Stratigraphy and Hydrothermal Alteration of the Gagne Lake Prospect: An Occurrence of Volcanogenic-Type Massive Sulfides Near Mine Centre, Northwestern Ontario, Canada.

A Thesis

Submitted to the Faculty of the Graduate School

of the University of Minnesota

by

Douglas Stuart Davis

In Partial Fulfillment of the Requirements

for the Degree of

Master of Science

September 1987

Aknowledgements

The author gratefully acknowledges his advisor Dr. Ronald Morton of the University of Minnesota-Duluth and Dr. K.H. Poulsen of the Geologic Survey of Canada for initiating this thesis.

In addition, Dr. Penelope Morton, Dr. Richard Ojakangas, and Dr. Vincent Magnuson of the University of Minnesota-Duluth deserve recognition for serving as my advisory committee.

Funding for this thesis was provided by the Geologic Survey of Canada, and access to the Gagne Lake prospect was permitted by Corporation Falconbridge Copper.

Special thanks are given to Wendy Johnson-Rodzacky and Frank Pezzutto who performed some of the X-Ray mineralogy work needed to complete this thesis.

Abstract

East-west trending, steeply dipping (85° +), overturned, Archean-age volcanic, sedimentary and intrusive rocks (sills) of predominantly greenschist-amphibolite transition facies grade are exposed in the Wabigoon Subprovince of northwestern Ontario, Canada approximately 1.5 km southeast of Gagne Lake.

Volcanic rocks associated with the Gagne Lake prospect, a showing of volcanogenic massive sulfide-type mineralization (chalcopyrite, sphalerite, pyrite and galena), are primarily rhyolitic lava flows and pyroclastic (hydrovolcanic) rocks. The pyroclastic rocks serve as the host rock for the prospect. Mafic lava flows are interlayered with the felsic volcanics but constitute only a minor portion of the stratigraphy.

Tonalitic and mafic sills comprise nearly 50% of the stratigraphy and range in time of emplacement from prior to formation of the Gagne Lake prospect to after intrusion of the Little Ottertail Lake Stock.

Based on preserved primary textures and structures, the volcanic succession is thought to have formed under both subaerial and subaqueous conditions. Regional stratigraphic relationships suggest that the succession at one time formed part of an emergent volcanic island.

Volcanic rocks and tonalitic sills underlying the prospect have been variably altered by hydrothermal solutions. Distribution and geochemistry of the altered rocks is such that four alteration assemblages can be defined: 1) least altered assemblage, 2) sericite (biotite)- chlorite-iron carbonate assemblage, 3) actinolite-chlorite-epidote assemblage and 4) dalmatianite (sericite, chlorite, iron carbonate). The alteration assemblages delimit a concentrically zoned alteration pipe below the prospect in which actinolite-rich rocks are enveloped by sericite or biotite-rich rocks and a stratigraphically semi-conformable zone of sericitc alteration within the hydrovolcanic rocks. A relatively small zone of dalmatianite (spotted alteration) envelopes the Gagne Lake prospect. Crosscutting relationships indicate that actinolite-rich rocks and dalmatianite formed at the expense of sericite and/or biotite-rich rocks.

Alteration assemblages are believed to have formed by the circulation of hydrothermal solutions through the volcanic succession. Shallow circulating sea water reacted with felsic rocks and evolved into an acidic, potassium-rich brine. Reactions between this solution and felsic rocks in the field area produced the sericite/biotite-rich rocks by addition of potassium and magnesium to and leaching of calcium and sodium from the rocks. Deeper circulating solutions encountered mafic rocks at depth. Reactions between these fluids and the rocks produced a solution enriched in calcium, magnesium and iron. With ascent, this brine encountered sericite and biotite-rich rocks of the study area. The resulting reactions produced actinolite-rich rocks by addition of calcium, magnesium and iron to and leaching of potassium from the rocks. As this solution mixed with sea water near the water-rock interface, it became enriched in magnesium. Reactions

between this magnesium-rich solution and sericite-rich rocks produced a chlorite-quartz alteration assemblage that became dalmatianite during prograde metamorphism.

Table of Contents

List of Plates and Figures

List of Tables

I. INTRODUCTION

PURPOSE of STUDY

As a result of recent exploration for sulfide and precious metal deposits in northwestern Ontario, remapping of the Rainy Lake area has been undertaken by various mining companies and the Canadian Federal and Provincial governments as a means of evaluating the region for resource potential. This particular project was undertaken in conjunction with the Federal Government and Corporation Falconbridge Copper to study the stratigraphy and hydrothermal alteration of the footwall and immediate hanging wall rocks of the Gagne Lake prospect, an occurrence of volcanogenic-type massive sulfide minerals. Specifically, the objectives of this thesis are:

1) To determine the volcanic rock types and their stratigraphic relationships.
2) To develop a model of the volcanic environment in which the rocks were deposited.
3) To define the mineralogical and chemical changes caused by hydrothermal alteration in the rocks and develop an alteration model.

LOCATION, ACCESS and PHYSIOGRAPHY

Situated in the southwest quarter of Farrington Township, Rainy River District, northwestern Ontario, the study area is approximately half-way between the towns of Fort Frances and Mine Centre and 3.5 km south of highway 11 (Fig. 1). The study area can be reached in two ways: either by taking highway 11 east out of Fort Frances for 50 km to the eastern boundary of Rainy Lake Indian Reserve 26A, or by boat going eastward up Swell Bay into the inlet that receives drainage directly from Gagne Lake. From either point, the study area can be reached via flagged bulldozed roads and trails.

The topography of the map area consists of bedrock ridges that trend parallel to the strike of bedding. These ridges are separated by valleys that are localized along contacts between strata. Maximum elavation in the study area is 412 meters and maximum relief is 48.50 meters.

The study area is poorly drained making swamps a common feature, particularly along lake shores. However, outcrop exposure is nearly 50%.

PREVIOUS WORK

One of the earliest detailed works produced concerning the geology of the Fort Frances-Mine Centre area was the mapping of the stratigraphy in the Rice Bay area by A. C.

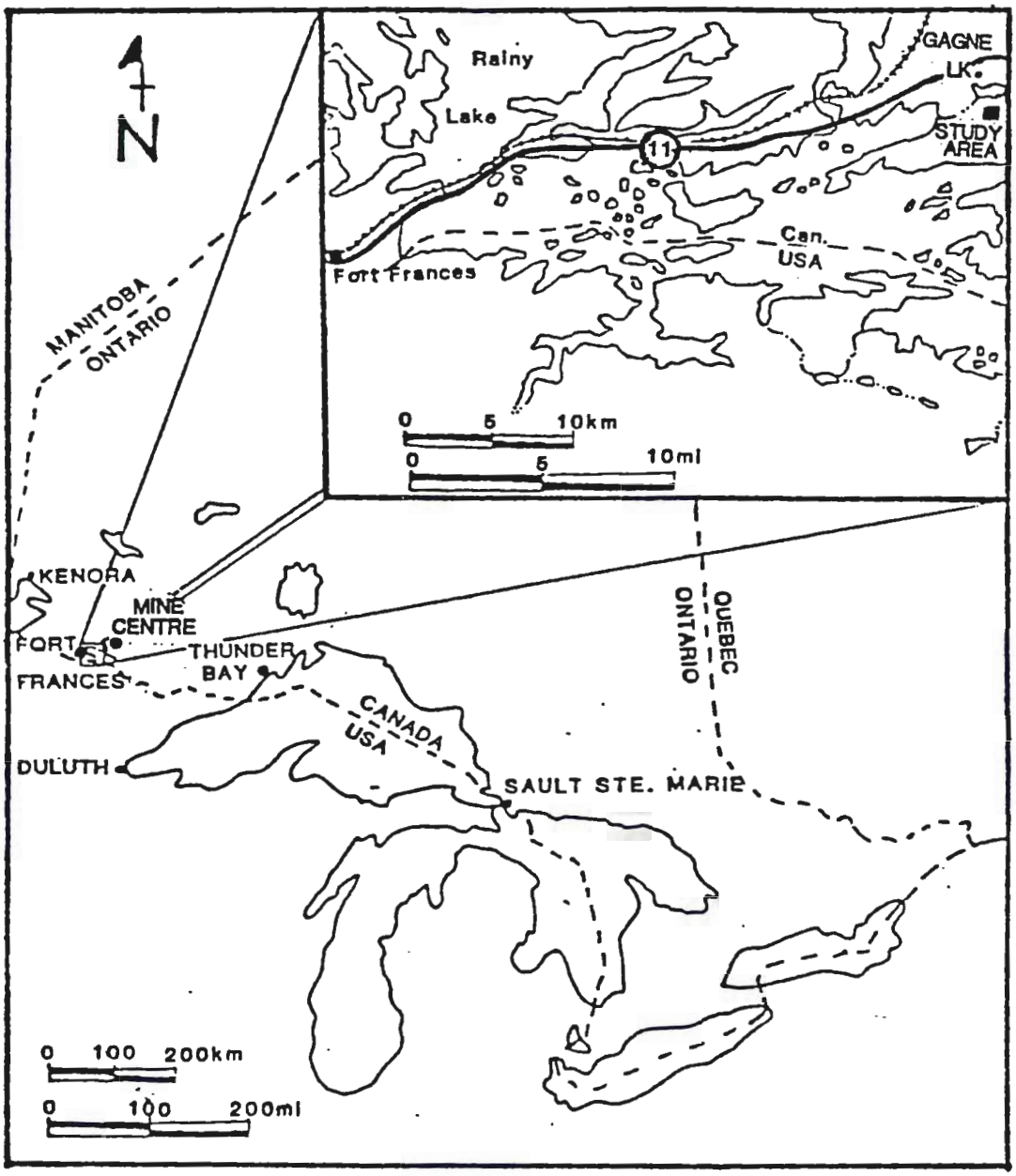

Figure 1. Location of study area.

Lawson (Lawson, 1913). He developed a nomenclature of three groups: the metavolcanic Keewatin Group, and the metasedimentary Coutchiching and Seine Groups. Using principles of structural superposition, Lawson concluded that the Coutchiching was the oldest followed in age by the Keewatin and Seine Groups respectively (Lawson, 1913).

This interpretation prevailed until Grout (1925) showed by younging directions from sedimentary features that the Coutchiching was younger than the Keewatin and may be a lateral facies of the Seine Group. Grout's interpretation was not fully accepted and many subsequent studies concerning the stratigraphy of the area (e.g. Merritt, 1934; Ojakangas, 1972; Harris, 1974) addressed this problem as well as redefining the basic stratigraphy.

In 1980, the Rice Bay area originally mapped by Lawson was found to be a dome formed by three deformational events, and that the Keewatin Group was, in fact, the oldest of the three Groups (Poulsen et al., 1980).

Goodwin (1977) in detailing the volcanism of the Superior Province showed that the volcanic stratigraphy is dominated by sequences that are mafic to ultramafic at the base and proportionately more felsic toward the top. These volcanic successions are lensoid in shape and

overall similarities to Quaternary island arcs led Goodwin (1977) to conclude that some type of interplate tectonics may have occurred during the Archean. Subsequent works on volcanic-sedimentary sequences within the Superior Province and the Wabigoon Subprovince have led others to postulate a model of island-arc type plate tectonics for the formation of Archean volcanic-sedimentary sequences (Langford and Morrin, 1976; Blackburn, 1980; Blackburn et al., 1985). Earlier models were fixist in that Archean rocks were autochthonous, and rifting and diapiric intrusion were the major crust-forming processes (McGlynn and Henderson, 1970).

METHODS of STUDY

Geologic mapping and rock sampling in a 4 square kilometer area were done during June and July of 1985 along a cut and flagged grid established by Corporation Falconbridge Copper. Results from mapping were compiled on mylar overlays in the field at a scale of 1:2500 and later transferred to a base map of the same scale provided by Corporation Falconbridge Copper.

Two hundred twenty rock samples were collected and made into thin sections to study mineralogy, primary textures, hydrothermal alteration, and metamorphism. Detailed modal analyses are tabulated in Appendix I.

Sixty-eight samples were also analyzed for major oxides and trace elements by the Geologic Survey of Canada for use in mass-balance computations. Analytical methods and results are compiled in Appendix II.

Sixteen samples were analyzed by X-ray diffraction in order to determine the chlorite species and to determine if cordierite is present in the rocks.

Eight altered samples were stained with alizerin red S and potassium ferricyanide using the methods of Freidman (1959) and Evamy (1962) for the determination of the carbonate species. Results for X-ray analyses and chemical staining are compiled in Appendix III.

REGIONAL GEOLOGY

Bounded on the north by the Quetico Fault and on the south by the Seine River-Rainy Lake Fault, the Archean-age rocks of the Fort Frances-Mine Centre area form a fault-bounded wedge of crust between the Wabigoon Subprovince to the north and the Quetico Subprovince to the south (Fig. 2). Both subprovinces are part of the Superior Province (Poulsen, 1982). Because of similarities in lithology, the bounday zone is typically included within the Wabigoon Subprovince.

The three areas are structurally discordant in that the Wabigoon is dominated by domal features resulting from diapiric intrusions and the refolding of earlier

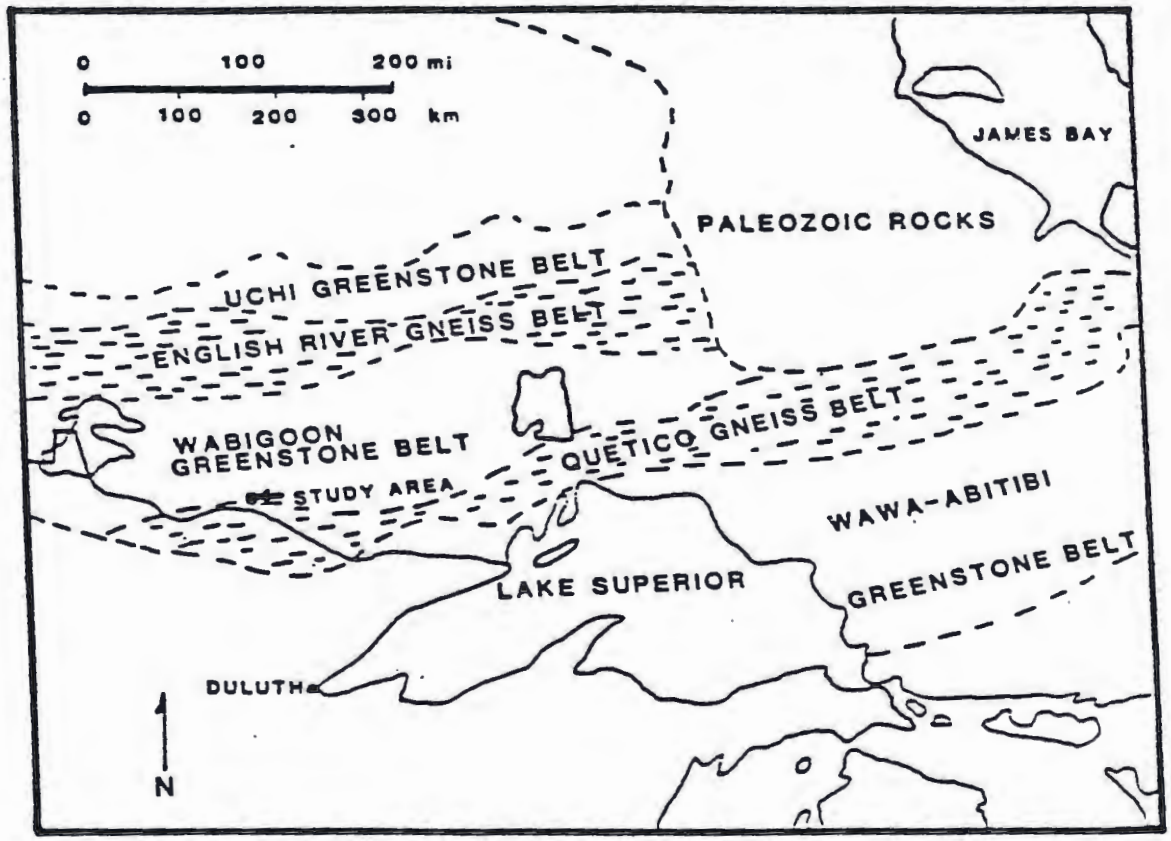

Figure 2. Distribution of greenstone and gneiss belts of northwestern Ontario (After Condie,1981)

nappe structures (Schwerdtner et al., 1979; Poulsen et al., 1980). The Quetico consists of steeply dipping metasedimentary strata with uniform east-trending strikes subparallel to the Seine River-Rainy Lake Fault (Poulsen, 1981). The boundary zone, which includes the study area, is a dextral wrench zone resulting from right-lateral movements on both of the faults (Poulsen, 1981). Locally, intrusion of the Little Ottertyail Lake Stock (Proterozoic) has metamorphosed rocks in the boundary zone to the greenschist-amphibolite transition facies (Poulsen, 1981).

Rocks of the Fort Frances-Mine Centre area consist of mafic to felsic metavolcanics, interbedded metasediments, including minor iron formation, and granitic plutons. Locally, the sequence is 15 km thick (Fig. 3).

The metavolcanic rocks form a succession of predominantly felsic metavolcanic rocks with mafic and intermediate compositions occurring near the base. The volcanic succession is intruded by a series of gabbroic and granitic sills and granitic stocks.

The mafic rocks range in composition and mode of occurrence from olivine gabbro intrusions to tholiitic basalt lava flows (Goodwin et al., 1972; Goodwin, 1977). Mafic and intermediate (andesitic) metavolcanic rocks exhibit pillowed, fragmental and massive textures whereas

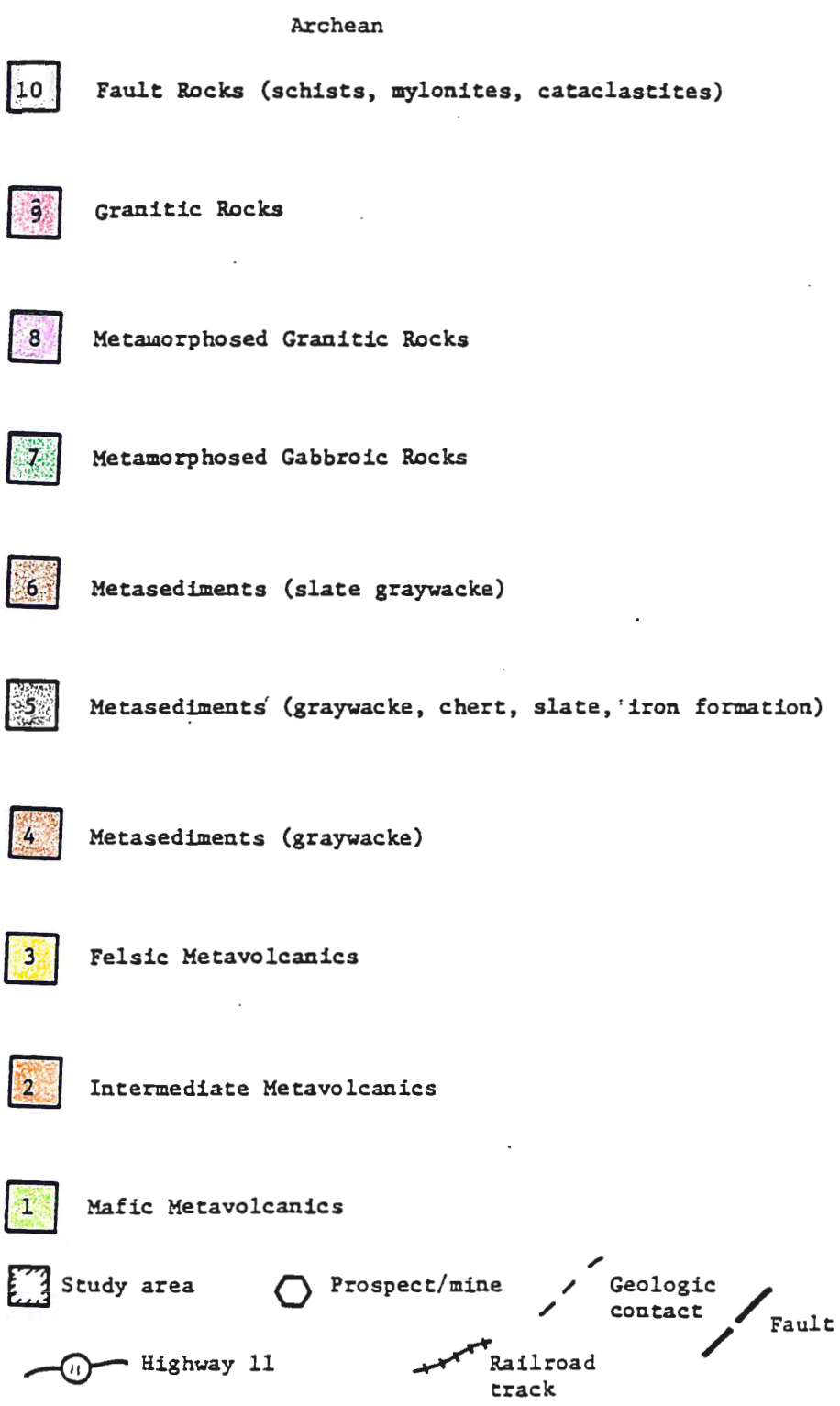

Figure 3. Legend for regional geology map.

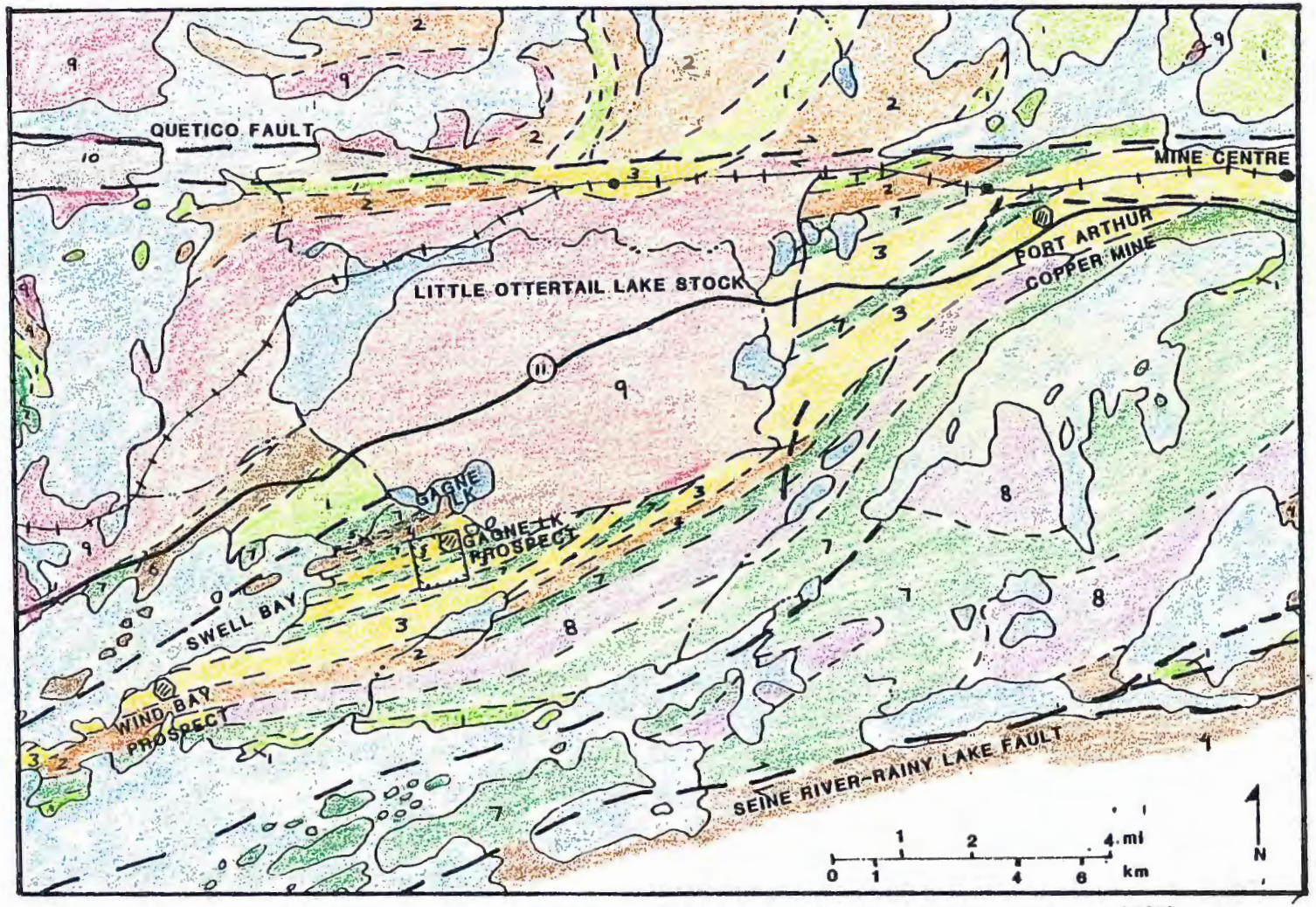

Figure 3. Regional geology of the Fort Frances-Mine Centre area (Blackburn, 1975; Poulsen, 1982)

the felsic metavolcanics are fragmental or massive (Poulsen, 1982).

The granitic plutons can be grouped into two broad categories (Blackburn, 1978):

1) Metamorphosed granitic rocks

2) Nonmetamorphosed granitic rocks

For simplicity, nonmetamorphosed granitic rocks will be referred to as granitic rocks only. The granitic rocks compose a spectrum of compositions ranging from monzonite to granite while the metamorphosed granitic rocks are more bimodal in composition and consist of granite and tonalite without significant volumes of intermediate compositions (Goodwin,1972; Poulsen, 1981).

As well as being compositionally different, the two groups also have contrasting modes of occurrence. The metamorphosed granitic rocks tend to occur as sills and dikes; granitic rocks form batholiths.

Metasediments are prdominantly metagraywacke, but local variations have led to the division of the metasediments into three groups (Blackburn, 1978):

1) Metagraywacke

2) Metagraywacke with chert, slate and iron formation

3) Slate with metagraywacke

Each group is arranged in decending order by abundance.

Metagraywackes have been interpreted to be turbidites and the abundance of volcanic detritus incorporated into the metagraywackes suggests that deposition and volcanism were penecontemporaneous (Ojakangas, 1985).

Rocks found in fault zones consist of schists, mylonites, and cataclastites that have been interpreted to be sheared equivalents of the igneous and sedimentary rocks of the region (Ojakangas, 1972; Poulsen, 1982).

II. LITHOLOGY and STRATIGRAPHY

INTRODUCTION

The distribution of rocks in the study area is shown on Plate 1 (back jacket), and modal mineral abundances for represenative samples of each lithology are compiled in Appendix I.

The rocks have a consistent east-west strike and dip either vertically or steeply (85^{o}+) to the south. Other top indicators in the region, as well as graded bedding within the study area, indicate that the strata are slightly overturned to the south. A vertical, bedding-parallel foliation occurs in the area but is not pervasive in outcrop; in thin section, however, foliation and bedding are virtually indistinguishable.

With the exception of unit 8, which has not undergone metamorphism, the intrusion of the Little Ottertail Lake stock (Fig. 3) metamorphosed the rocks in the area to the greenschist-amphibolite transition facies with temperature and pressure conditions of metamorphism having been approximately 500-550 ^{o}C at 2.0-3.5 kbar (Winkler, 1976; Poulsen, 1982). For brevity, the prefix meta will not be used in this text.

Despite having been both metamorphosed and hydrothermally altered, the rocks display primary igneous textures in outcrop and thin section that allow for the

determination of the original character of the rock.

The stratigraphy of the Gagne Lake area (Fig. 4) consists of rhyolitic lava flows and bedded pyroclastic rocks interlayered with plagioclase-phyric mafic flows and tonalitic and mafic sills.

LAVA FLOWS

Mafic and felsic lava flows constitute 80-90% of the volcanic rocks and 50-60% of the stratigraphy in the study area. Although typically massive, locally the lava flows are porphyritic, amygdaloidal, and/or flow banded. Flow breccias are absent, but ash-sized fragments are locally incorporated into the quartz-feldspar porphyry lava flow.

Absence of features such as shards, abundant lithic/pumice fragments and interbedded air fall tuffs commonly associated with ash tuffs (Bonnichsen and Kauffman, 1987; Chapin and Lowell, 1979) indicates that these units are lava flows rather than pyroclastic rocks.

Felsic Lava Flows

Quartz-Feldspar Porphyry

(Unit 1, Plate 1)

A rhyolitic, quartz--feldspar porphyry (QFP) lava flow crops out in the southwest corner of the field area and constitutes 5 to 7% of the volcanic stratigraphy. The unit is thick (up to 120 m) and pinches out to the east.

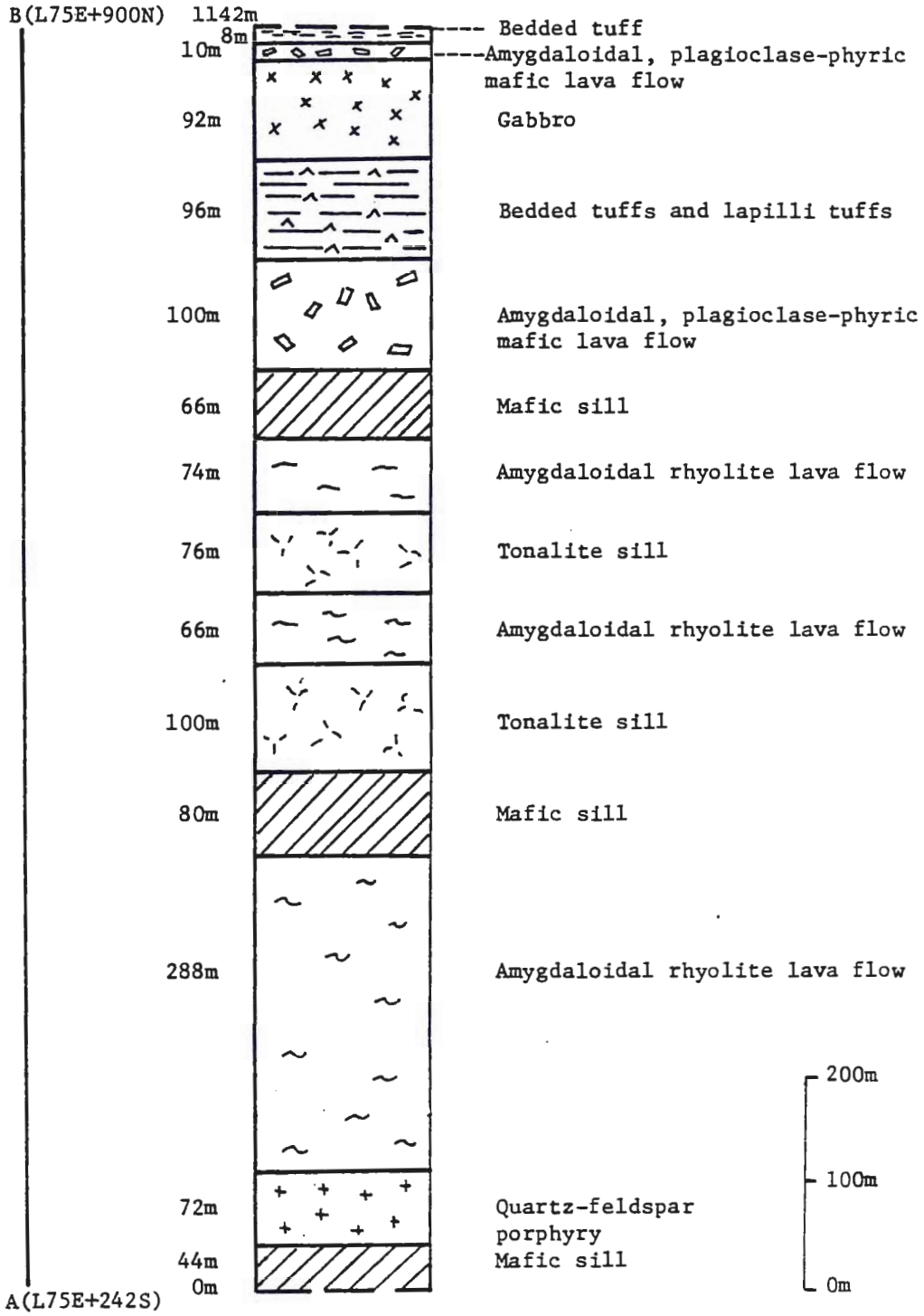

Figure 4. Stratigraphy of the Gagne Lake area measured along AB, L75E, Plate 1.

In outcrop, the QFP is massive to porphyritic and differentiated from the other rhyolite lava flows by the presence of medium-grained (1.0-5.0 mm) phenocrysts of quartz and plagioclase.

In thin section, fine to medium-grained, broken phenocrysts make up 2 to 7% of the QFP and consist of pilotaxitic andesine (An_{33-37}) laths and quartz that is either anhedral or exhibits a beta-quartz (bipyramidal) habit (Fig. 5). The unit is a serriate porphyry and locally glomeroporphyritic.

Small (<1.0 mm) quartz-filled amygdules are present and comprise 1 to 12% of the unit. The amygdules are round to elliptical in shape and may occur in trains parallel to flow banding and/or metamorphic foliation that is defined by the segregation of light and dark minerals and the preferred orientation of biotite and/chlorite. Ash size (<1.0 mm) siliceous fragments are locally present and comprise up to 12% of the QFP.

The matrix of the QFP is composed predominantly (30-90%) of fine-grained (<0.5 mm) recrystallized quartz, albite and minor cordierite (determined by X-ray diffraction and thin section analysis). Recrystallized spherulites (<1.0 mm) are locally abundant (1-10%) indicating the original matrix was glassy. Fine-grained biotite (15-30%) occurs in veinlets or disseminated

throughout the rock and is commonly intergrown with chlorite. Magnetite (1-4%), sphene (<2%) and apatite (<1%) are the major accessory minerals (Appendix I). Sericite, chlorite and iron carbonate are present and thought to represent minerals formed during hydrothermal alteration.

Amygdaloidal Rhyolite Lava Flows

(Unit 2, Plate 1)

Constituting 60 to 70% of the volcanic rocks, amygdaloidal rhyolite lava flows are the most voluminous rock type in the study area and differentiated from the QFP by the absence of megascopic phenocrysts. These units form thick (50 to 400 m) units, some of which can be traced along strike for at least 2.0 km. In outcrop, the amygdaloidal rhyolites are typically massive and aphanitic. Locally, however, some outcrops are coarse grained enough to display a megascopic foliation subparallel to the regional strike. The foliation is defined by the preferred orientation of biotite and chlorite and may represent flow banding or a metamorphic effect. The amygdaloidal rhyolites are mottled reddish brown and gray on weathered surfaces and light gray to black on fresh surfaces. Weathering of sulfides produces pits on the outcrop that are encrusted by limonite.

In thin section, round to elliptically shaped

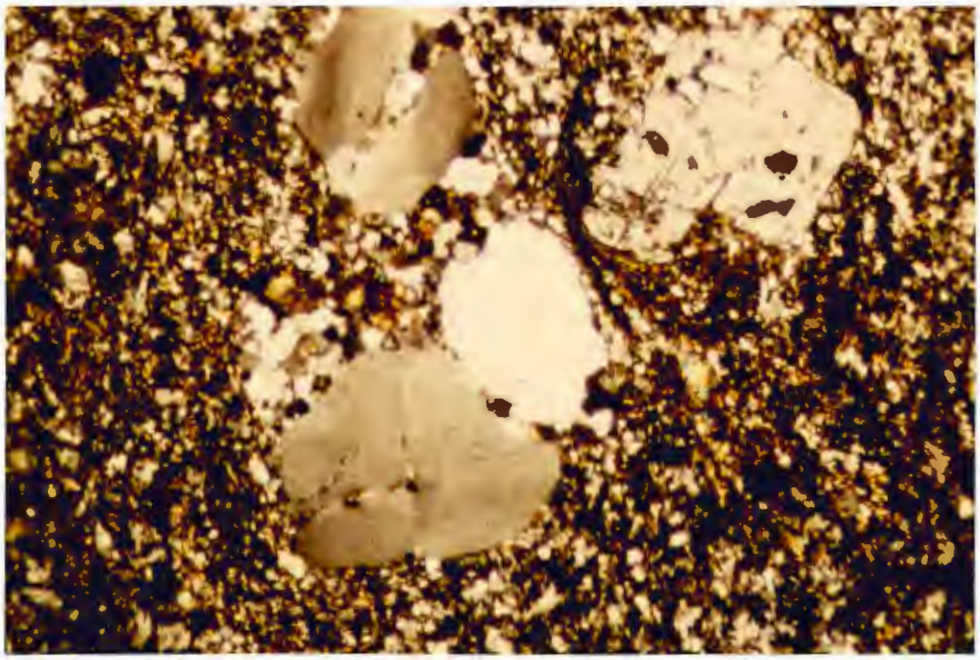

Figure 5. Photomicrograph of plagioclase (upper right) and quartz (center) phenocrysts in QFP. Matrix is composed of plagioclase, quartz, biotite and minor cordierite. Crossed polars, field of view 5x7mm.

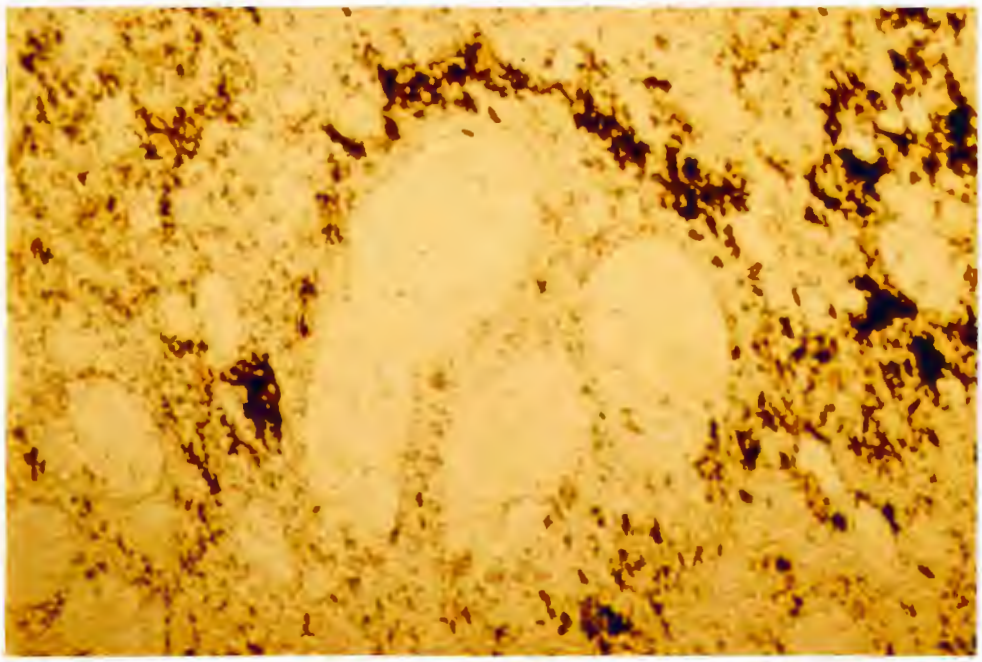

Figure 6. Photomicrograph of quartz-filled amygdules in amygdaloidal rhyolite lava flow. Plane polarized light, field of view 5x7mm.

amygdules typically constitute from 3 to 6% of the rock but may be present in amounts up to 15%. The amygdules are small (<1.5 mm) and filled by either quartz (Fig. 6) or quartz in association with biotite, chlorite or sericite. Quartz and quartz-biotite-filled amygdules predominate. Cataclastized microphenocrysts (<1.0 mm) of pilotaxitic andesine (An_{32-38}) and anhedral quartz compose 1 to 6% of the rock. The percentage of phenocrysts increases stratigraphically upwards.

Flow bands are thin (<5.0 mm) and defined by the segregation of light and dark minerals. Flow banding is typically plane parallel but may become convoluted and discontinuous around phenocrysts and amygdules. Aligned trains of very-fine-grained amygdules may reflect original flow banding.

Fine-grained (<1.0 mm) recrystallized spherulites (2-15%) have been observed in thin section and indicate that the original matrix was glassy. The spherulites are round to elliptical in shape and may exhibit a radiating texture.

Based on X-ray diffraction and thin-section study, quartz, albite and cordierite (<10%) are found to form 40 to 90% of the fine-grained (<0.50 mm) matrix of the rhyolites. These minerals occur as either a massive, recrystallized mosaic of grains or in a radiating,

"leafy", texture that is interpreted to be a relict devitrification feature. Fine-grained (<1.0 mm) biotite (10-25%) is found disseminated throughout the rock or, locally, it occurs as veinlets or filling amygdules with quartz. Sphene (1-4%), magnetite (1-4%) and apatite (<2%) are the accessory minerals (Appendix I). Sericite, chlorite, actinolite, epidote and iron carbonate are locally abundant and believed to represent minerals formed during hydrothermal alteration. Veinlet and disseminated sulfide mineralization consisting of pyrite with lesser sphalerite (<1%) and/or chalcopyrite (<1%) are present in amounts up to 3%. Limonite staining occurs with the sulfide mineralization.

Mafic Lava Flows

Amygdaloidal, Plagioclase-Phyric, Mafic Lava Flows

(Unit 3, Plate 1)

Two plagioclase-phyric mafic lava flows outcrop in the study area and make up 10 to 20% of the volcanic stratigraphy. The stratigraphically lowest of the two flows has a strike length of at least 2.0 km. Thinning to the east, the flow varies in thickness from 70 to 100 m. The stratigraphically higher lava flow pinches out to the east and is thinner (5-20 m). Both flows are dark green to black in outcrop and slightly foliated. The best exsposures of these units occur in the northwest corner

of the field area and near the north shore of One Island Lake (Plate 1).

In thin section, the mafic lava flows are serriate porphyries in which andesine (An_{38-42}) phenocrysts grade into a matrix of predominantly chlorite and quartz (Fig. 7). Phenocrysts comprise 8 to 15% of the rock and range in size from less than 0.30 mm to 0.80 mm with an average grain size of 0.50 mm. The phenocrysts appear to be randomly oriented and cataclasis is common. The percentage of phenocrysts decreases to the east to less than 2%.

In the stratigraphically lowest lava flow, the phenocrysts are smaller and invariably pseudomorphed by iron carbonate whereas phenocrysts in the upper lava flow exhibit only partial replacement around crystal edges by carbonate or sericite.

Each flow contains 5 to 12% quartz-filled amygdules. The amygdules are small (<1.0 mm) and elliptical in shape.

Chlorite is the dominant matrix mineral (30-40%) and occurs in fibrous or radiating masses that are intergrown with biotite (2-10%). X-ray diffraction studies indicate that chlorite varies in composition from penninite to ferroan clinochlore (Berry, 1974, Switzer, 1977); the anomalous indigo interference color observed in thin

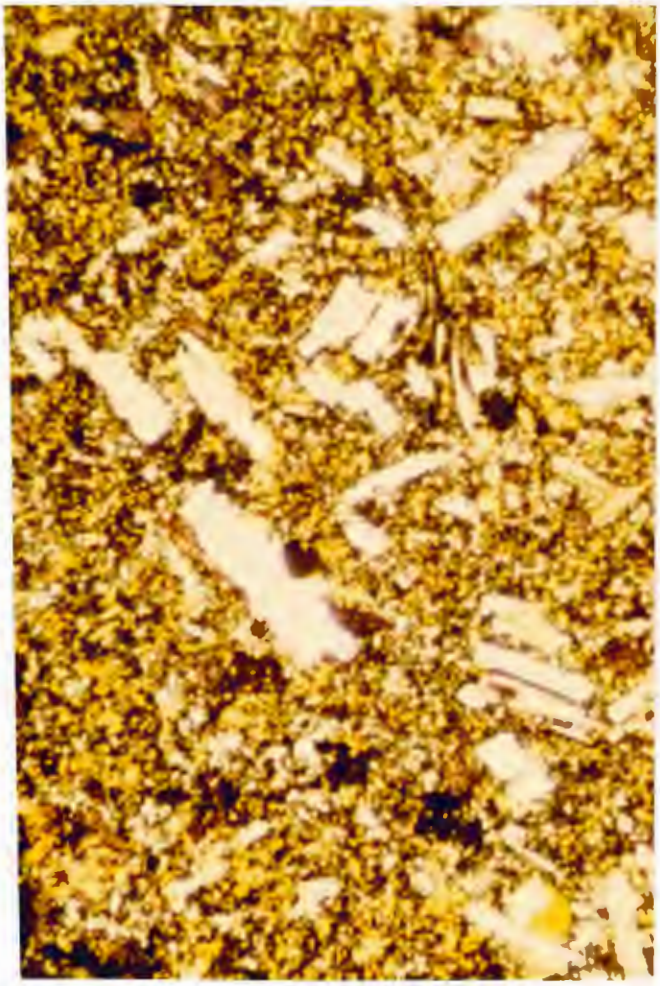

Figure 7. Photomicrograph of serriate plagioclase phenocrysts in mafic lava flow. Matrix is composed of chlorite, biotite, quartz and plagioclase. Crossed polars, field of view 5x7mm.

section indicates that the perminite is iron enriched (Phillips and Griffen, 1981). Fine-grained, bladed to fibrous hornblende (8-15%) and anhedral quartz (10-20%) and plagioclase (5-10%)are also present in the matrix. Epidote (4-11%) magnetite (1-3%) sphene (1-4%) and ilmenite (0-1%) constitute the accessory minerals (Appendix I). Platy sphene grains and sphene grains with ilmenite cores indicates that sphene occurs as a pseudomorph after ilmenite.

PYROCLASTIC ROCKS

Pyroclastic rocks comprise 10 to 20% of the volcanic rocks and 5 to 10% of the rocks in the study area. These fine-grained units consist of well-bedded, and locally, graded tuffs and lapilli tuffs.

Bedded Tuffs and Lapilli Tuffs

(Unit 4, Plate 1)

Interlayered, felsic bedded tuffs and lapilli tuffs comprise 10 to 15% of the volcanic stratigraphy in the area and are the host rocks for the sulfide mineralization (Gagne Lake prospect). Varying from 80 to 160 m in thickness, the tuffs thin to the west and have strike lengths that exceed 2.0 km. The units are thinly bedded (<5.0 cm) and light brown to black on both fresh and weathered surfaces. A vertical, bedding-parallel foliation is present on some outcrops.

Lapilli tuffs are characterized by thin (<0.5 m) normally graded beds which are lapilli-rich (10-50%) at the base and grade upward into finely-bedded ash-size material. The elliptically shaped lapilli (2.0-8.0 mm) compose from 3 to 50% of an individual bed and are aligned in the plane of bedding (Fig. 8). The elliptical shape of the lapilli may be the result of compaction and/or post-deposition deformation.

Typically, the beds are plane parallel, but, locally, convoluted and lens-like bedding was observed. At least four units of the lapilli tuffs were counted in the field.

Eastward, the lapilli tuffs pass into uniformly bedded tuffs that are virtually fragment free (<1%). Bedding in these units is predominantly plane parallel (Fig. 9) but convoluted bedding (Fig. 10), load structures (Fig. 11) and symmetrical ripple marks (Fig. 12) are locally present suggesting that the units were deposited in a water-rich, turbulent flow (base surge?) (Fisher and Schmincke, 1984).

Near the base of the bedded tuffs and lapilli tuffs, in the western end of the study area, large (>64 mm) rounded to fusiform fragments composed of fine-grained quartz and feldspar are present (5-7%). Associated with these fragments are symmetrical to ballistically shaped

Figure 8. Lapilli aligned in plane of bedding of lapilli tuff. Unit tops to north (left). Lens cap is 52mm in diameter.

Figure 9. Plane parallel bedding in bedded tuff. Lens cap is 57mm in diameter.

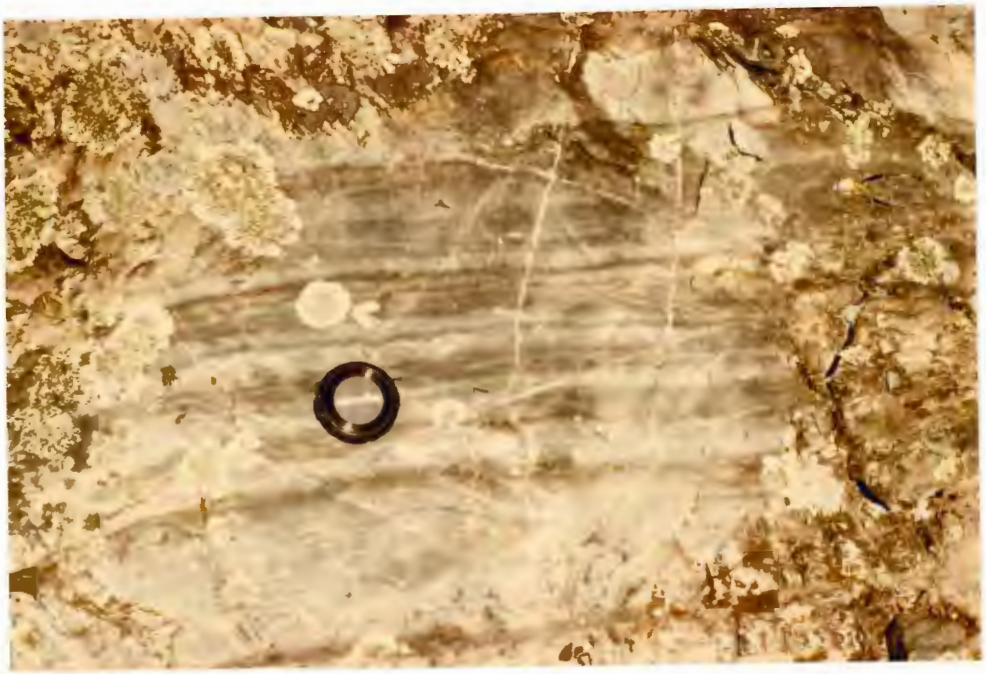

Figure 10. Convoluted bedding in bedded tuff. Lens cap is 57mm in diameter.

Figure 11. Load structures in bedded tuff.

bomb-sagged bedding features (Fig. 13).

In thin section, lapilli were observed to be predominantly siliceous, possibly juvenile, fragments rather than pumiceous (Fig. 14). Constituting 3 to 50% of an individual bed, the fragments are subrounded, commonly broken, and range in size from coarse ash (0.5-1.0 mm) to lapilli (2.0-8.0 mm). Ash-sized, chloritized pumice fragments occur locally and constitute up to 4% of the rock. The pumice fragments are slightly flattened and exhibit a weak preferred orientation subparallel to bedding. Ash-sized fragments of graphically intergrown quartz and feldspar (orthoclase?) are present but only in minor (<1%) amounts. Fragments of the rhyolite flows (<1.0%) occur as accessory fragments.

Fine-grained (<1 mm) phenocrysts are composed of either pilotaxitic plagioclase (1-5%) or anhedral quartz (1-8%). Both plagioclase and quartz phenocrysts are serriate and cataclastized.

The matrix is composed primarily of a recrystallized mosaic of very fine-grained (<0.25 mm) quartz, albite and minor cordierite that constitutes 40 to 90% of the rock with biotite (5-40%) and magnetite (1-4%) as the major accessory minerals (Appendix I).

Biotite flakes (<0.25 mm) are disseminated throughout the rock and commonly aligned in the plane of bedding or

Figure 12. Symmetrical ripple marks in bedded tuff. Unit tops to north (top of page).

Figure 13. Fusiform, block-sized fragment and bomb-sagged bedding features in lapilli tuff. Unit tops to north,(top of page).

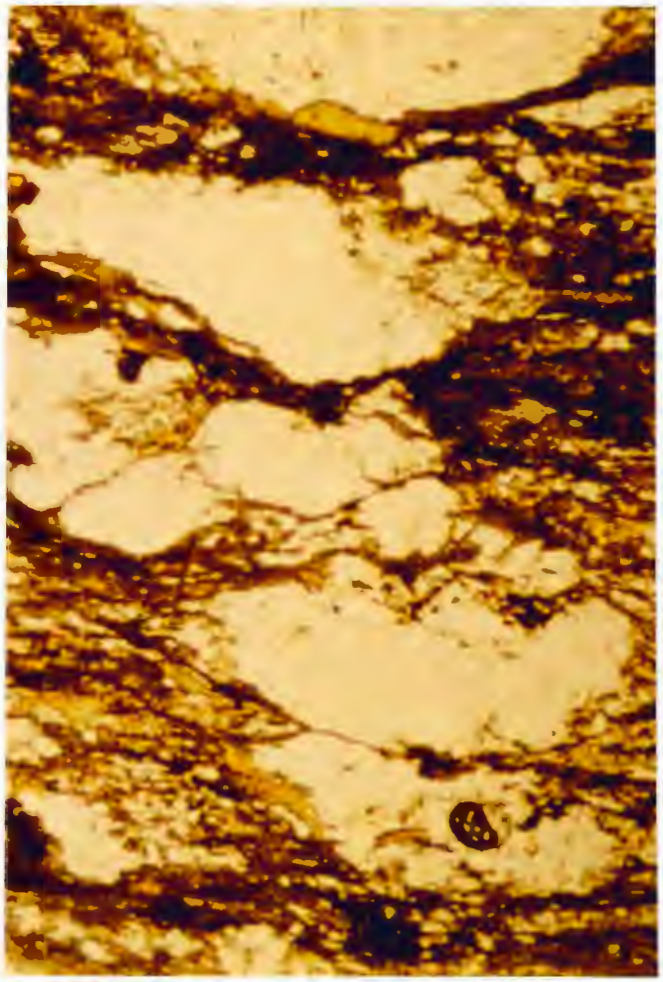

Figure 14. Photomicrograph of broken lapilli. Plane polarized light, field of view 5x7mm.

foliation. Chlorite is typically intergrown with biotite in fibrous or radiating masses. Poikolitic intergrowths of muscovite and quartz are present but rare (<1%). Magnetite is disseminated throughout the rock. Sericite, chlorite, epidote and iron carbonate are considered to be minerals formed by hydrothermal alteration and will be discussed more thoroughly in the chapter on hydrothermal alteration. Sulfide mineralization varies from 1 to 7% disseminated sulfides and consists of pyrite with lesser sphalerite (<1%) and/or chalcopyrite (<1%).

Bedded Tuff

(Unit 5, Plate 1)

Outcropping in the northwest corner of the study area is a thin (5-10 m), chlorite-rich tuffaceous unit that may be sedimentary in origin rather than volcanic. The bedded tuff pinches out towards the east and comprises less than 3% of the rocks in the map area. The unit is thinly bedded (<5.0 cm) and displays plane parallel bedding (Fig. 15). Dark green to black, the bedded tuff is composed primarily of medium-grained (1-5mm), crenulated, biotite and chlorite that is aligned in the plane of bedding and/or foliation.

In thin section, biotite (15-20%) and chlorite (30-35%) are intergrown into fibrous masses (Fig. 16). Fine-grained, anhedral quartz (20-25%) and fine-grained

Figure 15. Plane parallel bedding in bedded tuff. Lens cap is 52mm in diameter.

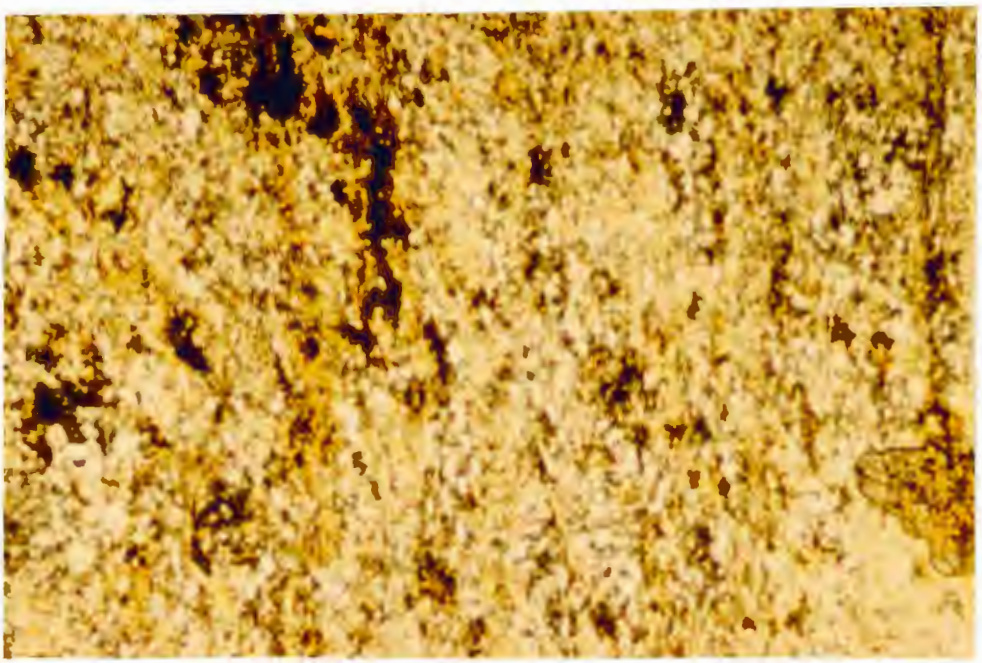

Figure 16. Photomicrograph of bedded tuff. Biotite (yellow) and chlorite (green) with quartz. Crossed polars, field of view 5x7mm.

plagioclase laths (2-6%) constitute the other major minerals. The plagioclase is pilotaxitic, subparallel to the biotite and chlorite masses and pseudomorphed by carbonate. Quartz typically occurs as anhedral grains but is also present as veinlet filling material with carbonate. Ash-sized (<2.0 mm) lithic fragments make up 1 to 3% of the rock. The fragments are elliptical and highly chloritized. Sphene (1-3%), tourmaline (1-2%) and apatite (<1%) are the accessory minerals.

INTRUSIVE ROCKS

Intrusive rocks make up 30 to 40% of the rocks in the study area and range in time of emplacement from prior to hydrothermal alteration for the tonalite sills to post-emplacement of the Little Ottertail Lake stock.

Tonalite Sills

(unit 6, Plate 1)

The tonalite sills are greenish gray in color on both weathered and fresh surfaces, 20 to 90 m thick, and slightly foliated. Strike lengths for these sills exceeds 2.0 km. Similarities in mineralogy between these units and the felsic volcanics suggests that the two rock types may be genetically related.

Mineralogically, andesine (An_{35-39}), quartz, biotite and chlorite form the bulk of the rock (Fig. 17). Plagioclase (10-30%) occurs as fine to medium-grained

(<5.0 mm) laths with partially corroded edges or as graphic intergrowths with quartz similar to the fragments in the lapilli tuffs. Grains of graphically intergrown quartz and plagioclase may be up to 3.0 mm but are generally in the 1.0 to 2.0 mm range. Quartz (10-20%) also occurs as small (<2.0 mm) anhedral grains. Biotite (5-30%) and chlorite (6-30%) are invariably intergrown into fibrous masses. The individual grains are fine grained, but the masses of intergrown biotite and chlorite are up to several millimeters in length and show a weak preferred orientation. Disseminated pyrite (<1.0 mm) is present in some samples in amounts up to 2% (Appendix I).

Actinolite, epidote and iron carbonate are also present and along with chlorite are interpreted to be hydrothermal alteration minerals. Although sericite is present, its abundance is so low (1-5%) and its occurrence is so pervasive that its classification as a hydrothermal alteration mineral is speculative.

Mafic Sills

(unit 7, Plate 1)

Laterally extensive (>2.0 km) and massive to slightly foliated in outcrop, these 26 to 100 m thick units are quite similar in appearance to the tonalite sills. On a fresh surface, however, gray to white, fine to

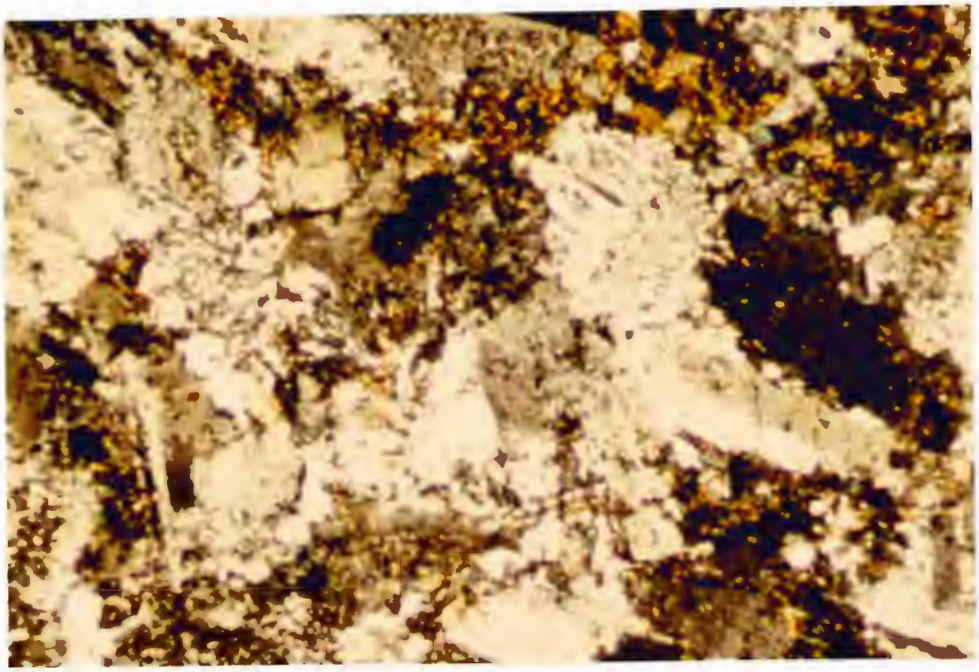

Figure 17. Photomicrograph of tonalite sill. Plagioclase, quartz, biotite, chlorite and graphically intergrown quartz and plagioclase. Crossed polars, field of view 5x7mm.

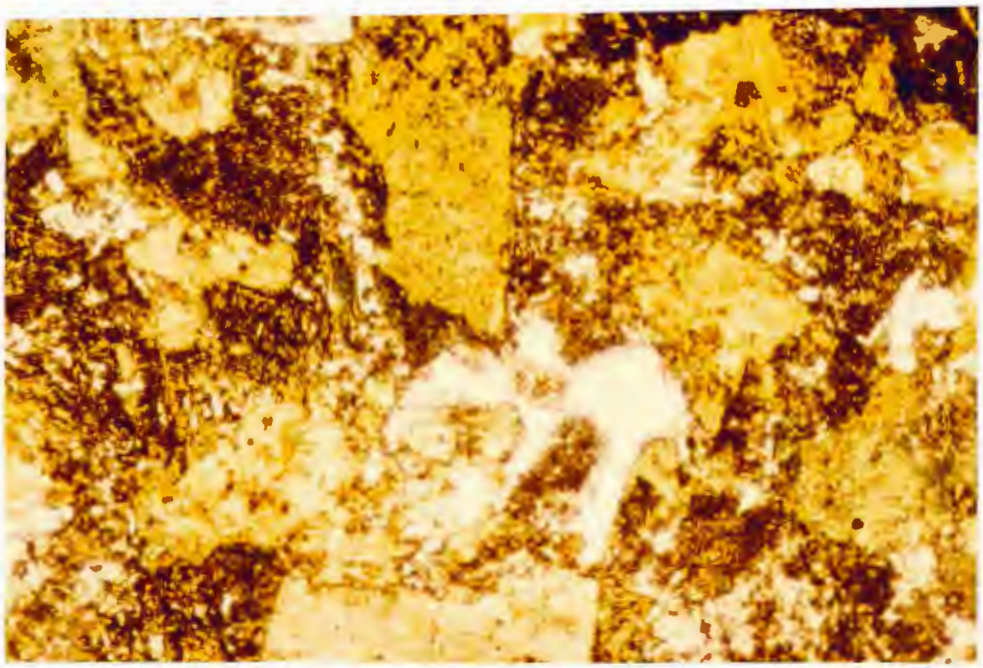

Figure 18. Photomicrograph of mafic sill. Hornblende with quartz, chlorite and grapically intergrown quartz and plagioclase in which the plagioclase has been saussuritized. Plane polarized light, field of view 5x7mm.

medium-grained plagioclase grains and pink to flesh colored graphic intergrowths of quartz and plagioclase can be seen against a green matrix. Previous geochemical work (Poulsen, 1982) has shown these rocks to be originally basaltic in composition.

In thin section, the mineralogy of these rocks is hornblende, andesine (An_{35-42}), chlorite, epidote, and sphene (replacing ilmenite) with minor quartz and apatite as well as the graphic intergrowths (Appendix I). Medium grained (1.0-4.0 mm) bladed to fibrous hornblende (25-60%) with interstitial, massive to fibrous chlorite (chamosite?) (10-20%) dominate (Fig. 18). Plagioclase (7-15%) occurs as individual laths (0.5-2.0 mm) or as graphic intergrowths with quartz. Commonly, the plagioclase that is intergrown with the quartz is pseudomorphed by chlorite and epidote. Quartz (10-18%) is also present as small (<1.0 mm) anhedral grains that grade into the matrix. Euhedral, fine-grained epidote (3-25%) occurs disseminated throughout the sample or in anastomosing veinlets. Apatite (<2%) and ilmenite (1-7%) are the major accessory minerals. Sphene (1-5%) commonly occurs as a pseudomorph of ilmenite. Where the replacement of ilmenite is incomplete, cores of ilmenite mantled by sphene are present.

Gabbro

(unit 8, Plate 1)

This 90 to 100 m thick sill is also laterally extensive (>2.0 km) and recognized in outcrop by its ophitic texture. Differential weathering of pyroxene and plagioclase has produced a spotted, knobby texture on the outcrop surface in which resistant pyroxene grains are darker in color and stand up in relief against the plagioclase (Fig. 19). The unit is medium to coarse grained (2.0-7.0 mm), thickens to the east, and weathers to dark green or shades of brown.

Under the microscope, the rock is composed of uralitized, euhedral augite oikocrysts (30-40%) interstitial to which are either an assemblage of fibrous to massive chlorite (20-30%), and fine-grained, euhedral epidote (zoisite) (15-30%) from the saussuritization of plagioclase or partially saussuritized plagioclase (2-20%) (Appendix I). Quartz phenocrysts (<2%) are fine grained and grade into the matrix where quartz comprises 1 to 8 % of the rock. Larger quartz phenocrysts are present in outcrop as blue quartz. When abundant, the phenocrysts are grouped together in patches. Ilmenite (1-5%) that is either partially or totally replaced by sphene is the major accessory mineral and apatite is present as a minor constituent (<1%).

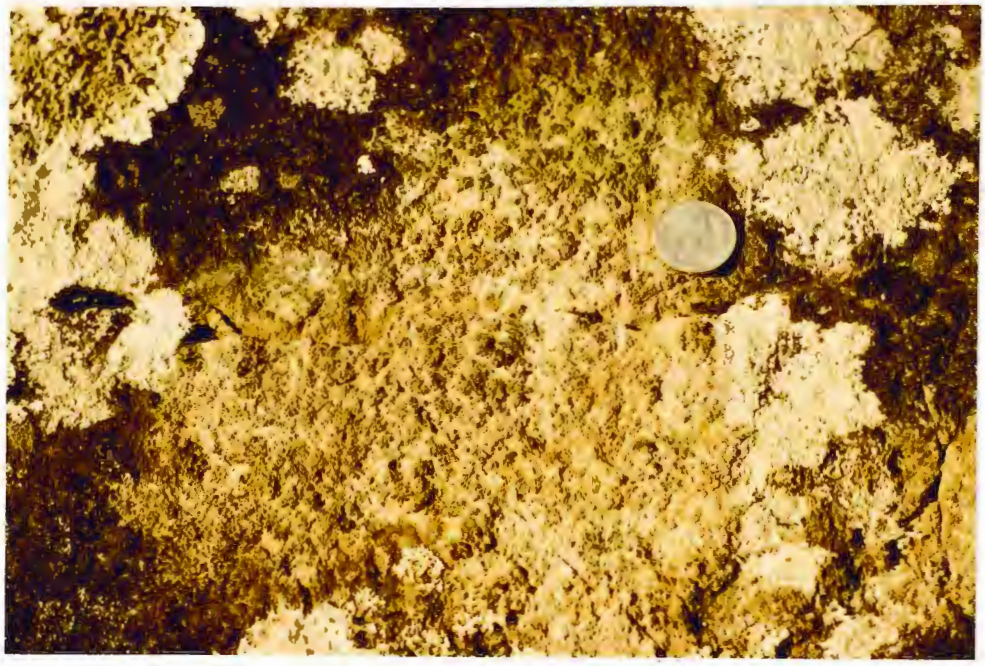

Figure 19. "Knobby" texture in gabbro produced by differential weathering of pyroxene (dark brown) and plagioclase.

VOLCANOLOGIC INTERPRETATION

The volcanic stratigraphy in the Gagne Lake area consists of a relatively thick sequence of rhyolite lava flows which passes stratigraphically upwards into a sequence of interbedded mafic lava flows, bedded tuffs and lapilli tuffs (Fig. 20). Field evidence indicates that the eruption of the volcanic rocks occurred under both subaerial and subaqueous conditions. The following is a proposed volcanologic model for the formation of the rocks in the map area.

Rhyolitic lava flows dominate the volcanic stratigraphy in the study area. The rhyolites are thick (up to 400 m) units that may have strike lengths in excess of 2.0 km. The aerial extent of these units suggests that they may have been erupted at relatively high temperatures (900-1000 °C) for rhyolites and possibly gas charged (Hausback, 1987; Bonnichsen and Kauffman, 1987). Typically massive but locally flow banded, porphyritic, amygdaloidal or spherulitic, these units are texturally similar to rhyolite lava flows and domes near Mine Centre (Poulsen, 1982).

Absence of features within the sequence of rhyolite flows (domes?) such as hyaloclastite material, quench textures, and interbedded sedimentary rocks which are commonly associated with subaqueous rhyolite flows (i.e. Rouyn-Noranda, Quebec, Blahnukur, Iceland (De

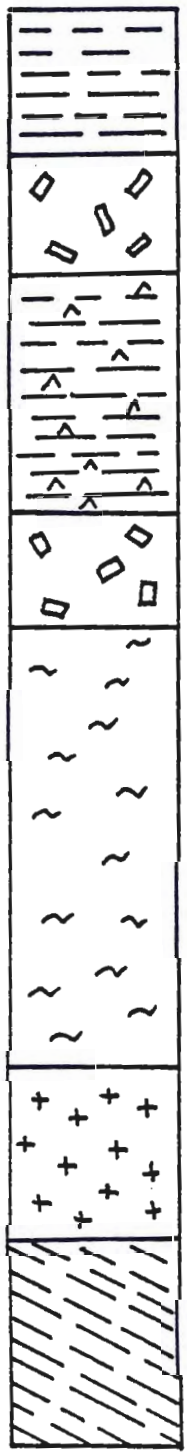

Figure 20. Diagramatic columnar section of the volcanic stratigraphy of the Gagne Lake area showing proposed facies changes with time

Rosen-Spence et al., 1980) and Hill End Trough, New South Wales, Australia (Cas, 1978)) combined with the absence of pillow structures and hyaloclastite material in the overlying mafic lava flow suggest that the rhyolites and overlying mafic flow were formed in a subaerial environment. Further evidence that these units are subaerial is the presence (outside the field area) of a highly vesicular, flow-banded rhyolite lava flow stratigraphically below the rhyolite lava flows in the study area that has been interpreted to be subaerial (B. Boily, pers. comm., 1985) (Fig. 20).

Felsic bedded tuffs and lapilli tuffs overlie the rhyolite and mafic lava flows. The thin (<0.5 m), locally graded bedding, near horizontal bedding angles, sedimentary structures, quenched juvenile fragments, extremely fine grain size, and limited vertical extent of the units are characteristic of hydroclastic deposits formed by explosive hydrovolcanic (phreatomagmatic) eruptions (Heiken, 1971; Wohletz and Sheridan, 1983).

Hydroclastic deposits like those in the field area are characteristic of tuff rings. Tuff rings are relatively small (<3.0 km in diameter), typically asymmetric volcanic edifaces of low relief that occur in clusters and are commonly associated with maar volcanoes (Wohletz and Sheridan, 1983).

Explosive hydrovolcanic eruptions are believed to be the result of fuel-coolant interactions (FCI) in which the fuel is a magma, and the coolant is an external source of water (either ground water or a standing body of water) (Sheridan and Wohletz, 1983). An FCI typically involves the contact of the two fluids with the fuel being above the boiling point of the coolant. During an FCI, the coolant may be vaporized, resulting in its rapid expansion, and the fuel chilled or quenched (Sheridan and Wohletz, 1983).

Experimental studies (Wohletz and McQueen, 1984) and detailed studies of tuff ring evolution and morphology (Wohletz and Sheridan, 1983; Sheridan and Wohletz, 1983) have determined that the explosivity of the FCI and, consequently, the nature of the hydrovolcanic eruption is controlled by the coolant/fuel (water/magma) ratio. The volume of water that interacts with magma during a hydrovolcanic eruption is governed by the actual abundance of water present, accessibility of the water to the magma, and the amount of magma. For example, during a hydrovolcanic eruption, if the available water has only limited access to the magma, then the eruption will take place at a low water/magma ratio even though the amount of water available may be large (Sheridan and Wohletz, 1983).

For felsic magmas, when the water/magma ratio is low (subaerial conditions?), the eruption is predominantly magmatic and results in lava flows or pumice fall and flow deposits. With increasing water/magma ratios (available ground water?), the water is flashed to steam and expands rapidly resulting in highly energetic and inflated base surge eruptions of superheated steam and ash with associated ash falls. These result in the deposition of well-bedded, fine-grained ash and lapilli as a tuff ring. Higher water/magma ratios (shallow surface water?) result in less energetic eruptions of water-saturated surges and ash falls (and possibly vent lahars) that deposit thick, massive ash beds as tuff cones. At very high water/magma ratios (deep water?), relatively passive eruptions occur that deposit pillow lavas and hyaloclastites (Wohletz and Sheridan, 1983; Osterberg, 1985).

As stated previously, the hyalotuffs in the map area exhibit characteristics similar to those of tuff rings (Sheridan and Wohletz, 1983; Heiken, 1971). Formation of a tuff ring indicates that the hydrovolcanic eruption occurred at a low water/magma ratio (Wohletz and Sheridan, 1983).

Penecontemporaneous with the hydrovolcanism, the Gagne Lake prospect was formed by the precipitation of sulfides

in a subaqueous environment from a hydrothermal system. Such systems usually invove evolved sea water (Franklin et al., 1981). During formation of the prospect, the rocks were hydrothermally altered. (Franklin et al., 1981). The presence of a volcanogenic-type massive sulfide deposit within the tuff ring indicates that deposition of the felsic bedded tuffs and lapilli tuffs, in part, occurred in a shallow subaqueous environment.

Volcanism within the study area concluded with the deposition of the mafic lava flow and chlorite-rich bedded tuff that outcrop in the northwest corner of the map area (Plate 1). The thinly bedded nature of the bedded tuff is a characteristic of volcaniclastic sedimentary rocks (Fiske and Matsuda, 1964; Pettijohn et al., 1972; Fisher and Schmincke, 1984). Coupled with the presense of volcanogenic-type massive sulfides within the bedded tuffs and lapilli tuffs stratigraphically below, the mafic lava flow and bedded tuff were deposited in a subaqueous environment.

Intrusion of sills into the volcanic succession occurred in three stages. First, the abundance of minerals (actinolite, chlorite, and iron carbonate) thought to have formed by hydrothermal alteration in the tonalite sills indicates that these units are synvolcanic and emplaced prior to deposition of the sulfide minerals.

Secondly, because the mineral assemblage of the mafic sills is characteristic of a basalt that has underegone metamorphism to the greenschist-amphibolite transition facies (Winkler, 1976; Williams, Turner and Gilbert, 1982) these sills were emplaced after hydrothermal activity ceased but prior to emplacement of the Little Ottertail Lake stock. Intrusion of the gabbro represents a final, late-stage igneous event in the map area that post-dates intrusion of the Little Ottertail Lake stock.

Although explosion breccias which commonly occur near the vents of tuff rings (Sheridan and Wohletz, 1983) are absent, the presence of block-size fragments within the bedded tuffs and lapilli tuffs, and the presence of tonalite sills that, based on similar mineralogy, may be genetically related to the rhyolite lava flows they intrude indicates that the volcanic stratigraphy of the Gagne Lake area represents a near-to-medial source facies (Williams and McBirney, 1979; Fisher and Schmincke, 1984). The center of volcanism for the area has been interpreted to be northwest of the field area near Mine Centre (Poulsen, 1982).

Units of pillowed basalt and pillowed intermediate volcanics have been mapped in the Fort Frances-Mine Centre area and outcrop stratigraphically above and below the rocks of the study area (Fig. 3). Pillowed flows

indicate that these horizons formed in a subaqueous environment (Ballard and Moore, 1977). This progression of subaqueous lava flows through a sequence of subaerial rhyolite lava flows, hydrovolcanic rocks and back into subaqueous volcanic rocks with interbedded sedimentary rocks (Fig. 3) is evidence that the rocks of the Gagne Lake area were part of an emergent volcanic island (island arc?) built up on a platform of subaqueous volcanic rocks which subsided by volcano-tectonic processes with continued eruption (Williams and McBirney, 1979; Fisher and Schmincke, 1984).

III. HYDROTHERMAL ALTERATION

INTRODUCTION

The Gagne Lake prospect is a volcanogenic-type massive sulfide deposit of sub-ore grade that is stratabound within units of bedded and lapilli-rich tuffs. Mineralization at the main pit (L80E, Plate 1) occurs in two stratiform zones 10 to 20 cm wide. Sulfide mineralization consists of sphalerite, pyrite, and chalcopyrite with associated galena and malachite. The two zones of mineralization are separated by 3 to 5 meters of hydrothermally altered rock; contacts with the sulfides are gradational.

Rocks at the Gagne Lake prospect have been variably altered by hydrothermal solutions. Hydrothermally altered rocks are here defined as those containing actinolite, chlorite, epidote, sericite, biotite or iron carbonate in modal abundances that are inconsistant with primary igneous or greenschist-amphibolite facies metamorphic minerals for the rock type altered.

Distribution and geochemistry (mineralogy) of altered rocks is such that four distinct assemblages can be defined: a) a least altered rock assemblage, b) a sericite/biotite, chlorite and iron carbonate assemblage and c) an actinolite, chlorite, and epidote assemblage, and d) dalmatianite. Alteration assemblages b and c will

be referred to as the sericite or biotite and actinolite assemblages respectively. A spotted alteration, locally referred to as dalmatianite (Franklin et al., 1981), is present in the area of the prospect (Plate 2). This alteration is characterized by a porphyroblastic ("spotted") texture and is mineralogically composed of sericite, chlorite and iron carbonate. Although the mineralogy of the dalmatianite is similar to the sericite assemblage, the two have been separated on the basis of the porphyroblastic texture and alteration geochemistry (Chapter IV).

GEOMETRY of ALTERATION ZONES

Distribution of hydrothermally altered rocks in the study area is shown on plate 2 (back jacket). The alteration assemblages form a concentric pipe-like alteration zone beneath the Gagne Lake prospect which becomes stratigraphically semi-conformable upwards within the bedded tuffs and lapilli tuffs (Plate 2). The alteration pipe consists of a core of actinolitic alteration that is enveloped by sericitic or biotitic alteration. Within the bedded tuffs and lapilli tuffs, the stratigraphically conformable alteration consists of a zone of dalmatianite that is surrounded by sericitic alteration. Contacts between different alteration zones are gradational.

In addition to the alteration pipe, isolated patches of sericitic alteration occur stratigraphically below the Gagne Lake prospect within the rhyolite lava flows.

ALTERATION ASSEMBLAGES

Least Altered Assemblage

Rocks considered to be least altered are those in which the mineralogy is predominantly metamorphic or igneous in origin. Least altered felsic rocks are composed of quartz, plagioclase (albite and andesine) and biotite with lesser amounts of cordierite, sphene, magnetite and apatite. In the mafic rocks, hornblende, andesine, chlorite, epidote and sphene make up the metamorphosed sills and lava flows whereas augite, plagioclase, epidote, ilmenite, and chlorite occur in the gabbro. For more detailed analyses, the reader is referred to chapter two of this study as the rock descriptions are based primarily on the least altered rocks.

Sericite/Biotite Assemblage

(sericite or biotite, chlorite, iron carbonate)

This alteration assemblage is the most widespread and occurs below the Gagne Lake prospect either enveloping the actinolitic alteration, to form the outer margins of the alteration pipe, or as patches of alteration within the rhyolite lava flows. Within the bedded tuffs and

lapilli tuffs, sericitic alteration forms a broad, semiconformable zone. In outcrop, sericitic alteration imparts a foliation and pale greenish-gray color to the rock.

The mineralogy of this assemblage is dependant upon the rock type altered, but the alteration chemistry (Chapter IV) is, essentially, the same. In the felsic volcanic rocks, sericite is the dominant alteration mineral (10-45%) with lesser amounts of chlorite (1-15%) and iron carbonate (1-6%) (Fig. 21). In the tonalite sills and mafic lava flow, biotite (15-40%) and chlorite (10-40%) are predominant giving these units a spilitized appearance while sericite (1-7%) is virtually absent (Fig. 22). Iron carbonate comprises 1 to 6% of the biotite-rich rocks.

X-ray diffraction analysis indicates that the chlorite species varies in composition from penninite to ferroan clinochlore or possibly ripidolite (Berry, 1974; Switzer, 1977) with the iron-rich species (ripidolite) occurring in the biotite-rich rocks. X-ray diffraction analysis also detected the presence of cordierite (<10%) in some rhyolite lava flow samples. Using chemical staining techniques developed by Freidman (1959) and Evamy (1962), the iron carbonate species was determined to be ferroan dolomite or ankerite.

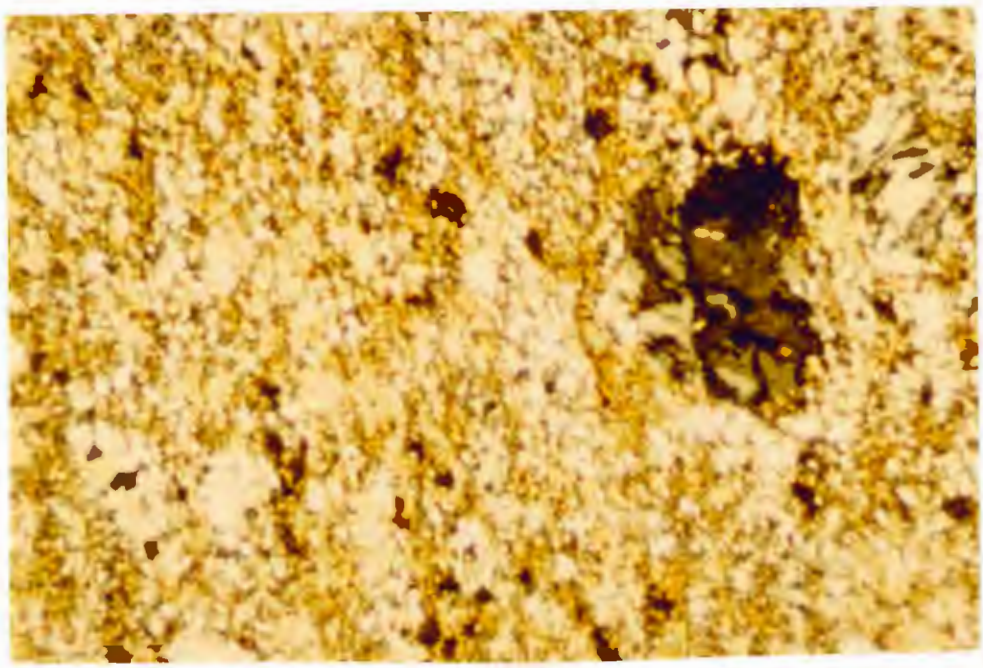

Figure 21. Photomicrograph of sericitic alteration in amygdaloidal rhyolite lava flow. Fine-grained matrix is intensely altered to sericite while phenocryst is altered along crystal edge only. Crossed polars, field of view 5x7mm.

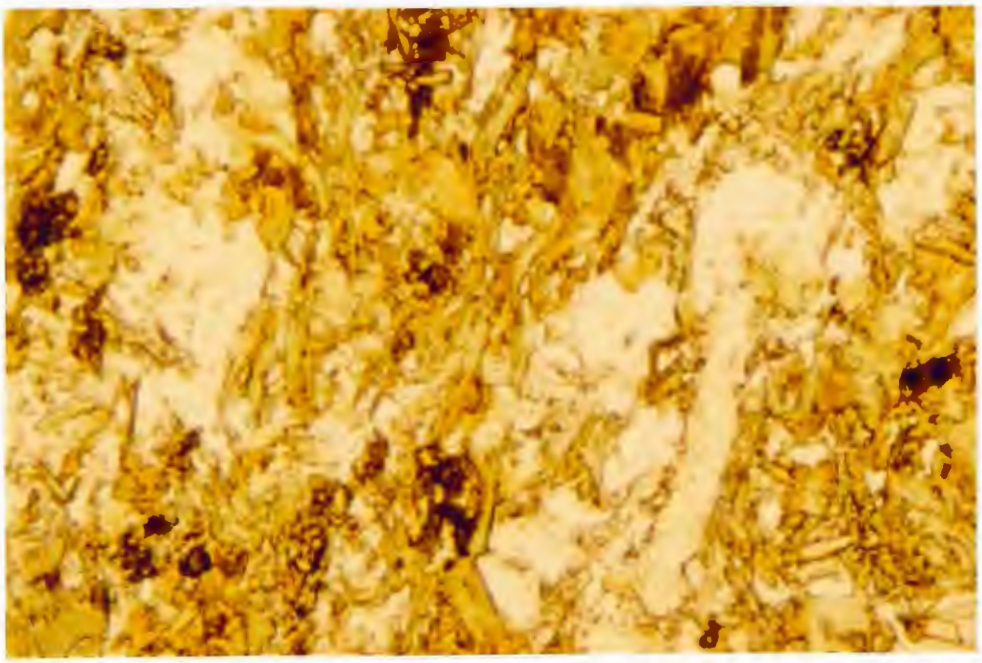

Figure 22. Photomicrograph of biotitic alteration in tonalite sill. Plane polarized light, field of view 5x7mm.

In felsic volcanics, sericite occurs as disseminations, in veinlets that may exhibit crenulations, or as a replacement mineral of plagioclase. The disseminated and veinlet sericite is subparallel to the flow banding or foliation. Biotite (10-15%) in sericite-rich rocks occurs as small clots or veinlets intergrown with chlorite or as a black "grunge" of indistinguishable minerals.

In the mafic rocks, biotite and chlorite occur as intergrown euhedral to fibrous grains or as veinlets subparallel to the bedding or foliation. Interstitial to the biotite and chlorite, clusters of fine-grained epidote (1-15%) occur. Sericite in biotite-rich rocks occurs disseminated throughout, typically as a replacement of plagioclase.

Quartz is ubiquitous to both sericite and biotite-rich rocks (Appendix I) and occurs as anhedral grains in the matrix or, in the felsic volcanics, as a phenocryst.

Ferroan dolomite/ankerite is usually intergrown with masses of sericite or biotite and chlorite but pseudomorphs of iron carbonate after plagioclase and carbonate veinlets do occur.

In thin section, the ferroan dolomite/ankerite is stained by a dark, nearly opaque brown material that is pervasive or controlled by the cleavage. This material is

interpreted to be a mixture of iron oxides and hydroxides (Groves, 1984).

Sericitic alteration in felsic volcanics is preferential in nature. Within the bedded and lapilli-rich tuffs, the recrystallized ash-size matrix is intensely altered; lithic fragments are generally altered only along their edges whereas pumice fragments may be completely altered. In the rhyolite lava flows, the amygdaloidal portions of the flow tend to be altered with more intensity than massive portions. Except for iron carbonate pseudomorphs, plagioclase phenocrysts typically show only a slight alteration along crystal edges (usually sericitization), and quartz phenocrysts are unaltered. Biotitic alteration in the mafic rocks is pervasive.

Actinolite Assemblage

(actinolite, chlorite, epidote $\pm$ iron carbonate)

A zone of actinolitic alteration occurs below the Gagne Lake prospect, cross-cuts stratigraphy and forms the core of the alteration pipe. Smaller patches of actinolite-rich rocks occur within the alteration pipe separated from the main area of actinolitic alteration by sericite or biotite-rich rocks. These patches are confined to the felsic rocks (Plate 2). In outcrop, actinolitic alteration imparts a black color to the fresh

surface of the rock.

Actinolite is the dominant mineral of this assemblage (Fig. 23) making up 15 to 45% of the rock. The actinolite is typically bladed but may also be acicular or fibrous in habit; combinations exist in which larger grains (1.0-2.0 mm) of actinolite are bladed and display fibrous terminations. Interstitial to the actinolite is fine-grained, fibrous to massive chlorite (7-20%) that is commonly intergrown with biotite. X-ray analyses on samples from different strata show that the chlorite species range in composition from ferroan clinochlore to ripidolite (Berry, 1974; Switzer, 1977). Chlorite is green and slightly pleochroic in thin section with a dark green to gray birefringence. Epidote is ubiquitous but not necessarily abundant (3-15%). It occurs as small (<1.0 mm) euhedral grains disseminated throughout the sample or in veinlets with chlorite. Iron carbonate (0-4%) may be present as fine-grained (<1.0 mm), anhedral grains or in veinlets. Chemical staining using the techniques of Freidman (1958) and Evamy (1962) indicates that the iron carbonate may be ferroan dolomite or ankerite.

When present, plagioclase (0-15%) occurs as subhedral laths (<1.5 mm) that are corroded on crystal edges and partially replaced by sericite and/or iron carbonate. The

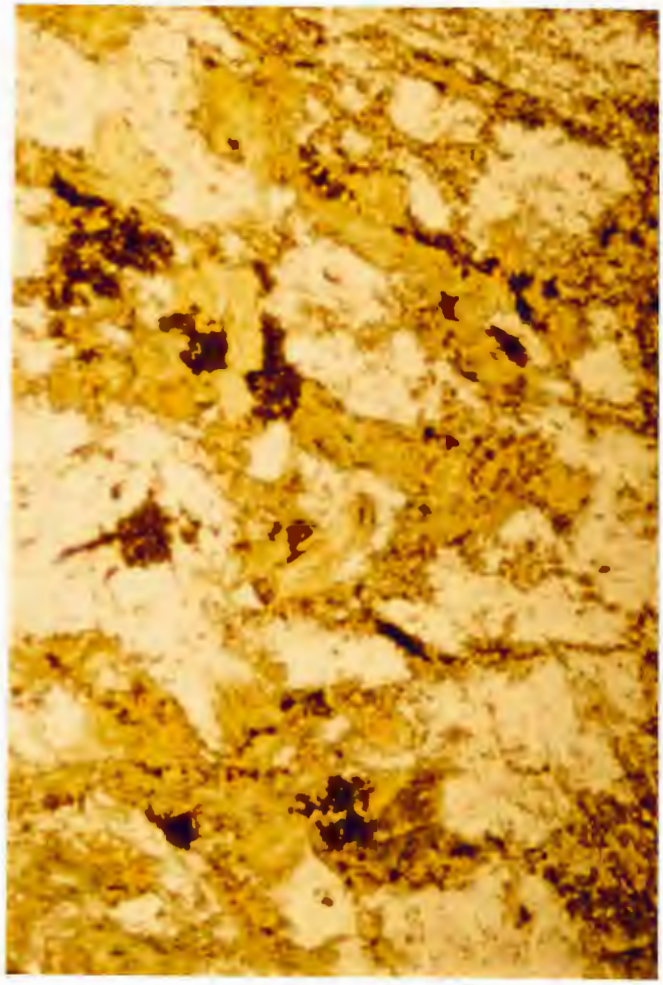

Figure 23. Photomicrograph of actinolitic alteration in tonalite sill. Bladed actinolite with quartz, chlorite and sphene. Plane polarized light, field of view 5x7mm.

amount of plagioclase is inversely proportional to the degree of hydrothermal alteration and occurs in altered tonalite sills only.

Dalmatianite

(sericite, chlorite, iron carbonate)

A small zone of dalmatianite is stratabound within the bedded tuffs and lapilli tuffs and outcrops around the sulfide showing near L80E (Plate 2). The dalmatianite is enveloped by the sericite assemblage and is centered above actinolite-rich rocks. Dalmatianite is recognized in outcrop by its porphyroblastic texture in which the porphyroblasts vary in size from a few millimeters to approximately 1.0 cm in diameter and are round to elliptical in shape (Fig. 24).

The dalmatianite is not pervasive; instead, it occurs as subround to elongated patches up to a few meters in length that are foliated on two scales. First, the long dimensions of the dalmatianite patches tend to parallel bedding, and, second, the porphyroblasts that constitute the patches also display a weak preferred orientation subparallel to bedding (Fig. 25).

Mineralogically, the dalmatianite is similar to the sericite assemblage with sericite and chlorite present in subequal amounts. The porphyroblasts are composed of fine-grained, massive sericite (80-90% of porphyroblast)

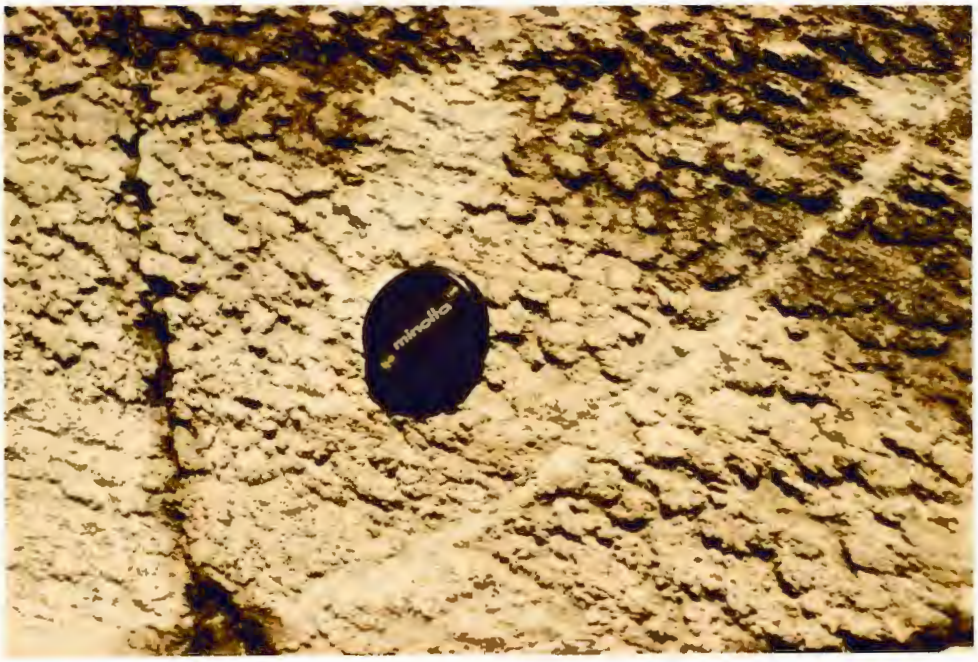

Figure 24. Dalmatianite near Gagne Lake prospect. Lens cap is 57mm in diameter.

Figure 25. Dalmatianite showing foliated nature of porphyroblasts. Bedded tuffs top to north (upper right) and bedding stikes east-west. Lens cap is 57mm in diameter.

and quartz (10-20% of porphyroblast) that are surrounded by a matrix of massive chlorite (17-50%), quartz (8-40%) and sericite (8-15%) (Fig. 26) with lesser amounts of biotite (2-12%), anthophyllite (1-3%), cordierite (0-5%) and trace amounts of tourmaline. Chlorite pseudomorphs after anthophyllite are present within the matrix.

The formation of dalmatianite is a metamorphic effect that is produced when magnesium-rich chlorite and quartz are metamorphosed to cordierite and anthophyllite at amphibolite facies conditions. The size and intensity of the porphyroblasts are directly proportional to the original amount of chlorite. (Franklin et al., 1981). Formation of cordierite and anthophyllite at the expense of chlorite and quartz during prograde metamorphism to produce dalmatianite at the Millenbach mine, Noranda, Quebec has been defined by the reaction:

$$\text{chlorite} + \text{quartz} = \text{cordierite} + \text{anthophyllite} + H_2O$$

for pressure and temperature conditions similar to those established for metamorphism in the Gagne Lake area (Riverin and Hodgson, 1980).

During retrograde metamorphism, the cordierite porphyroblasts become pinnitized to the sericite and

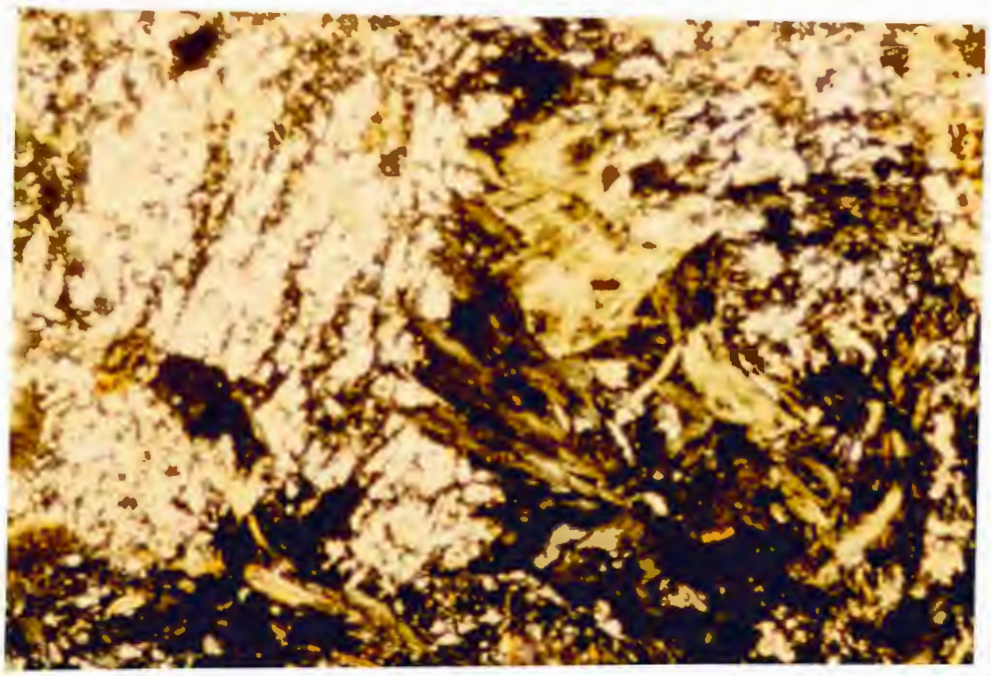

Figure 26. Photomicrograph of dalmatianite. Original porphyroblast of cordierite (left) is now pinnitized to sericite and quartz and set in a matrix of chlorite, quartz and iron carbonate. Crossed polars, field of view 5x7mm.

quartz assemblage that is now present (Franklin et al., 1981).

Besides dalmatianite, other interesting alteration effects are present in the area around the sulfide occurrence. Most dramatic of these is a pseudo or alteration breccia above the prospect in which clasts of weakly altered bedded tuff occur in a matrix of sericitic alteration. Abundant chlorite in the matrix gives the outcrop its black color (Fig. 27). Alteration breccias form in situ as the hydrothermal solution progressively alters the rock outward from the original fractures or permeable channels that it was migrating through (Nebel, 1982). The anastomosing nature of the hydrothermal solution as it passes through the rock causes formation of the clasts in a matrix of altered material. Lateral to the breccia, the alteration is pervasive (Fig. 28) suggesting that the hydrothermal solution was originally focused at the discharge site (the prospect) and underwent increasing diffusion effects as it spread out laterally.

Tourmaline (dravite) -bearing quartz veins (Fig. 29) occur near the sulfide mineralization. Smaller dravite-bearing quartz veins also outcrop near the sericitic alteration on L71E approximately 300 m north of L50N. Rosettes (<5.0 mm in diameter) of dravite occur on

Figure 27. Pseudo (alteration) breccia. Relatively unaltered clasts of bedded tuff (tan) in a matrix of altered rock. Lens cap is 57mm in diameter.

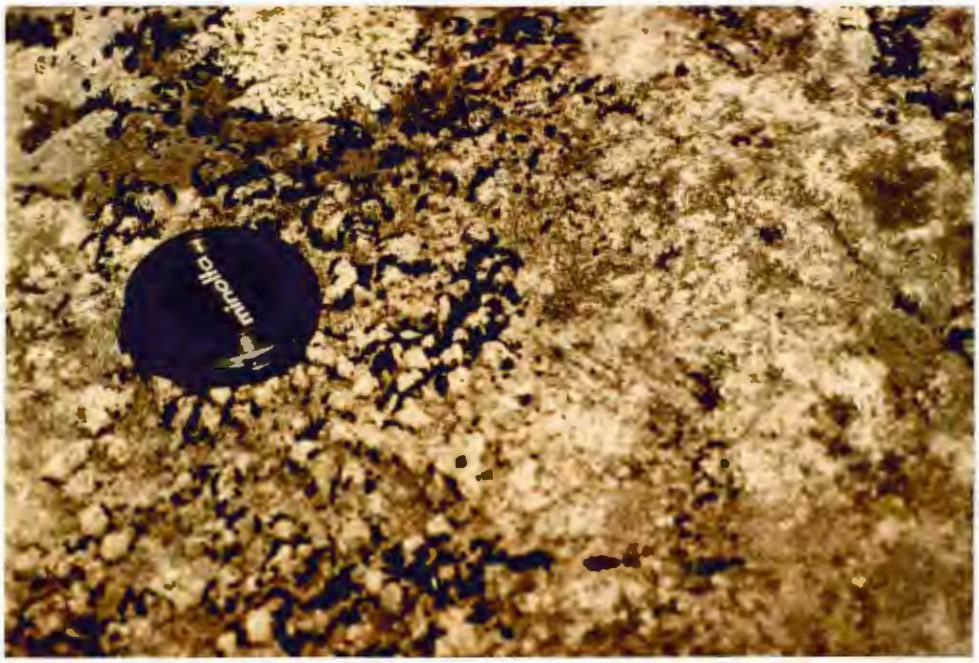

Figure 28. Pervasive alteration lateral to alteration breccia. Lens cap is 57mm in diameter.

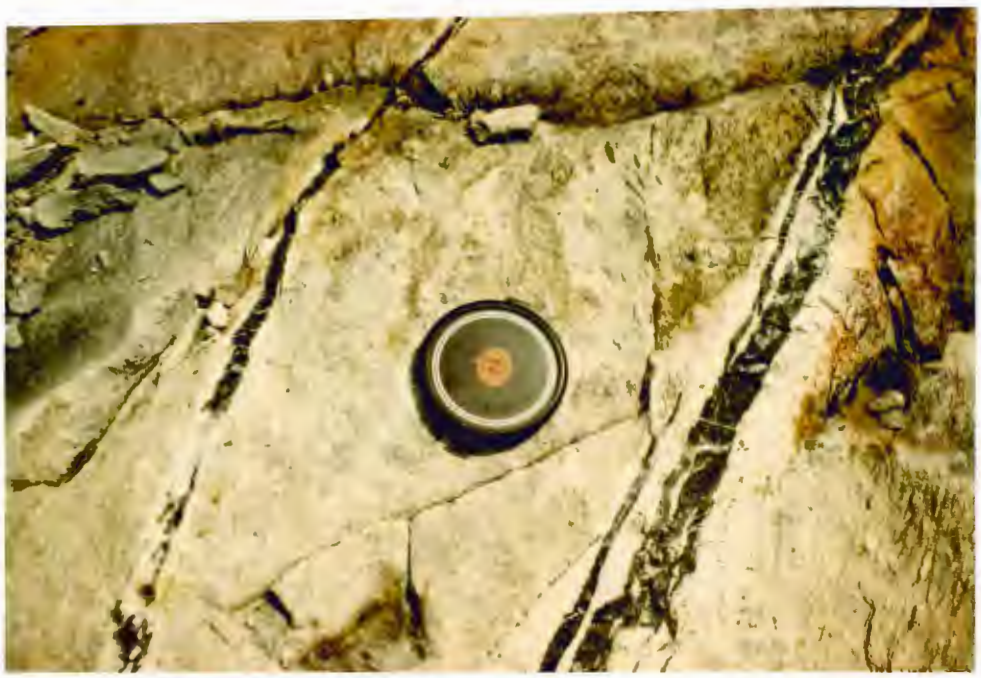

Figure 29. Dravite-bearing quartz veins near Gagne Lake prospect. Lens cap is 52mm in diameter.

outcrops of the immediate footwall rocks of the Gagne Lake prospect in close proximity to the sulfide mineralization. Although spatially associated with hydrothermally altered rocks, the actual relationship between the tourmaline and hydrothermal fluids that produced the alteration is not known.

IV. GEOCHEMISTRY

INTRODUCTION

In order to determine chemical variations within hydrothermally altered rocks of the Gagne Lake prospect and their least altered, stratigraphic equivalents, 68 samples representing the various alteration assemblages defined in Chapter III were analyzed for major oxides, 10 trace elements, H_2O and CO_2 by the Geological Survey of Canada. Concentrations of Fe^{3+} were determined from the equation: $Fe_2O_3(actual)=Fe_2O_3(XRF)-1.11134FeO$ (Osterberg, 1985). Analytical results and methods used are listed in Appendix II, and locations of chemically analyzed samples are shown on Plate 2.

MAJOR and TRACE ELEMENT GEOCHEMISTRY

Wide variations exist in many of the major and trace element abundances for similar samples from stratigraphically equivalent rock units. Table 1 shows the ranges of compositions for rock units of the study area. As a result of hydrothermal alteration, neither petrogenetic trends or chemical classifications for the rocks can be done accurately by means of standard petrochemical graphs such as AFM or Harker Variation diagrams. However, outcrops of amygdaloidal rhyolite flows that were determined to be least altered are abundant enough to allow for some comparisons to be made

Table 1.

Variations in major oxide and trace element contents for lithologic units in the study area, Fe*=total iron content. AT=bedded tuffs and lapilli tuffs, RF=amygdaloidal rhyolite lava flows, QFP=quartz feldspar porphyry, TS=tonalite sills, MF=mafic lava flow, N=nuber of samples. Major elements are given in weight percent while trace elements are givin in ppm.

	AT	RF	QFP	TS	MF
SiO_2	42.8-80.6	55.3-79.9	71.0-76.0	53.5-67.9	53.7-56.6
Al_2O_3	9.3-19.6	10.6-13.7	11.4-13.3	14.1-15.7	13.8-14.6
CaO	0.11-5.22	0.19-6.98	0.47-0.68	2.08-6.39	4.34-6.25
MgO	0.27-11.9	0.16-6.93	0.64-1.34	0.68-6.65	3.41-6.92
Na_2O	0.24-5.01	1.94-6.10	3.36-5.16	3.28-5.16	2.99-4.47
K_2O	1.11-6.37	1.31-5.62	1.39-4.06	0.32-2.15	0.51-1.15
Fe*	1.40-13.1	0.68-8.84	3.49-5.17	6.16-11.6	8.83-12.4
MnO	0.03-0.17	0.02-0.13	0.05-0.12	0.05-0.18	0.13-0.18
TiO_2	0.23-1.45	0.15-0.78	0.32-0.33	0.68-1.74	0.79-1.51
FeO	0.90-10.4	0.40-5.80	2.30-3.50	3.40-7.90	6.20-9.30
Fe_2O_3	0.40-1.54	0.23-2.39	0.93-1.21	2.27-3.37	1.92-2.06
H_2O	0.60-6.50	0.20-1.90	0.50-0.80	1.00-2.50	1.90-3.30
CO_2	0.01-0.25	0.01-0.79	0.03-0.08	0.01-1.50	0.01-1.00
Cu	0.50-1600	1.00-23.0	2.00-25.0	1.00-33.0	21.0-41.0
Zn	62-11000	31- 180	53- 140	49- 250	97- 130
Pb	2- 150	2- 28	2- 20	2- 6	2- 6
Cr	10- 40	10- 340	10- 20	10- 220	20- 340
Rb	40- 320	40- 200	70- 150	60- 130	30- 50
Sr	10- 210	10- 250	20- 30	70- 210	100- 290
Y	30- 150	10- 190	140	10- 90	10- 30
Zr	130- 620	120- 400	650- 670	120- 460	100- 120
Nb	10- 60	20- 60	30- 50	10- 30	10- 30
Ba	330-1620	390-1270	380-1200	140- 540	190- 370
N	21	19	4	18	5

between these units and other Archean rhyolite lava flows.

In general, the rhyolite lava flows of the field area are deficient in iron, particularly Fe^{2+}, magnesium, calcium, strontium, H_2O, and CO_2 and enriched in potassium and barium when compared to other Archean rhyolites in the area (Jolly, 1977; Goodwin, 1972, 1977; Gelinas et al., 1977).

Although these trends are similar to sericitic alteration (Riverin and Hodgson, 1980; Osterberg, 1985), low modal abundances of sericite (0-8%) in the least altered rocks indicates that hydrothermal alteration was not entirely responsible for these chemical trends but probably had some effect.

MASS BALANCE CALCULATIONS

In order to determine the changes in concentrations of components in hydrothermally altered rocks relative to their concentrations in least altered, stratigraphically equivalent rocks, mass balance calculations were done using the isocon method outlined by Grant (1986). The basic equation for the isocon method is:

$$C_i^A = M^O/M^A(C_i^O + \Delta C_i) \qquad (1)$$

in which:

ΔC_i=gain or loss in concentration of component i. When ΔC_i is positive, the component is gained during hydrothermal alteration; negative values indicate a loss.

M^A=mass of altered (final) sample

M^O=reference mass of original sample

C_i^A=concentration of component i in altered sample

C_i^O=concentration of component i in original sample

with concentration terms in units of mass/mass.

For each component, there is an equation of this form in which the ratio of equivalent masses before and after alteration (M^O/M^A) is constant.

For immobile components in which the change in concentration (ΔC_i) is equal to zero, M^O/M^A can be determined by solving a set of simultaneous equations of the form:

$$C_i^A=(M^O/M^A)C_i^O. \qquad (2)$$

The simultaneous equations can be solved graphically by plotting the analytical data C^A against C^O. The

immobile elements generate a straight line through the origin with a slope of M^O/M^A. This line, for which $\Delta C_i=0$, connects points of equal geochemical concentration and is referred to as an isocon (Grant, 1986; Gary et al., 1974). The isocon is defined by the equation:

$$C^A=(M^O/M^A)C^O \qquad (3)$$

and represented graphically by the best fit of a straight line through the origin and a series of data points defined by the ordered pairs (C_i^O,C_i^A) (Fig. 30).

Relative gains and losses of mobile components are determined from the displacements of representative data points for the components from the reference isocon. Components plotting above the isocon are believed to be gained during alteration while those plotting below are lost. To determine the change in concentration of a component relative to its concentration prior to hydrothermal alteration, both sides of eqation (1) are divided by C_i^O and the result rearranged to yield:

$$(\Delta C_i/C_i^O)=(M^A/M^O)(C^A/C^O)-1. \qquad (4)$$

M^A/M^O is determined from the best-fit isocon and

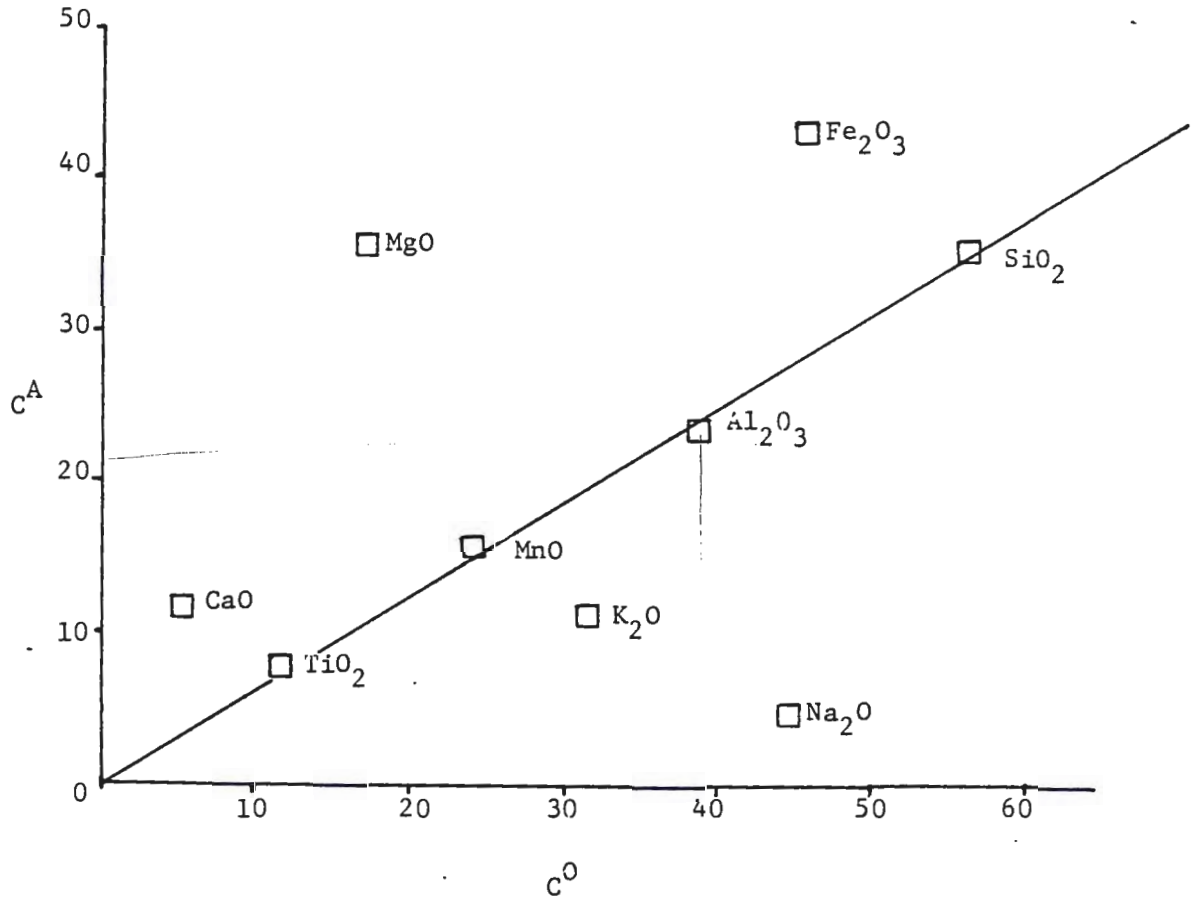

Figure 30. Example plot of C^O versus C^A for determination of gains and losses of components during alteration by the isocon method. The isocon is drawn through a near-linear array of data points, and gains and losses are determined from the displacement of a component's data point from the isocon.

equation (4) is then solved for ΔC_i to obtain the relative gain or loss of a particular component as a result of hydrothermal alteration (Grant, 1986).

If a component is assumed to be constant during alteration, equation (4) can be written as:

$$(\Delta C_i/C_i^O)=(C_x^O/C_x^A)(C_i^A/C_i^O)-1 \qquad (5)$$

with C_x^O and C_x^A representing the concentrations of the component assumed to be constant during alteration in the original and altered sample respectively. For example, if SiO_2 is assumed to be constant, then equation (5) would be written as:

$$(\Delta C_i/C_i^O)=(C_{SiO2}^O/C_{SiO2}^A)(C_i^A/C_i^O)-1 \qquad (6)$$

and ΔC_i for the mobile components would be determined from the isocon defined by the origin and SiO_2 data point. This method is also applicable when a series of components plot in a near linear array through the origin but deviate from the statistical, best-fit isocon. When such an array of data points exists, then those components can be considered immobile and used to define an isocon (Grant, 1986).

Changes in mass resulting from hydrothermal alteration

can be determined from the slope of the chosen isocon. As stated previously, the slope of the isocon yields M^O/M^A (e.g. 1.25) which is equivalent to M^A/M^O=0.80 and thus a mass decrease of 20% (Grant, 1986). Changes in mass determined this way can be used as an estimation of the volume change during alteration.

For the purpose of this study, average values for the concentrations of components from a suite of altered samples for a particular rock type (CA) will be compared to the average values for the concentrations of components from a suite interpreted to be the least altered (original), stratigraphic equivalent (CO). Table 2 shows the average values for each alteration type used in mass balance calculations. Because alumina is typically considered immobile during alteration (Morton, pers. comm.), gains and losses of components were determined using equation (5) and assuming constant Al_2O_3. Since major elements are plotted as weight percent of the oxides and trace elements as parts per million, a scale factor (shown on graphs) is used so that both can be represented on the same isocon graph with limited clustering of data points.

ALTERATION GEOCHEMISTRY

Sericitic or Biotitic Alteration

Gains and losses of components during the formation of

Table 2.

Average concentrations of components for alteration types used for mass balance calculations by means of the isocon method. Fe*=total iron content, AT=bedded tuffs and lapilli tuffs, RF=amygdaloidal rhyolite lava flows, QFP=quartz-feldspar porphyry, TS=tonalite sills, MF=mafic lava flow, N=number of samples. Major elements are given in weight percent, trace elements in ppm.

Least Altered Zone

	AT	RF	QFP	TS
SiO_2	74.53	76.85	76.00	59.77
Al_2O_3	11.90	11.92	11.70	14.46
CaO	0.39	0.72	0.68	4.27
MgO	1.67	0.34	0.68	4.40
Na_2O	4.11	4.48	5.16	4.41
K_2O	2.35	3.06	1.39	0.91
MnO	0.06	0.03	0.12	0.13
TiO_2	0.29	0.16	0.32	0.80
FeO	1.97	0.91	2.30	5.06
Fe_2O_3	1.13	0.86	0.93	2.67
H_2O	0.90	0.33	0.50	1.86
CO_2	0.01	0.04	0.01	0.02
Total	99.31	99.7	99.79	99.76
Fe*	3.32	1.87	3.49	8.30
Cu	35	7	4	25
Zn	79	62	53	149
Pb	5	4	2	2
Cr	33	16	20	126
Rb	90	102	70	30
Sr	27	58	30	156
Y	80	126	140	27
Zr	290	321	670	236
Nb	40	42	40	23
Ba	690	802	380	263
N	2	12	1	4

Table 2. continued

Sericite/biotite Alteration Zone

	AT	RF	QFP	TS	MF
SiO_2	74.05	76.33	73.15	63.65	55.07
Al_2O_3	11.0	11.93	12.35	13.35	14.17
CaO	1.03	0.49	0.70	3.44	4.77
MgO	2.01	0.44	0.99	2.10	3.94
Na_2O	1.48	3.69	3.98	4.00	3.75
K_2O	3.57	3.91	2.95	1.66	0.94
MnO	0.05	0.03	0.06	0.11	0.17
TiO_2	0.25	0.16	0.32	0.94	1.49
FeO	1.77	1.11	3.15	5.75	8.70
Fe_2O_3	1.09	0.69	2.39	2.05	2.56
H_2O	1.10	0.40	0.75	1.37	2.63
CO_2	0.06	0.14	0.06	0.52	0.42
Total	97.46	99.32	98.46	94.48	99.58
Fe*	3.06	1.94	4.68	8.45	12.23
Cu	130	10	14	17	23
Zn	945	57	113	155	123
Pb	22	7	2	3	5
Cr	10	13	15	35	20
Rb	189	120	110	70	47
Sr	80	22	20	140	173
Y	107	118	140	60	10
Zr	329	318	655	327	116
Nb	45	41	40	27	20
Ba	816	928	910	460	307
N	16	6	3	6	4

Table 2. continued

Actinolite Alteration Zone and Dalmatianite (ATD)

	RF	TS	MF	ATD
SiO_2	55.30	59.64	55.30	58.53
Al_2O_3	13.60	13.88	14.60	15.15
CaO	6.98	4.77	5.28	1.45
MgO	6.93	4.13	6.92	6.42
Na_2O	2.50	4.17	3.47	0.84
K_2O	1.31	1.11	0.51	2.43
MnO	0.13	0.13	0.15	0.12
TiO_2	0.78	1.22	0.79	1.07
FeO	5.80	5.56	6.20	6.65
Fe_2O_3	2.39	2.35	1.94	1.63
H_2O	1.90	1.60	3.10	4.12
CO_2	0.02	0.10	0.91	0.04
Total	97.64	98.66	99.17	98.45
Fe*	8.84	8.53	8.83	9.02
Cu	22	8	41	9
Zn	87	89	97	215
Pb	8	3	2	7
Cr	340	98	340	25
Rb	60	56	30	112
Sr	220	148	200	53
Y	10	19	10	58
Zr	120	180	110	302
Nb	20	25	10	27
Ba	390	304	200	720
N	1	8	1	3

sericite/biotite-rich rocks were determined by comparing least altered amygdaloidal rhyolite flow, quartz-feldspar porphyry (QFP), bedded tuff, lapilli tuff and tonalite samples with their altered, stratigraphic equivalents. Figures 31 and 32 are isocon graphs for respective rock types and Table 3 summarizes the alteration trends.

Gains and losses of components during formation of biotitic alteration of the mafic lava flow could not be calculated since least altered, stratigraphic equivalents were not exsposed in the field area.

Changes in mass during alteration determined from the isocons range from a mass increase of 9% for the bedded tuffs and lapilli tuffs to a mass decrease of 9% in the tonalite sills indicating that alteration occurred at near constant volume.

For the formation of sericite in the felsic volcanic rocks SiO_2, TiO_2, and Nb consistantly plot near the isocon indicating these components were relatively immobile during sericitization.

K_2O, Rb, Ba, MgO, CO_2, Fe* and H_2O consistently plot as components gained during sericitization. Rb is believed to have substituted for K^+ in sericite.

Na_2O, CaO and Cr plot as components lost during alteration while the remaining components exhibit no consistant pattern.

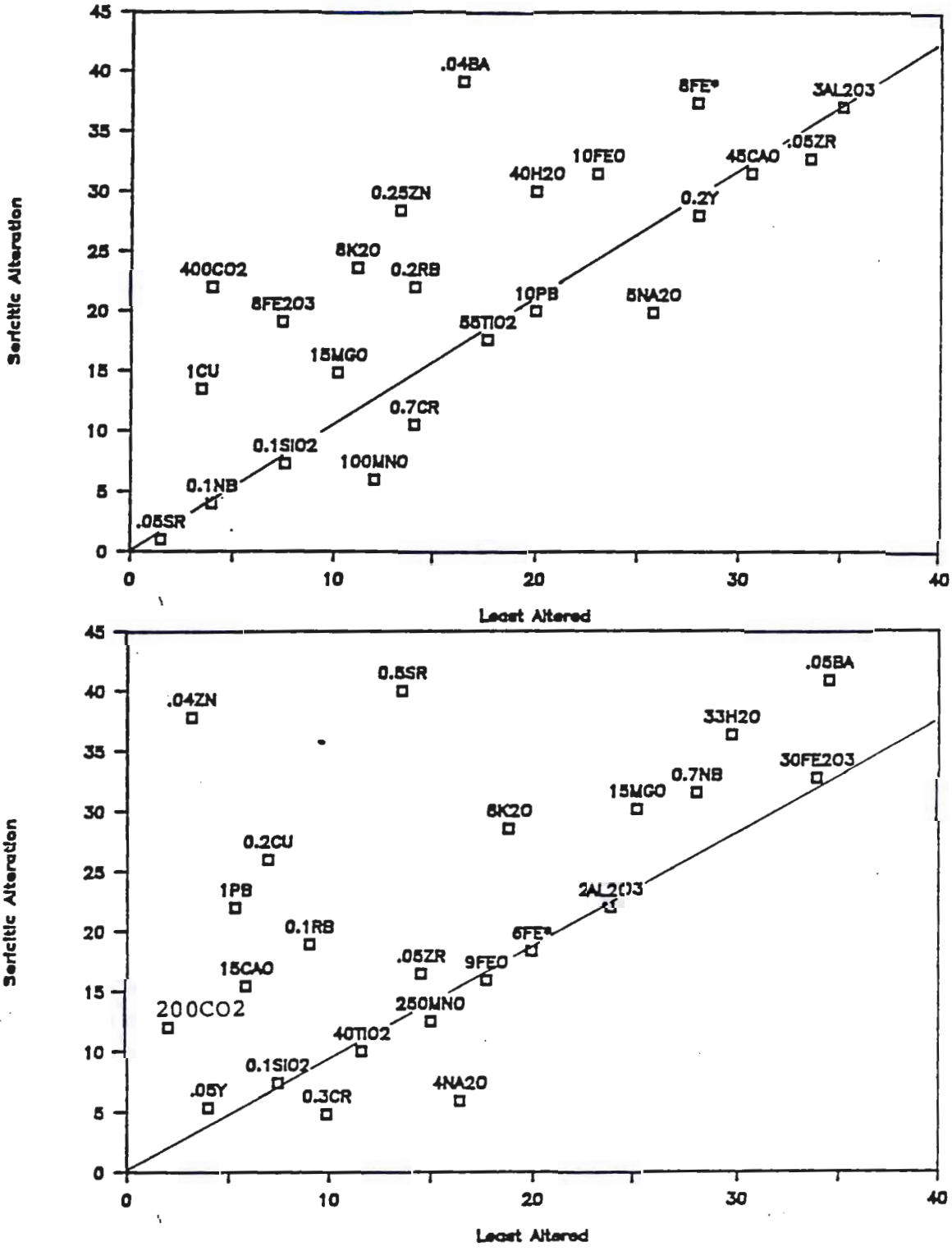

Figure 31. Isocon plots comparing least altered to sericite-rich rocks for QFP (top) and bedded tuffs and lapilli tuffs. Gains and losses of components are given in Table 3.

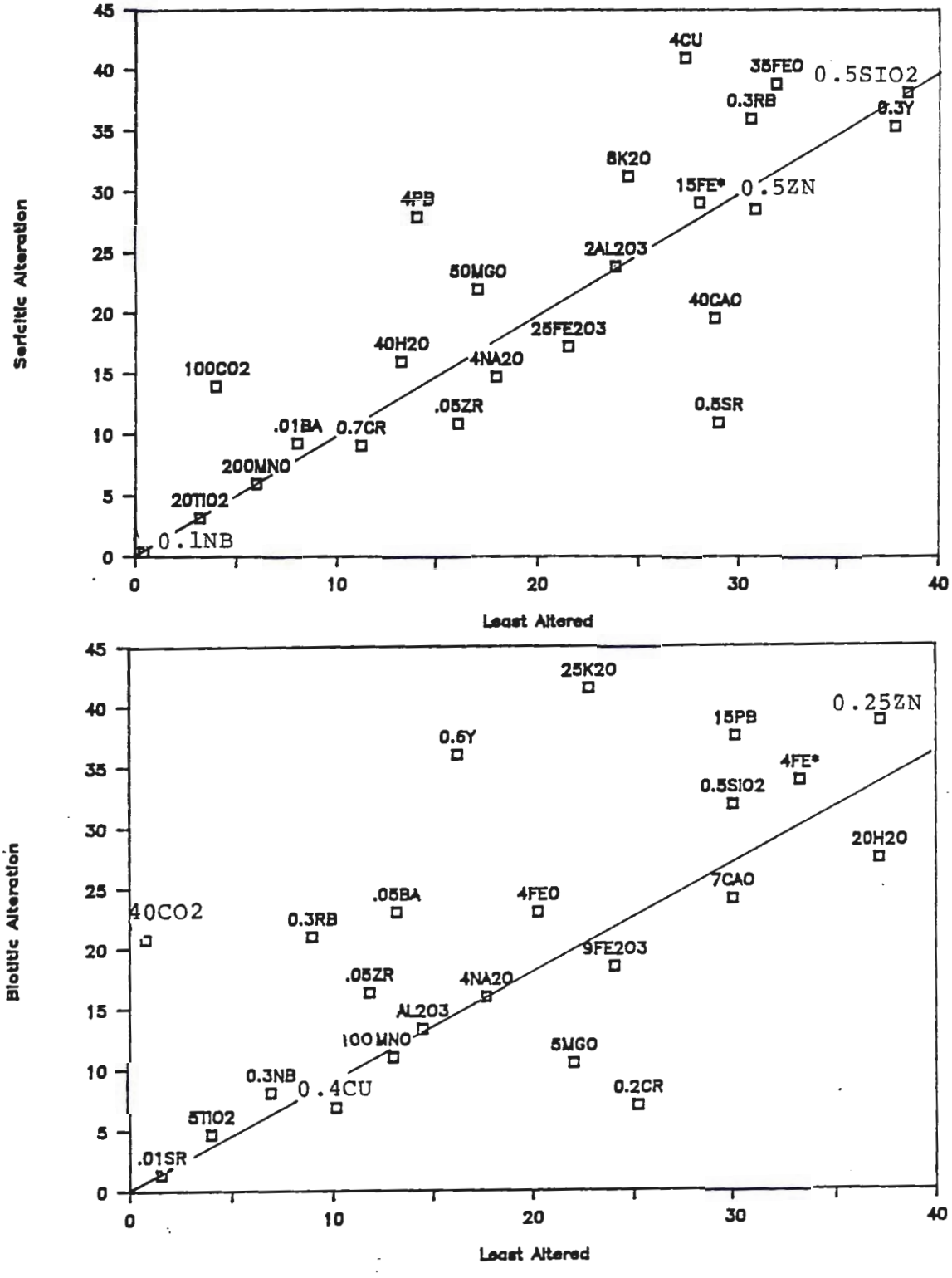

Figure 32. Isocon plots comparing least altered to sericite-rich rocks for amygdaloidal rhyolite lava flows (top) and biotite-rich rocks for tonalite sills. Gains and losses of components are listed in Table 3.

Table 3.

Gains and losses of components (ΔC_i) during formation of sericitic alteration. QFP=quartz-feldspar porphyry, AT=bedded tuffs and lapilli tuffs, RF=amygdaloidal rhyolite lava flows, TS=tonalite sills, Fe*=total iron, N_1=number of least altered samples, N_2=number of sericite-rich samples and ΔM=change in mass. Al_2O_3 assumed constant during alteration, ΔC_i is multiplied by 100 and read as a percent gain or loss relative to concentration in original (least altered) samples. Major elements are given in weight percent, trace elements in ppm.

	QFP	AT	RF	TS
SiO_2	-0.09	0.07	-0.01	0.15
Al_2O_3	0.00	0.00	0.00	0.00
CaO	-0.02	1.86	-0.32	-0.13
MgO	0.38	0.30	0.29	-0.48
Na_2O	-0.27	-0.61	-0.18	-0.02
K_2O	1.01	0.64	0.28	0.98
Fe*	0.27	0.00	0.04	0.10
MnO	-0.53	-0.10	0.00	-0.08
TiO_2	-0.05	-0.07	0.00	0.27
FeO	0.30	-0.03	0.22	0.23
Fe_2O_3	1.43	0.04	-0.20	-0.17
H_2O	0.42	0.32	0.21	-0.20
CO_2	4.21	5.49	2.50	27.16
Cu	2.65	3.06	0.50	-0.27
Zn	1.03	11.94	-0.07	0.13
Pb	-0.05	3.47	1.00	0.35
Cr	0.29	-0.48	-0.19	-0.70
Rb	0.49	1.27	0.18	1.53
Sr	-0.37	2.21	-0.62	-0.03
Y	-0.05	0.45	-0.06	1.41
Zr	-0.07	0.23	-0.32	0.50
Nb	-0.05	0.22	-0.02	0.27
Ba	1.27	0.28	0.16	0.89
ΔM	-6%	9%	0	-9%
N_1	1	2	12	4
N_2	3	16	6	6

Formation of sericite-rich rocks is typically attributed to the breakdown of plagioclase feldspar by base leaching reactions during alteration (Riverin and Hodgson, 1980; Morton and Nebel, 1984; Osterberg, 1985). Plagioclase species in least altered felsic volcanics were determined to be albite (groundmass) and andesine (phenocrysts). Morton and Nebel (1984) define the breakdown of albite to form sericite by the reaction:

$$\underset{\text{albite}}{NaAlSi_3O_8} + 0.33K^+ + 0.67H^+ = \underset{\text{sericite}}{0.33KAl_3Si_3O_{10}(OH)_2} + \underset{\text{quartz}}{2SiO_2} + Na^+ \qquad (7)$$

While sericitization of andesine can occur by the reaction:

$$\underset{\text{andesine}}{Ca_{0.5}Na_{0.5}Al_{1.5}Si_{2.5}O_8} + 0.50K^+ + H^+ = \underset{\text{sericite}}{0.50KAl_3Si_3O_{10}(OH)_2} + \underset{\text{quartz}}{SiO_2} + 0.5Na^+ + 0.5Ca^{2+} \qquad (8)$$

Addition of MgO to the rocks during alteration resulted in the formation of the magnesian chlorites (penninite, ferroan clinochlore) determined by X-ray diffraction analysis. Morton and Nebel (1984) suggest

that chlorite can develop as a result of destruction of albite that was not converted to sericite by the reaction:

$$\underset{\text{albite}}{NaAlSi_3O_8} + 2.5(Mg, Fe)^{2+} + \underset{\text{quartz}}{0.32SiO_2} + 7.63H_2O = \underset{\text{chlorite}}{0.5(Mg, Fe)_5Al_2Si_3O_{10}(OH)_8} + 4H^+ + 1.82H_4SiO_4 + Na^+. \quad (9)$$

The intergrown nature of chlorite and biotite observed in thin sections of altered rocks and the presence of biotite in least altered samples suggests that chlorite may also have formed as a replacement of biotite. As an example, a hypothetical, iron-rich biotite can alter to a hypothetical, magnesium-rich chlorite by the reaction:

$$\underset{\text{biotite}}{KMgFe_2AlSi_3O_{10}(OH)_2} + Mg^{2+} + 2H^+ = \underset{\text{chlorite}}{0.5Mg_4Fe_1Al_2Si_3O_{10}(OH)_8} + K^+ + \underset{\text{quartz}}{1.5SiO_2} + 1.5Fe^{2+}. \quad (10)$$

The chlorite composition in this reaction (Phillips and Griffen, 1981) is similar to compositions of chlorites in the sericitic alteration zone as determined by X-ray

diffraction analyses.

Addition of CO_2 and FeO to the rocks resulted in the formation of feroan dolomite or ankerite. Loss of calcium during alteration suggests that iron carbonates may have formed as a replacement of preexisting, diagenetic calcite.

Within the tonalite sills, addition of potassium and iron resulted in the formation of biotite rather than sericite. Chemically the most significant difference between the sericite and biotite alteration is the loss of significant amounts of water during the formation of biotite.

Biotite can also form from the alteration of andesine, by the reaction:

$$\overset{\text{andesine}}{Ca_{0.5}Na_{0.5}Al_{1.5}Si_{2.5}O_8} + 1.5K^+ + 4.5(Mg, Fe)^{2+} + 3H_4SiO_4 = \overset{\text{biotite}}{1.5K(Mg,Fe)_3AlSi_3O_{10}(OH)_2} + 0.5Ca^{2+} + 0.5Na + \overset{\text{quartz}}{SiO_2} + 9H^+. \quad (11)$$

The intergrown nature of chlorite and biotite suggests that chlorite in this assemblage may represent a metamorphic mineral that formed at the expense of biotite by a reaction similar to reaction (10).

Because a least altered, stratigraphic equivalent is not exposed in the map area, mass balance analysis for the formation of biotite in the mafic lava flow was not possible. However, it is reasonable to assume that biotite may have formed from the breakdown of plagioclase at least as calcic as andesine.

Actinolitic Alteration

Spatial distribution of the alteration zones indicates that the actinolite-rich rocks crosscut and, therefore, formed at the expense of sericite-rich and biotite-rich rocks. In order to analyze geochemical trends associated with the formation of actinolitic alteration, mass balance computations were done by comparing sericitized samples from amygdaloidal rhyolite lava flows, and biotite-rich samples from the tonalites and the mafic lava flow with their actinolite-rich, stratigraphic equivalents. Figures 33 and 34 represent isocon graphs for actinolitic alteration, and alteration trends are summarized in Table 4.

Mass changes determined from the isocons range from a mass decrease of 2.9% for the mafic lava flow to a mass decrease of 12.3% for the rhyolite lava flows indicating that a small volume loss may have occurred during alteration.

MnO and Sr consistantly plot near the isocon

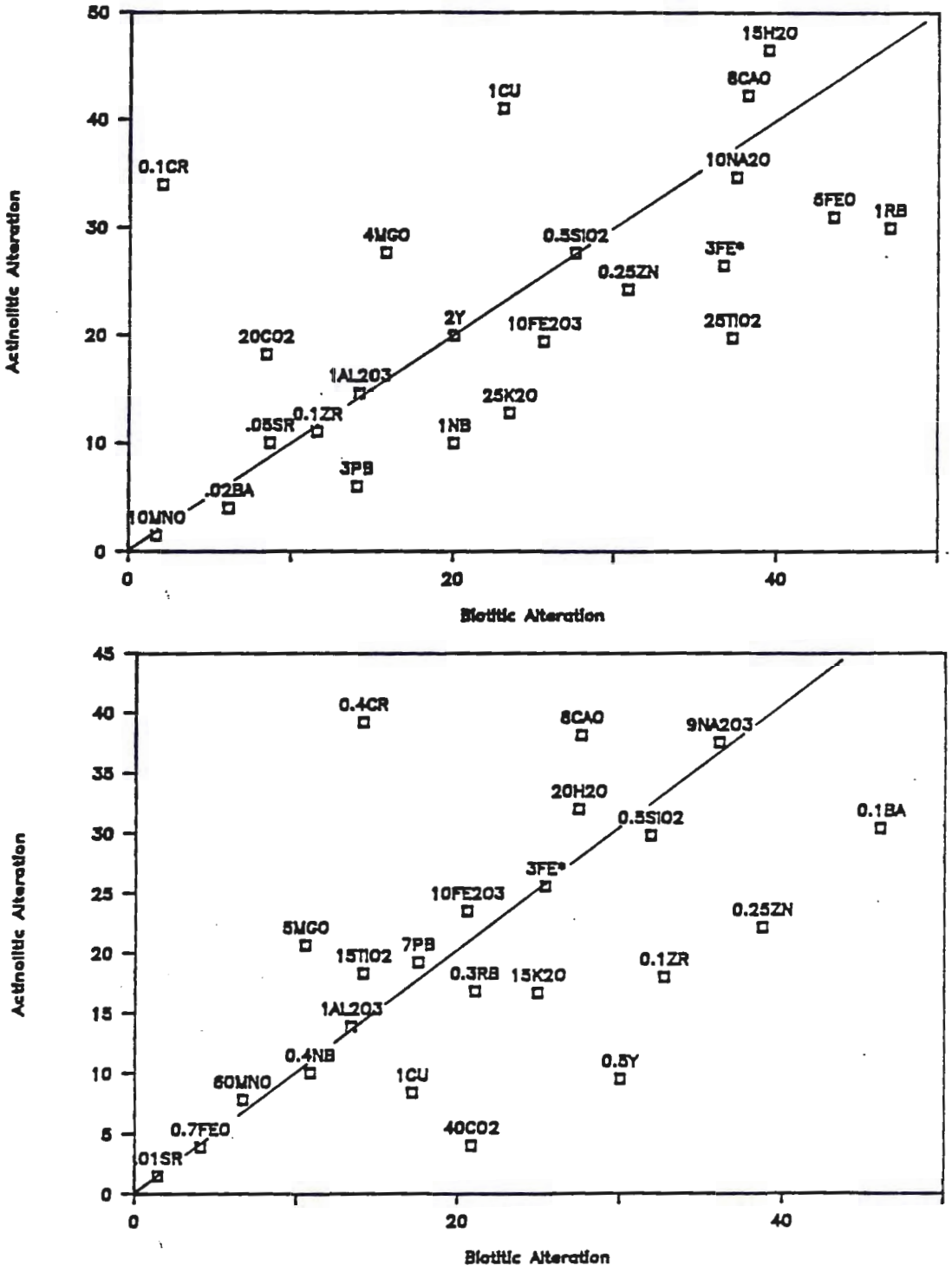

Figure 33. Isocon plots comparing biotite-rich rocks to actinolite-rich rocks for the mafic lava flow (top) and tonalite sills. Gains and losses of components are given in Table 4.

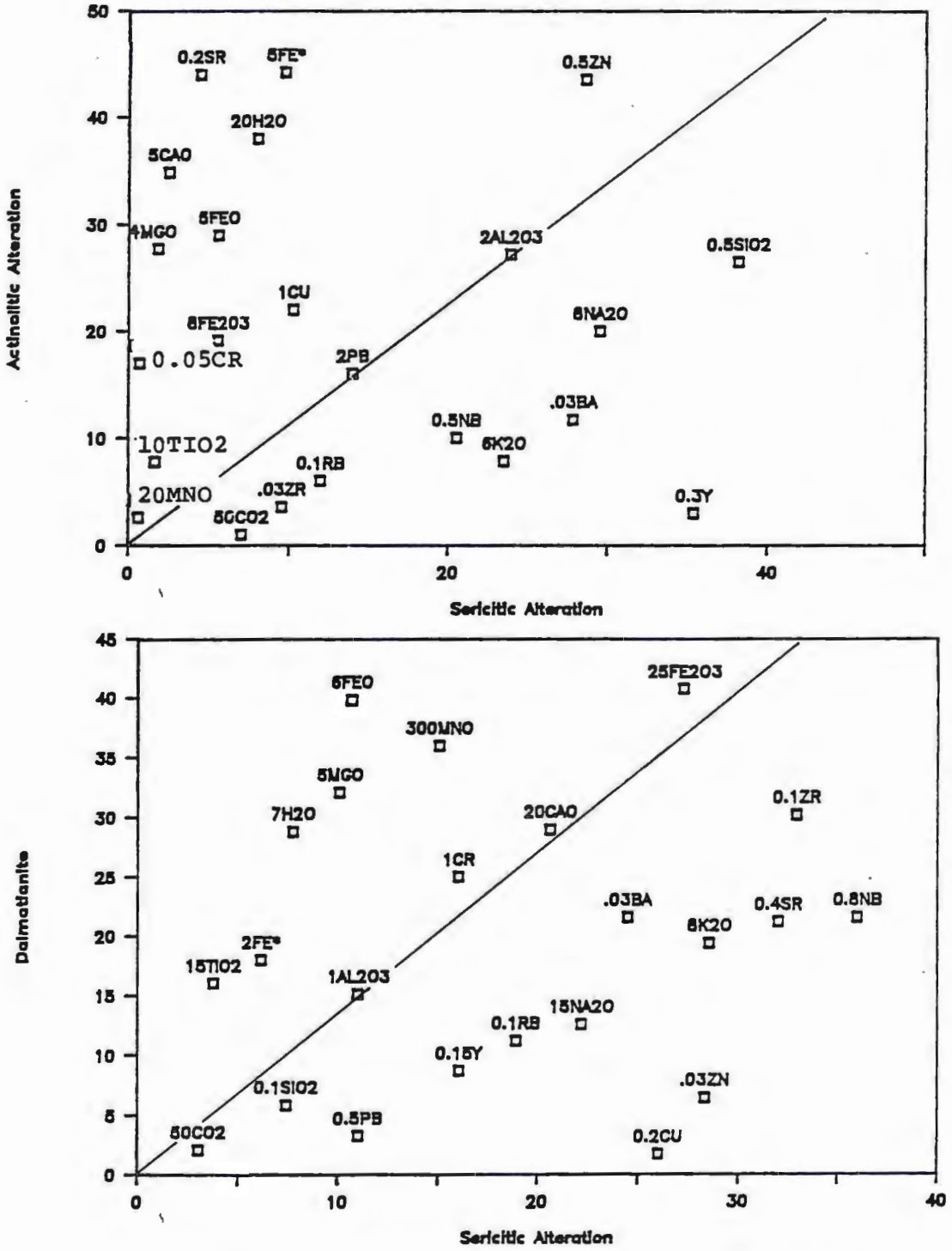

Figure 34. Isocon plots comparing sericite-rich rocks to actinolite-rich rocks for amygdaloidal rhyolite lava flows (top) and to dalmatianite for bedded tuffs and lapilli tuffs. Gains and losses of components are given in Table 4.

Table 4.

Gains and losses of components (ΔC_i) during formation of actinolitic alteration in mafic lava flow (MF), tonalite sills (TS), and amygdaloidal rhyolite lava flows (RF), and formation of dalmatianite in bedded tuffs and lapilli tuffs (AT). N_1=number of sericite-rich (original) samples, N_2=number of actinolite-rich or dalmatianite samples, ΔM-change in mass during alteration. Al_2O_3 assumed constant during alteration, ΔC_i is multiplied by 100 and read as a percent gain or loss relative to concentration in original (least altered) samples. Major elements are given in weight percent, trace elements in ppm.

	MF	TS	RF	AT
SiO_2	-0.03	-0.10	-0.39	-0.43
Al_2O_3	0.00	0.00	0.00	0.00
CaO	0.07	0.33	11.50	0.02
MgO	0.07	0.89	12.82	1.32
Na_2O	-0.10	0.00	-0.41	-0.59
K_2	-0.47	-0.36	-0.71	-0.51
Fe*	-0.30	-0.03	3.00	1.41
MnO	-0.14	0.14	2.80	0.74
TiO_2	-0.49	0.25	3.28	2.11
FeO	-0.31	-0.07	3.58	1.73
Fe_2O_3	-0.26	0.10	2.04	0.09
H_2O	0.41	0.12	3.17	1.72
CO_2	1.10	-0.82	-0.87	-0.49
Cu	0.73	-0.53	0.88	-0.95
Zn	-0.24	-0.45	0.33	-0.83
Pb	0.58	0.06	0.00	-0.79
Cr	15.50	1.69	21.94	0.13
Rb	-0.38	-0.23	-0.56	-0.57
Sr	0.12	0.02	7.77	-0.52
Y	-0.03	-0.70	-0.93	-0.61
Zr	-0.08	-0.47	-0.67	-0.33
Nb	-0.51	-0.11	-0.57	-0.56
Ba	-0.37	-0.36	-0.63	-0.36
ΔM	-2.9%	-3.85%	-12.3%	-27.5%
N_1	4	6	6	16
N_2	1	8	1	3

indicating that these components, along with Al_2O_3, were relatively immobile during formation of actinolite-rich rocks.

The most striking geochemical trend is addition of large amounts of CaO, as well as MgO, Fe_2O_3 and H_2O with or without FeO and loss of K_2O and Rb. This is attributed to the formation of actinolite at the expense of sericite and biotite by base fixing reactions. Cr is also added during alteration and assumed to substitute for Fe^{2+} and Mg^{2+} in actinolite and Fe^{3+} in magnetite. CO_2 loss is attributed to decarbonization during alteration and/or metamorphism and represented in thin section by the virtual absence of iron carbonate in actinolite-rich rocks. SiO_2, Na_2O, Zr, Ba, and Y typically plot as components lost whereas TiO_2 and Sr plot as components gained.

During hydrothermal alteration, actinolite and epidote can form directly from sericite by the reaction:

$$\underset{\text{sericite}}{KAl_3Si_3O_{10}(OH)_2} + 5(Mg, Fe)^{2+} + 5Ca^{2+} + \underset{\text{quartz}}{9.5SiO_2} + 12.5H_2O = \underset{\text{actinolite}}{Ca_2(Mg, Fe)_5Si_8O_{22}(OH)_2} + \underset{\text{epidote}}{1.5Ca_2Al_2FeSi_3O_{12}(OH)} + K^+ + 23.5H^+. \quad (12)$$

or from biotite by the reaction:

$$\underset{\text{biotite}}{K(Mg,Fe)_3AlSi_3O_{10}(OH)_2} + 2.2Ca^{2+} + \underset{\text{quartz}}{0.5Fe^{3+} + 3.3SiO_2} + 2.3H_2O = \underset{\text{actinolite}}{0.6Ca_2(Mg,\ Fe)_5Si_8O_{22}(OH)_2} + \underset{\text{epidote}}{0.5Ca_2Al_2FeSi_3O_{12}(OH)} + K^+ + 4.9H^+ \qquad (13)$$

From the isocon graphs it is readily perceived that total iron as either Fe_2O_3 or FeO is not necessarilly gained in large quantities and may actually be lost during alteration. Combined with the weak pleochroism of the actinolite observed in thin section, these geochemical trends indicate that the actinolite is a low-iron variety near the composition of the tremolite ($Ca_2Mg_5Si_8O_{22}(OH)_2$) end member of the tremolite-ferroactinolite solid solution series.

Addition of MgO and FeO resulted in the formation of chlorite. Chlorite can form at the expense of sericite, possibly by the reaction:

$$\underset{\text{sericite}}{KAl_3Si_3O_{10}(OH)_2} + 7.5(Fe, Mg)^{2+} + \underset{\text{quartz}}{1.5SiO_2} + 12H_2O = \underset{\text{chlorite}}{1.5(Mg, Fe)_5Al_2Si_3O_{10}(OH)_8} + K^+ + 14H^+. \quad (14)$$

Chlorite could have formed from biotite by a reaction similar to reaction (9).

Dalmatianite

Field relationships indicate that dalmatianite formed at the expense of the sericite-rich bedded tuffs and lapilli tuffs. To determine geochemical trends for the formation of dalmatianite, sericitized bedded tuffs and lapilli tuffs were compared with stratigraphically equivalent dalmatianite samples to produce an isocon graph (Fig. 34). Alteration trends are summarized in Table 4.

A mass decrease of 27.5% determined from the isocon indicates that, compared to the other alteration types, a relatively large volume decrease occurred during the formation of dalmatianite.

Cr and CaO plot near the isocon and are considered to be relatively immobile during alteration.

Major geochemical trends are the addition of MgO, Fe* (as FeO and Fe_2O_3) and H_2O while K_2O and Rb,

SiO_2 and CO_2 are lost. Na_2O, Y, and Nb are also lost whereas TiO_2 is gained.

Dalmatianite is believed to have formed at the expense of sericite-rich rocks. Because dalmatianite also forms from prograde metamorphism of chloritic alteration (Franklin et al., 1981), it is reasoned that the additions of MgO, Fe* and H_2O represent the formation of an initial chlorite-rich alteration zone metamorphosed to dalmatianite (anthophyllite and cordierite).

Chlorite could have formed at the expense of sericite as defined by equation (14) or by the breakdown of albite that was not converted to sericite during alteration as defined by equation (9). Subsequent prograde metamorphism to the greenschist-amphibolite transition facies formed the dalmatianite by the reaction given in Chapter III.

MgO and FeO not partitioned into chlorite can be accommadated with CaO in the ferruginous dolomite/ankerite present in this alteration zone.

V. ALTERATION MODEL

Hydrothermal alteration associated with the formation of volcanogenic-type massive sulfide deposits results from the interaction of hydrothermal solutions circulating in a geothermal system (Franklin et al., 1981). A heat source at depth, such as a subvolcanic pluton, is thought to drive the convective circulation of the fluids through permeable rocks and along fracture systems by establishing a steep temperature gradient (Franklin and Thorpe, 1982; Reed, 1984). Isotopic studies (Hutchinson, 1982) indicate that the fluids are of sea water origin, but contributions from connate and magmatic sources cannot be excluded (Franklin et al., 1981).

By combining the above characteristics with the mineralogy, chemistry and distribution of the alteration zones, a geothermal system capable of producing the alteration at the Gagne Lake prospect can be reconstructed.

A heat source at depth, probably related to volcanism, initiated convective circulation of sea water throughout the volcanic succession of the Fort Frances-Mine Centre area. At shallow depths (<2 km), circulating sea water would react with felsic volcanic rocks in the upper portion of the volcanic succession. Chemical reactions between heated (200-300 ^{o}C) sea water and rhyolitic

volcanic rocks on the descending limb of the convection system would result in the addition of magnesium and sodium to the rocks while the solution would evolve into an acidic ($pH \leq 5$) brine enriched in potassium, iron and possibly calcium. pH of the fluid decreases as magnesium is withdrawn as $Mg(OH)_2$ generating H^+ (Hajash and Chandler, 1981; Dickson, 1977; Mottl, 1983)). Additions of calcium to solution are balanced by precipitation of anhydrite; therefore, a net gain of calcium need not occur (Hajash and Chandler, 1981; Dickson, 1977; Mottl, 1983). Although sea water becomes depleted in magnesium during these chemical reactions, substantial amounts can remain in solution at sufficiently high water/rock ratios (Hajash and Chandler, 1981).

In the proposed model, downward circulation of sea water occurred predominantly outside the field area, perhaps on a scale of kilometers, and left the rocks enriched in magnesium and sodium and depleted in potassium. However, magnesium chlorites in least altered rocks in the field area may represent early alteration by the descending limb of a convection system (Mottl, 1983).

With continued heating, the acidic, potassium-enriched brine would buoyantly ascend along fractures and permeable strata into overlying, relatively unaltered felsic volcanics including rocks of the study area.

Chemical reactions between the ascending fluid and rocks in the study area caused the breakdown of plagioclase to form seicite, biotite, quartz and possibly chlorite, and the breakdown of biotite to form chlorite and quartz by addition of potassium and minor magnesium to and leaching of sodium and calcium from the rocks (Fig. 35). Addition of magnesium to the rocks indicates that water/rock reactions on the descending limb occurred at high water/rock ratios (Hajash and Chandler, 1981).

Decrease in hydrostatic pressure with ascent would also decrease the solubility of carbon dioxide, possibly by boiling, and cause the precipitation of ferroan dolomite/ankerite within the sericite and biotite alteration zones (Nebel, 1982; Holland and Malinin, 1979).

Formation of sericite, biotite and chlorite would decrease the porosity and permeability of the altered rocks resulting in the formation of a cap rock over part of the geothermal system (Riverin and Hodgson, 1980).

Underlying the felsic succession are subaqueous, pillowed and brecciated intermediate and mafic volcanics (Poulsen, 1981). Being brecciated, these units may have served as a reservoir for connate sea water. Evolved solutions of sea water origin circulating through deeper (>3 km) portions of the hydrothermal system would mix

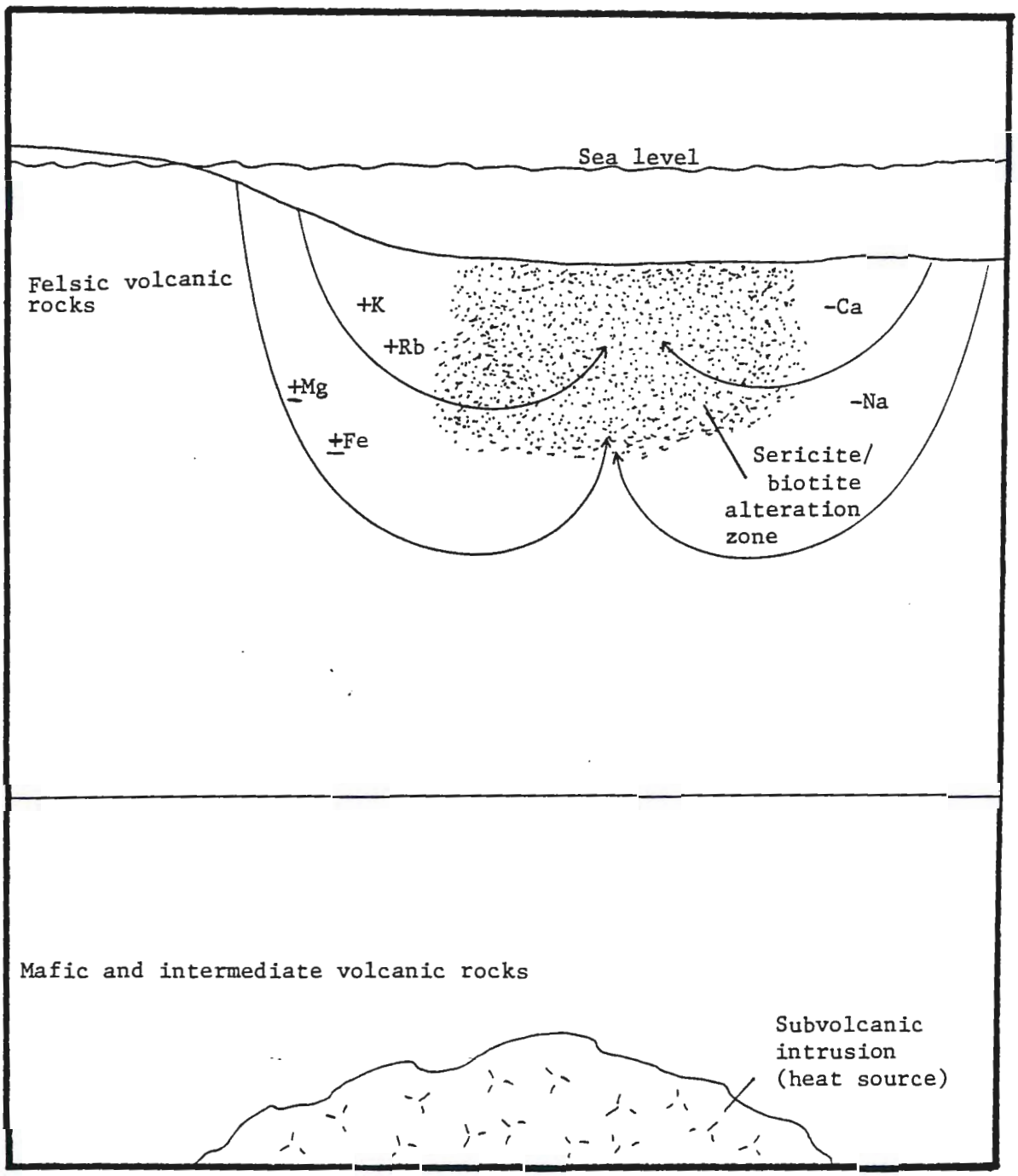

Figure 35. Diagramatic cross section of volcanic succession showing development of sericite/biotite alteration zones by convective circulation of sea water at shallow and moderate depths through felsic volcanic rocks. Chemical changes (i.e. +K) reflect changes in rock chemistry during hydrothermal alteration.

with this connate sea water and the resulting fluid would chemically react with the mafic and intermediate volcanic rocks. Reactions between these deep circulating fluids and volcanic rocks would have occurred at low to moderate water/rock ratios since much of the fluid would have been tapped off in upper portions of the system at depths less than 3 km (Osterberg, 1985).

For andesites and basalts, sea water-rock reactions at low to moderate water/rock ratios result in the addition of magnesium to the rock in exchange for calcium as primary minerals are converted to various magnesium silicates (i.e. smectite, actinolite). Solution pH during reaction is acidic to neutral (Seyfried and Bischoff, 1981; Hajash and Chandler, 1981; Seyfried and Mottl, 1982). Over a temperature range of 150 to 350 ^{o}C and moderate (10-50) water/rock ratios, solution pH is slightly acidic (3-6) and buffered by silicate hydrolysis reactions (Seyfried and Bischoff, 1977; Seyfried and Mottl, 1982). Under these conditions, substantial magnesium remains in the calcium-enriched solution, particularly at intermediate stages of reaction, and heavy metal content is typically low since solution pH is too high and temperature too low to efficiently leach base metals from the rocks at the moderate water/rock ratios (Seyfried and Bischoff, 1977; Seyfried and Mottl,

1982).

With deeper circulation, the water/rock ratio would decrease as more fluid is tapped off in upper portions of the system. Under these rock-dominated conditions, most of the magnesium and calcium in solution would be lost to the surrounding rocks resulting in a fluid enriched in iron, manganese and base metals (Seyfried and Bischoff, 1977, 1981).

Chemical changes in the rocks of the field area indicate that the fluids were enriched in calcium and magnesium; therefore, in the proposed model, water-rock interactions between the hydrothermal fluids and mafic rocks took place at low to moderate water/rock ratios, moderate temperatures (150-350 ^{o}C) and shallow circulation depths. Under these conditions, the pH of the solution would have been too high and temperature too low to efficiently leach base metals from the rocks.

This calcium-enriched solution would have buoyantly risen with continued heating until it encountered the cap rock of sericite/biotite alteration. Increasing hydrostatic pressure below the cap rock caused fracturing to occur that released the solution. This fluid reacted with the sericite and biotite alteration zones to produce the actinolite alteration zone by the addition of calcium, magnesium and iron to and leaching of potassium

from the rocks. Decreasing hydrostatic pressure with ascent, mixing with relatively cold sea water and possibly boiling caused base metals in solution to become insoluble and precipitate with the alteration phases or as sulfides. At or near the sea water-rock interface, precipitation of base metals as sulfides formed the Gagne Lake prospect (Fig 36). Two hypotheses can account for the low abundance of base metal sulfides at the Gagne Lake prospect. First, the base metal content of the hydrothermal fluids may have been low because conditions of water-rock interactions (high pH, low temperature) deeper in the system inhibited the leaching of base metals from the rocks. Secondly, boiling of the solution as pressure decreased with ascent could have caused the "dumping" of base metals over a wide area as disseminated sulfides in the subsurface. This process may be reflected in the high zinc and copper values in the rocks (Appendix II).

Near the sea water-rock interface, the rising solution, now depleted in calcium and magnesium from the formation of actinolite and chlorite lower in the system, mixed with connate sea water in the bedded tuffs and lapilli tuffs and sea water drawn down into the system along discharge zones. Chemical reactions between this recharged solution and the pyroclastic rocks resulted in

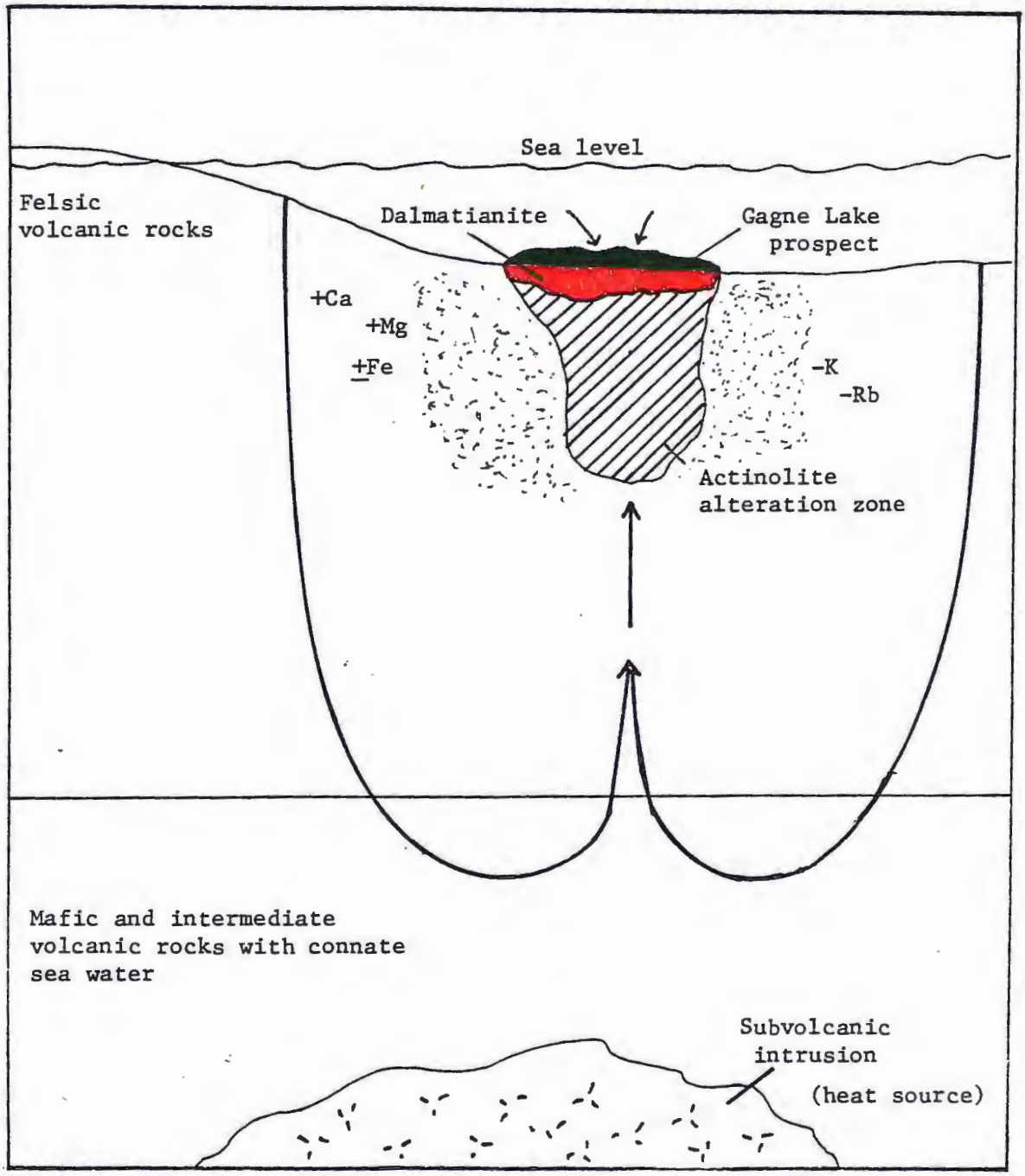

Figure 36. Diagramatic cross section of volcanic succession showing development of actinolite alteration zone and dalmatianite at expense of sericite/biotite alteration zones by convective circulation of evolved sea water through mafic and intermediate volcanic rocks at depth and draw down of sea water into the system near the water-rock interface. Changes in chemistry (i.e. +Ca) reflect changes in rock chemistry during hydrothermal alteration.

the formation of a magnesium chlorite and quartz alteration zone at the expense of sericite-rich rocks. This alteration zone became dalmatianite during prograde metamorphism (Fig. 36).

VI. SUMMARY and CONCLUSIONS

The volcanic stratigraphy of the Gagne Lake area consists of felsic lava flows and pyroclastic rocks interlayered with a much lesser volume of mafic lava flows and volcaniclastic rock.

Rhyolite lava flows dominate the lower portion of the stratigraphy. These units compose 70-80% of the volcanic succession and may be up to 400 m thick. Typically amygdaloidal and spherulitic, individual rhyolite lava flows may be porphyritic and/or flow banded.

Field evidence and petrographic studies indicate that these rhyolite lava flows and an overlying, porphyritic mafic lava flow were deposited under subaerial conditions.

A package of felsic bedded tuffs and lapilli tuffs overlie these subaerial lava flows and are the host rock for the Gagne Lake prospect. The lapilli tuffs are normally graded with lapilli forming from 3 to 50% of an individual bed. Eastward the lapilli tuffs pass into bedded tuffs that are virtually fragment free. Large (>64 mm) fragments occur near the base of the pyroclastic rock and phenocrysts of quartz and plagioclase occur locally. Lapilli are predominantly siliceous, possibly juvenile, fragments, but pumice fragments occur locally in minor

amounts.

The bedding and grain-size characteristics of these units are characteristic of tuff rings formed by explosive hydrovolcanic eruptions under low water/magma conditions. The presence of volcanogenic-type massive sulfide mineralization within the tuffs indicates that the tuff ring was, in part, deposited under subaqueous conditions.

Overlying the bedded tuffs and lapilli tuffs are a porphyritic mafic lava flow and chlorite-rich bedded tuff. Similarities between the bedded tuff and volcaniclastic sediments, and the presence of the Gagne Lake prospect stratigraphically below these units suggests that they were deposited under subaqueous conditions and that the tuff may be sedimentary rather than pyroclastic.

The volcanic sequence has been intruded by tonalitic and mafic sills that range in time of emplacement from prior to hydrothermal alteration to after emplacement of the Little Ottertail Lake Stock.

Intrusion of the Little Ottertail Lake Stock has metamorphosed the rocks to the greenschist-amphibolite transition facies, and the entire sequence is part of a dextral wrench zone resulting from right-lateral movement on the Quetico and Seine River-Rainy Lake Faults.

Prior to being metamorphosed, rocks of the Gagne Lake prospect were hydrothermally altered. Petrographic and chemical analyses allow for the definition of four distinct alteration assemblages. A least altered assemblage, defined as those rocks composed of minerals that are primarily igneous or metamorphic in origin, a sericite/biotite-chlorite-iron carbonate assemblage, an actinolite-chlorite-epidote assemblage and dalmatianite which consists of sericite, chlorite, and iron carbonate but separated from the previously mentioned alteration assemblage by its porphyroblastic texture.

The alteration assemblages occur in a concentrically zoned alteration pipe below the Gagne Lake prospect that becomes semi-conformable to stratigraphy within the bedded tuffs and lapilli tuffs. The alteration pipe consists of a core of actinolite alteration that is enveloped by sericite or biotite alteration. The semi-conformable alteration zone consists of dalmatianite surrounded by sericitic alteration.

Enveloping the Gagne Lake prospect is a zone of dalmatianite that is similar in mineralogy to sericitic alteration but separated into a different alteration zone on the basis of its porphyroblastic texture and alteration geochemistry.

Chemically, the sericite/biotite alteration is defined

by the addition of potassium, rubidium and magnesium to and loss of sodium and calcium from the rocks. These chemical trends are attributed to the formation of sericite and biotite at the expense of plagioclase and the formation of magnesium chlorites at the expense biotite and/or plagioclase.

The mineralogy of this assemblage depends upon the rock type altered. In felsic volcanic rocks, sericite is predominant while biotite and chlorite predominate in the tonalite sills and mafic lava flow. Similar distribution and alteration geochemistry of these alteration zones indicates that the bulk chemistry of the rock being altered controled the mineralogy.

Actinolite alteration is defined by the addition of calcium, magnesium and iron to and loss of potassium from the rocks. Based on cross-cutting relationships, these chemical trends are attributed to the formation of actinolite, iron chlorites and epidote at the expense of pre-existing sericite/biotite alteration.

Dalmatianite is characterized by the addition of magnesium to and loss of potassium from the rocks. These trends resulted in the formation of a magnesium chlorite and quartz alteration zone at the expense of sericitic alteration that became dalmatianite during prograde metamorphism.

Hydrothermal alteration resulted from the circulation of sea, and possibly connate, water through the rocks in a convection cell driven by a heat source at depth.

Shallow-circulating water reacted with felsic rocks in the region at moderate to high water/rock ratios and moderate (200-300 ^{o}C) temperatures. On the downwelling limb of the convection cell, the water reacted with felsic rocks and evolved into a potassium-rich, acidic (pH<5) solution depleted in magnesium and sodium. With ascent, this solution encountered rocks of the study area. Base-leaching reactions between the solution and rocks produced the sericite/biotite alteration.

Deeper-circulating solutions encountered mafic rocks. Reactions between the solution and mafic rocks occurred at moderate to low water/rock ratios and moderate (150-350 ^{o}C) temperatures and resulted in the addition of magnesium to and loss of calcium, iron and base metals from the rocks. Conditions of the reactions were such that substantial magnesium was left in solution. pH of the solution would have been acidic but near neutrality and base metal content low.

With ascent this calcium-enriched solution would have encountered the previously altered rocks of the study area. Base-fixing reactions between the fluid and the rocks resulted in the formation of actinolite, iron

chlorites and epidote at the expense of sericite, biotite, and magnesium chlorites.

During formation of actinolite alteration, sea water drawn down into the system along discharge sites replenished the solution in magnesium. Reactions between this solution and sericitized hyalotuffs resulted in the formation of a magnesium chlorite-quartz alteration assemblage that became dalmatianite during prograde metamorphism.

At or near the sea water-rock interface, base metals precipitated out of solution to form the Gagne Lake prospect. The sub-ore grade of the deposit is thought to be the result of low base metal content of the solution and loss of base metals as disseminated sulfides in the footwall rocks.

References Cited

Ayers, L.D., 1978, Metamorphism in the Superior Province of Northwestern Ontario and its Relationship to Crustal Development., in Metamorphism in the Canadian Shield, Geological Survey of Canada, Paper 78-10, J.A. Frasier, W.W. Heywood, eds., p.25-36, 367p.

Ballard, R.D., and Moore, J.G., 1977, Photographic Atlas of the Mid-Atlantic Ridge Rift Valley. Springer-Verlag, New York, 114p.

Berry, L.G., ed., 1974, Selected Powder Diffraction Data for Minerals, Joint Committee on Powder Difraction Standards.

Blackburn, C.E., 1975, Ontario Geological Survey Map 2443, Kenora-Fort Frances, Geologic Compilation Series.

Blackburn, C.E., 1980, Toward a Mobilist Tectonic Model for Part of the Archean of Northwestern Ontario., Geoscience Canada, 7, 2, p.64-72

Blackburn, C.E., Bond, W.D., Breaks, F.W., Davis, D.W., Edwards, G.R., Poulsen, K.H., Trowell, N.F., Wood, J., 1985, Evolution of Archean Volcanic-Sedimentary Sequences of the Western Wabigoon Subprovince and its Margins., in Evolution of Archean Supacrustal Sequences, L.D. Ayers, P.C. Thurston, K.D. Card and W. Weber, eds., Geological Association of Canada Special Paper 28, p89-117.

Boily, B. 1985, Pers. Comm., Corporation Falconbridge Copper, Toronto, Ontario, Canada

Bonnichsen, Bill and Kauffman, Daniel, F., 1987, Physical Features of Rhyolite Lava Flows in the Snake River Plain Volcanic Province, Southwestern Idaho., in The Emplacement of Silicic Domes and Lava Flows., Geological Society of America Special Paper 212, Jonathan Fink, ed. p119-145.

Cas, R., 1978, Silicic Lavas in Paleozoic Flyschlike Deposits in New South Wales, Australia: Behaviour of Deep Subaqueous Silicic Flows. Geologic Society of America Bulletin, 77, p.671-684.

Chapin, C.E., and Lowell, G.R., 1979, Primary and Secondary Flow Structures in Ash-Flow Tuffs of the Gribbles Run Paleovalley, Central Colorado., in Ash-Flow Tuffs, Geological Society of America Special Paper 180., Charles Chapin and Wolfgang Elston, eds., p137-152.

Christiansen, R.L., and Lipman, P.W., 1966, Emplacement and Thermal History of a Rhyolitic Lava Flow Near Fortymile Canyon, Southern Nevada., Geological Society of America Bulletin, 77, p.671-684

De Rosen-Spence, A.F., 1980, Archean Subaqueous Felsic Flows, Rouyn-Noranda, Quebec, Canada, and Their Quaternary Equivalents., Precambrian Research, 12, p.43-77

Dikson, F.W., 1977, The Reaction of Granite with Seawater at 300 ^{O}C and 1000 bars., EOS, (American Geophysical Union Transactions), 58, p.1251.

Evamy, B.D., 1963, The Application of Chemical Staining to a Study of Dedolomitization., Sedimentology, 2, p.164-170.

Fischer, R.V., Schminke, H.V., 1984, Pyroclastic Rocks., Springer-Verlag, New York, N.Y., 472p.

Fiske, R.S., and Matsuda, T., 1964, Submarine Equivalents of Ash Flows in the Tokiwa Formation, Japan, American Journal of Science., 262, p76-106.

Franklin, J.M., Sangster, D.M., and Lydon, J.W., 1981, Volcanic-Associated Massive Sulfide Deposits, in Economic Geology 75th Anniversary Volume, B.J. Skinner, ed., Economic Geology Publishing Company, 964p.

Freidman, G.M., 1959, Identification of Carbonate Minerals by Staining Methods., Journal of Sedimentary Petrology, 29, p81-97.

Gary, M., McAfee, R. Jr., and Wolf, C.L. eds., 1974, Glossary of Geology: Washington D.C., American Geological Institute., 860p.

Gelinas, L., Brooks, C., Perrault, G., Carignan, J., Trudel, P., Grasso, F., 1977, Chemo-Stratigraphic Divisions Within the Abittibi Volcanic Belt, Rouyn-Noranda District, Quebec., in Volcanic Regimes in Canada, Geologic Association of Canada Special Paper 16, W.R.A. Barager, L.C. Coleman, J.M. Hall, eds., p265-296.

Gibbon, D.L., 1969, Origin of the Star Mountain Rhyolite., Bulletin Volcanologique, 33, p.438-474.

Goodwin, A.M., Ambrose, J.W., Ayres, L.D., Clifford, P.M., Currie, K.L., Ermanovics, I.M., Fahrig, W.F., Gibb, R.A., Hall, D.H., Innes, M.J.S., Irvine, T.N., McLaren, A.S., Norris, A.W., Pettijohn, J.F., and Riddler, R.H., 1972, The Superior Province, Geological Association of Canada Special Paper 11, p527-624.

Goodwin, A.M., 1977, Archean Volcanism in the Superior Province, Canadian Shield., Geological Association of Canada Special Paper 16, p205-243.

Grant, James, A., 1986, The Isocon Diagram--A Simple Solution to Gresens' Equation for Metasomatic Alteration., Economic Geology, 81, p1976-1982.

Grout, F.F., 1925, The Coutchiching Problem., Geolgical Society of America Bulletin, 36, p351-364.

Groves, D.A., 1984, Stratigraphy and Alteration of the Footwall Volcanic Rocks Beneath the Archean Mattabi Massive Sulfide Deposit, Sturgeon Lake, Ontario., Unpublished MSc. Thesis, University if Minnesota-Duluth., Duluth, Minnesota., 115p.

Hajash, A. and Chandler, G., 1981, An Experimental Investigation of High Temperature Interactions Between Sea Water and Rhyolite, Andesite, Basalt and Peridotite., Contrib. Mineral. Petrology, 78, p240-254

Harris, F.R., 1974, Geology of the Rainy Lake Area, District of Rainy River., Ontario Division of Mines Geological Report 115, 94p.

Hausback, Brian, 1987, An Extensive, Hot, Vapor-Charged Rhyodacite Flow, Baja California, Mexico., in The Emplacement of Silicic Domes and Flows., Geological Association of America Special Paper 212, Jonathan Fink, ed., p111-118.

Heiken, G.H., 1971, Tuff Rings: Examples from the Fort Rock-Christmas Lake Valley Basin, South-Central Oregon., Journal of Geophysical Research, 76, 23, p5615-5626.

Holland, H.D., Malinin, S.D., 1979, The Solubility and Occurrence of Non-Ore Minerals., in Geochemistry of Hydrothermal Ore Deposits., H.L. Barnes, ed., p461-508

Hutchinson, R.W., 1982, Syndepositional Hydrothermal Processes and Precambrian Sulphide Deposits., in Precambrian Sulphide Deposits, Geological Association of Canada Special Paper 25., H.S. Robinson Memorial Volume, R.W. Hutchinson, C.D. Spence and J.M. Franklin, eds., p761-787.

Hyndman, D.W., 1972, Petrology of Igneous and Metamorphic Rocks, McGraw-Hill Book Co., 533p.

Jolly, W.T., 1977, Relations Between Archean Lavas and Intrusive Bodies of the Abattibi Greenstone Belt, Ontario-Quebec., in Volcanic Regimes in Canada, Geologic Association of Canada Special Paper 16., W.R.A. Barager, L.C. Coleman, J.M. Hall, eds., p311-330

Langford, F.F., and Morin, J.A., 1976, The Development of the Superior Province of Northwestern Ontario by Merging Island Arcs., American Journal of Science, 276, p1023-1034.

Lawson, A.C., 1913, The Archean Geology of Rainy Lake, Re-studied., Geological Survey of Canada, Memoir 40, 111p.

McGlynn, J.C., and Henderson, J.B., 1970, Archean Volcanism and Sedimentation in the Slave Structural Province., in Symposium on Basins and Geosynclines of the Canadian Shield, Geological Survey Canada Paper 70-40, p31-44.

Merritt, P.L., 1934, Seine-Coutchiching Problem., Geological Society of America Bulletin, 45, p333-374

Morton, R.L., 1986 pers. comm., University of Minnesota-Duluth, Duluth, Minnesota.

Morton, R.L., Nebel, M.L., 1983, Physical Character of Archean Felsic Volcanism in the Vicinity of the Helen Iron Mine, Wawa, Ontario, Canada., Precambrian Research, 20, p39-62.

_____, 1984, Hydrothermal Alteration of Felsic Volcanic Rocks at the Helen Siderite Deposit, Wawa, Ontario., Economic Geology and the Bulletin of the Society of Economic Geologists, 79, 6, p1319-1333.

Mottl, M.J., 1983, Metabasalts, Axial Hot Springs and the Structure of Hydrothermal Systems at Mid-Ocean Ridges., Geol. Soc. Amer. Bull., 94, p161-180.

Nebel, M.L., 1982, Stratigraphy, Depositional Environment and Alteration of Archean Felsic Volcanic Rocks, Wawa, Ontario., Unpublished MSc. Thesis, University of Minnesota-Duluth., Duluth, Minnesota., 114p.

Ojakangas, R.W., 1972, Rainy Lake Area., in Geology of Minnesota: A Centenial Volume., P.K. Simms, G.B. Morey, eds., Minnesota Geological Survey, p163-171.

Ojakangas, R.W., 1985, Review of Archean Clastic Sedimentation, Canadian Shield: Major Felsic Volcanic Contributions to Turbidite and Alluvial Fan-Fluvial Facies Associations., in Evolution of Archean Supracrustal Sequences., L.D. Ayers, P.C. Thurston, K.D. Card and W. Weber, eds., Geological Association of Canada Special Paper 28., p23-47.

Osterberg, S.A., 1985, Volcanic Stratigraphy and Hydrothermal Alteration in the Vicinity of the Headway-Coulee Massive Sulfide Prospect, Onaman River Area, Ontario., Unpublished MSc. Theses, University of Minnesota-Duluth, Duluth, MN, 115p.

Phillips, W.R., Griffen, D.T., 1981, Optical Mineralogy, the Nonopaque Minerals., W.H. Freeman and Company, San Francisco, 677p.

Pettijohn, F.J., Potter, P.E., Siever, R., 1972, Sand and Sandstone., Springer-Verlag, New York., 600p.

Poulsen, K.H., Borradaile, G.J., and Kehlenbeck, M.M., 1980, An Inverted Archean Succession at Rainy Lake, Ontario., Canadian Journal of Earth Sciences, 17, p1358-1369.

Poulsen, K.H., 1980, The Geological Setting of Mineralization in the Mine Centre-Fort Frances Area, District of Rainy River., in Summary of Field Work, 1980, by the Ontario Geological Survey., J. Wood, O.L. White, R.B. Barlow, and A.C. Colvine, eds., Ontario Geological Survey, Misc. Paper 100, 255p.

_____, 1982, Institute on Lake Superior Geology Field Trip Guide Book.

Reed, M.H., 1984, Geology, Wall-Rock Alteration and Massive Sulfide Mineralization in a Portion of the West Shasta District, California., Econ. Geol., 79, p1299-1318.

Riverin, G., and Hodgson, C.J., 1980, Wall-Rock Alteration at the Millenbach Cu-Zn Mine, Noranda, Quebec., Econ. Geol., 75, p424-444.

Sangster, D.F., 1972, Precambrian Volcanogenic Massive Sulfide Deposits in Canada: A Review., Canada Geological Survey Paper 72-22, 44p.

Schwerdtner, W.M., Stone, D., Osadetz, K., Morgan, J., and Scott, G.M., 1979, Granitoid Complexes and the Archean Tectonic Record in the Southern Part of Northwestern Ontario., Canadian Journal of Earth Sciences, 16, p1965-1977.

Seyfried, W., Bischoff, J., 1977, Hydrothermal Transport of Heavy Metals by Sea Water: The Role of Seawater/ Basalt Ratio., Earth and Planetary Science Letters., 34, p71-77.

_____, 1981, Experimental Seawater-Basalt Interaction at 300 ^{o}C, 500 bars, Chemical Exchange, Secondary Mineral Formation and Implications for Transport of Heavy Metals., Geochem. Cosmichem. Acta, 45, p135-147.

Seyfried, W., Mottl, M., 1982, Hydrothermal Alteration of Basalt by Sea Water Under Seawater Dominated Conditions., Geochem. Cosmichem. Acta, 46, p985-1002.

Sheridan, M.F., and Wohletz, K.H., 1983, Hydrovolcanism: Basic Considerations and Review., Journal of Volcanology and Geothermal Research, 17, p1-30.

Switzer, G., Apelrod, J., Lindberg, M., and Larsen, E., 1962, Tables of d Spacings for Angle 2O., United States Geological Survey Circular 29, 17p.

Thurston, P.C., Ayres, L.D., Edwards, G.R., Gelinas, L., Ludden, J.N., Verpaelst, P., 1985, Archean Bimodal Volcanism., in Evolution of Archean Supracrustal Sequences., Geological Association of Canada Special Paper 28, L.D. Ayres, P.C. Thurston, K.D. Card, and W. Weber, eds., p7-118.

Williams, H., McBirney, A.R., 1979, Volcanology., Freeman, Cooper and Company, San Francisco., 397p.

Williams, H., Turner, F.J., Gilbert, C.M., 1982, Petrography: An Introduction to the Study of Rocks in Thin Sections., Second Edition, W.H. Freeman and Company, San Francisco, 626p.

Winkler, H.G.F., 1976, Petrogenesis of Metamorphic Rocks. Fourth Edition, Springer-Verlag, New York Inc., 334p.

Wohletz K.H., and McQueen, R.G., 1981, Experimental Hydromagmatic Volcanism., EOS, (American Geophysical Union Transactions), 62, 45, p1085.

Wohletz, K.H., and Sheridan, M.F., 1979, A Model of Pyroclastic Surge., in Ash Flow Tuffs, Geological Society of America, Special Paper 180., C.E. Chapin, W.E. Elston, eds., p177-195.

Wohletz, K.H., and Sheridan, M.F., 1983, Hydrovolcanic Eruptions II. Evolution of Basaltic Tuff Rings and Tuff Cones., American Journal of Science, 283, p385-413

APPENDICES

Appendix I: Textures and Modes of Rock Units

The following tables represent modal compositions and textures seen in thin section and outcrop of each lithologic unit in the study area.

Minerals	Abbreviations
Quartz	QTZ
Plagioclase (andesine)	PLG
Recrystalized matrix material (quartz, plagioclase, cordierite)	QPC
Biotite	BIO
Sericite	SER
Chlorite	CHL
Hornblende	HNBD
Augite	AUG
Actinolite	ACT
Anthophyllite	ANTH
Tourmaline	TOUR
Epidote	EPI
Zircon	ZR
Sphene	SPH
Iron carbonate	CARB
Apatite	AP
Magnetite	MAG
Ilmenite	ILM
Sulfides	SUL

Textures	
Amygdaloidal	A
Porphyroblastic	P
Ophitic	O
Micrographic	M
Dalmatianite	D
Fragmental	
1) Pumicious fragments	PF
2) Silicious fragments	SF
Poikiloblastic	PK

All metamrphosed rocks are slightly foliated, and felsic metavolcanics diplay bedding. Modal values listed in the following tables are given in percent (%).

Table 5. Modal Compositions of Pyroclastic Rocks

Hyalotuffs

			PHENOCRYSTS										
T.S.#	TEXTURES	FRG	QTZ	PLG	QPC	QTZ	BIO	CHL	SER	CARB	SPH	SUL	MAG	OTHER
1A	D				60		10	17	12		Tr		1	
1B					80		8	7	5				Tr	
2A	P		2		57		20	5	15	1			Tr	
2B					65		25	5	5				Tr	TrZr
2C	P		1		84		5		10		Tr			TrTOUR
3	D				80		2	3	10					
4A					70		3	15	10				1	TrANTH
4B	D					25	2	25	40	1	4		1	2ANTH
4C	D				55	20	10	10	5	1			Tr	
5B	D					15	2	45	35	Tr	3		Tr	TrANTH
6					60		3	7	30	Tr				
7	P			3	70		15	2	10	Tr				
8	P		8	5	47		25		15					
3	LF	2			75		15	3	5				Tr	
15	P,PK,LF	10	5	2	20		6	20	33	2	Tr		2	TrTOUR,TrAP
16	P,LF,PF	7	3		40		10	3	33	1			Tr	
17	LF	8			56		12		20				1	3EPI
19	LF	1			48		20		30		Tr	Tr		1EPI
24	P,LF	5		1	60		5	2	22			3	1	
26	LF	1			80		1	4	10	1			1	1EPI
46FR	LF,P	30		1	30		25	2	10				2	
68					65		25		10			Tr	Tr	
71B					79		12		8					1EPI
75	D,LF	1			63	5	15	5	8	Tr		1		
81A					48		21	4	12	4		1	1	9EPI
83B	D				25	10	10	30	20	Tr	1	1		2EPI
84	PK				42		20	8	15	Tr	1	4	2	
125	LF	3			60		25	2	8					2EPI
Ash	LF	1			50		15		30			3	1	
Frag	LF	15			35		15		33				2	
MPHW					60		12	2	25			1		
MPFW					40		12	8	35				5	

Bedded Tuff

			PHENOCRYSTS										
T.S.#	TEXTURES	FRG	QTZ	PLG	OPC	QTZ	BIO	CHL	SER	CARB	SPH	SUL	MAG	OTHER
43	P,LF	4		2		30	25	30		Tr	8	Tr		1TOUR

Table 6. Modal Compositions of Lava Flows

Amygdaloidal rhyolite lava flows

		PHENOCRYSTS													
T.S.#	TEXTURES	QTZ	PLG	QPC	QTZ	PLG	BIO	CHL	SER	ACT	CARB	SPH	SUL	MAG	OTHER
37B	P	12	3	65			7	1	10		1			1	
48				41				1		7		1			5OEPI
49A	P	6	4	50			15		25			Tr		Tr	TrTOUR,TrAP
49B	P,A		3	55			25	3	15					2	
50	P,A	5		54			15	10	10		3	1		2	TrAP
52	P,A	1		52			1	10	12		1		1	2	15EPI,TrAP
53	P,A	1	1	55			25	3	8		3	1		3	
55	P,A	4	2	50			20	2	20					2	TrAP
57	P,A	7		65			15	3	7		1			2	
59	P,A	4	2	63			15		8		2	2		4	TrEPI
63	P,A	1			20	2	30	25		14		1			8EPI
64	A			75			10	10	2					3	
62					35	2	15	7		25		3			13EPI
76	P,A,FB	8	4	60			15	8	1					4	
89	A			58			25		15		1			1	1EPI
90	P,A,FB	7		45			25	5	15		1			1	1EPI
91	P,A,S,	2	3	55			15	5	10			1	1	3	
95	A			68			25	2	11					4	
96	P,S	1	1	80			15		3						
97	S			67			32		5					1	
105	P,S		1	70			15		12					2	
106	A			70			15	4	8		1			2	
114				73			9	6	10			1		1	TrEPI
116	A			75			15	5	4					1	
120	A			59			25	10	5					1	
122	P,A	2		55			15	1	20		4			3	
128	A,S	6		65			15	3	8			1	1	1	
134	P,A	1	1?	40	5	3	25	12		7		2			6EPI

Table 6. Continued

T.S.#	TEXTURES	phenocrysts QTZ	PLG	QPC	QTZ	PLG	BIO	CHL	SER	ACT	CARB	SPH	SUL	MAG	OTHER
135	A,S			50			25	3	20			1	1		
136	A,S			73			15	2	8			2			
139	A,S			65			6	10	15			1	1	2	TrEPI
142	FB			75			15	5	2					3	
143				71			22	1	5					1	
141B	P,A,S	6		55			25	4	6					4	
141C	S			79			3	12	1				3	2	
145	P,A	1	1	60			20	5	10					3	
150	A,S			50			5	22	7		1	1		3	1EPI
152	P	1		73			14	3	6					3	TrAP
155	P,S?	1		60			17	9	6		1		2	4	
162	S			75			4	12	3			1	3	2	
170	P,A	2	5	75			10	3	3					2	

Quartz-feldspar porphyry

T.S.#	TEXTURES	FRG	QTZ	PLG	QPC	BIO	CHL	SER	CARB	SPH	MAG	OTHER
93	A,S				60	17	1	6	1		5	
94	P,ALF		4	1	52	35		2		1		TrAP
103	P,A	4	4	2	30	30	1	15	1	3	1	
104	P,LF,A	12	3	2	45	27	1	6	1	3		
115	P,A		3	1	60	20	2	7	1	3	1	2EPI
119	A,FB,P		1	1	60	25	3	4			5	

Table 6. Continued

Mafic lava flows

T.S.#	TEXTURES	PHENOCRYSTS PLG	QTZ	PLG	HNBD	BIO	CHL	EPI	CARB	SPH	ILM	OTHER
12	P,A	20	6	10		3	45	5	1	2	Tr	TrSER
14	P	15	19	7		7	40	4	15*	4		3SER,TrMAG
25	A		20	15	15	3	35	11	1	1		1SER
33	P,A	2	30	15	25	7	14	2	2	4	1	TrAP,TrSER
124C			28	17	25	15	6	1		3	Tr	2SUL,3SER,TrTOUR
86	P,A	2	15	15	6	16	20	10	1	2	Tr	TrAP

* Iron carbonate occurs as a pseudomorph of plagioclase phenocrysts

Table 7. Modal Compositions of Intrusive Rocks

Tonalite Sills

T.S.#	TEXTURES	ACT	BIO	CHL	PLG	QTZ	EPI	SPH	OTHER
65		25	2	8	8	38	15	6	
66		30	12	12	5	30	8	2	
88			25	12	20	33	2	1	7SER,TrCARB
99A			20	20	40	12	3	5	TrSER
110	M		20	8	25	38	5		1MAG,TrCARB,TrAP,3SER
111		12	7	20	5	40	3	4	TrSER,TrAP
112A			15	21	25	21	8	5	4SER,1CARB,TrAP
112B		25	7	25	3	23	12	5	TrMAG
112D		12	10	28	12	30	1	2	4MAG,1SUL
113			30	30	10	15	1	6	3SER,4CARB,1MAG
127	M		28	6	34	26	4	1	1SUL,TrAP
129		5	10	25	10	39	5	2	3CARB,TrSER,1MAG
130		30	17	17	5	25	3	3	
132		30	10	20	4	31	3	2	
133		1	25	13	10	33	7	3	3SER,5CARB,TrMAG
137A		3	15	30	10	33	1	3	5CARB,TrSER
137B		2	30	20	15	26	4	3	
138		8	20	25	12	31	1	3	
138B		35	5	11	2	25	18	4	
140	M		30	7	26	35	Tr	1	1CARB,TrSER
147		3	30	10	12	36	5	4	
148		30	6	20	2	43	1	2	TrTOUR
MDI	M		23	10	33	31	2		1CARB,TrSER,TrMAG

Table 7. continued

Mafic Sills

T.S.#	TEXTURES	HNBD	CHL	BIO	PLG	QTZ	EPI	SPH	OTHER
51		40	7	2	35	9	4	2	TrAP
100A	M	37	10	4	5	12	30	2	TrSUL,TrILM
92	M	45	12	2	15	8	15	3	TrILM,TrAP
118BT		27	17	1	8	15	20	3	1ILM,1CARB
154		40	12	6	20	10	7	5	

Gabbro

T.S.#	TEXTURES	AUG*	CHL	BIO	PLG	QTZ	EPI	SPH	OTHER
10	0	45	15		20	3	14	2	TrILM
21	0	35	30	Tr	8	4	20	3	TrILM,TrCARB
23	O,P	40	30		10	2	15	3	
69	0	33	14		27	3	20	3	TrCARB,TrSUL
82A	0	35	13		22	8	17	2	3ILM,TrCARB

* Augite partially uralitized to actinolite

Appendix II. Chemical Analyses

The following tables are a compilation of major and trace element chemical analyses performed by the Geological Survey of Canada. Sample numbers correspond to sample locations on Plate 2.

Major and trace elements were analyzed by whole rock X-ray fluorescence except H_2O, CO_2, and FeO which were done by rapid chemical. Zn, Cu and Pb were done by the DC plasma method.

Major oxides are given as weight percents while trace elements are in parts per million.

Table 8. Major Element Geochemistry

Smpl #	SIO2	AL203	CAO	MGO	NA2O	K2O	FE* *	FEO	FE203	TIO2	H2O	CO2
Hyalotuffs												
17	75.70	11.30	0.36	1.05	3.11	2.81	4.43	2.4	1.76	0.23	1.1	0.04
16	72.80	12.70	2.19	1.75	1.06	3.12	2.67	1.3	1.23	0.19	1.0	0.12
32B	79.70	9.32	0.17	1.34	1.02	4.15	2.08	1.3	0.64	0.18	0.7	0.08
6	76.70	12.00	0.29	1.94	1.42	2.87	2.03	1.1	0.81	0.15	1.2	0.08
5B	59.80	14.80	1.23	6.09	1.13	2.14	9.36	7.3	1.25	1.01	4.1	0.11
15	69.90	13.60	0.47	3.84	0.62	3.26	4.91	3.1	1.46	0.25	2.4	0.01
3	80.00	11.10	0.35	1.02	3.86	1.52	1.40	0.9	0.40	0.14	0.8	0.01
68	76.60	11.00	2.07	0.85	1.87	2.76	2.94	1.7	1.05	0.20	0.6	0.02
2A	76.90	10.80	0.12	1.14	1.21	5.41	2.47	1.5	0.80	0.14	0.7	0.01
83B	63.30	14.50	2.45	3.21	1.52	2.35	7.69	4.5	2.69	1.16	2.9	0.01
2B	70.60	12.80	0.43	2.35	3.11	4.13	4.63	2.8	1.52	0.39	0.9	0.01
85	75.00	11.70	0.53	1.49	5.01	1.11	3.23	2.2	0.79	0.29	1.2	0.01
126	80.60	9.51	0.05	2.89	0.16	2.22	1.96	1.4	0.40	0.23	1.8	0.01
MPFW	54.30	19.60	0.11	8.09	0.56	6.37	3.46	2.1	1.13	0.24	2.1	0.02
171	68.20	12.90	0.73	4.51	0.49	2.50	5.92	4.4	1.03	0.66	3.0	0.04
67	78.00	11.20	0.22	1.17	4.22	1.80	2.10	0.9	1.10	0.20	0.6	0.01
19	74.30	11.50	1.63	1.08	0.69	4.47	3.24	1.8	1.24	0.25	0.9	0.15
18	76.50	11.10	0.19	0.27	2.64	4.80	2.05	1.3	0.61	0.18	0.6	0.04
4B	42.80	18.40	1.42	11.9	0.24	2.75	13.10	10.4	1.54	1.45	6.5	0.01
27	66.20	14.30	5.20	1.91	0.49	3.49	5.45	2.8	2.34	0.85	0.9	0.25
84	76.50	10.60	1.31	1.02	2.14	2.78	3.69	2.1	1.36	0.27	0.6	0.01
Mafic lava flows												
25	54.90	14.10	5.15	3.77	3.51	1.01	11.90	7.7	3.34	1.50	2.7	0.01
86	55.30	14.60	5.28	6.92	3.47	0.51	8.83	6.2	1.94	0.79	3.1	0.91
31B	56.20	14.10	6.25	3.41	2.99	0.92	10.60	6.7	3.15	1.47	2.1	0.01
14	53.70	14.60	4.81	4.21	3.28	0.65	12.40	9.3	2.06	1.51	3.3	1.00
33	56.60	13.80	4.34	3.83	4.47	1.15	12.40	9.1	2.29	1.47	1.9	0.25
QFP												
94	76.00	11.70	0.68	0.68	5.16	1.39	3.49	2.3	0.93	0.32	0.5	0.01
104	75.30	11.40	0.94	0.64	4.61	1.85	4.18	2.8	1.07	0.32	0.7	0.08
103	71.00	13.30	0.47	1.34	3.36	4.06	5.17	3.5	1.28	0.33	0.8	0.03
Rhyolite lava flows												
119	76.70	11.90	0.29	0.16	4.02	4.60	2.04	0.7	1.26	0.16	0.2	0.02
155	76.60	12.30	0.46	0.39	6.10	1.83	1.64	0.9	0.64	0.17	0.5	0.05
161	77.30	11.90	0.25	0.4	5.85	2.09	1.51	0.8	0.62	0.16	0.3	0.04
122	77.40	11.40	1.45	0.2	3.63	2.73	1.81	1.1	0.59	0.16	0.4	0.79
163	76.70	12.00	0.40	0.2	5.23	2.89	2.09	1.1	0.87	0.17	0.3	0.01
101	76.70	12.00	0.28	0.43	4.30	3.42	1.65	1.0	0.54	0.16	0.4	0.01
168	76.00	12.20	0.25	0.35	5.15	3.38	1.84	0.9	0.84	0.16	0.3	0.01
139	76.00	11.90	0.45	0.41	3.48	4.29	1.93	1.1	0.71	0.16	0.4	0.01
87	76.20	11.90	0.38	0.24	4.40	3.84	2.03	0.8	1.14	0.16	0.2	0.01
90	75.90	12.70	0.91	0.34	5.11	2.37	1.86	1.1	0.64	0.15	0.4	0.10
62	55.30	13.60	6.98	6.93	2.50	1.31	8.84	5.8	2.39	0.78	1.9	0.02
128	77.00	12.00	0.50	0.33	4.06	3.98	1.82	1.1	0.60	0.16	0.3	0.01
61	79.90	10.60	0.35	0.38	3.54	3.21	0.68	0.4	0.24	0.14	0.3	0.01
136	77.20	11.40	1.20	0.58	4.07	2.18	1.80	0.6	1.13	0.15	0.3	0.01
57	77.10	11.90	0.20	0.28	4.17	4.13	1.95	1.2	0.62	0.17	0.2	0.01
149	76.30	12.00	0.25	0.47	4.20	4.21	2.38	1.5	0.71	0.16	0.3	0.01
91	77.10	11.40	0.35	0.35	3.71	3.83	1.88	0.7	1.10	0.16	0.4	0.03
116	78.40	11.40	3.41	0.42	1.94	1.55	1.98	1.0	0.87	0.17	0.5	0.20
55	71.70	13.70	0.19	0.75	3.00	5.62	3.16	1.6	1.38	0.18	0.6	0.03

Table 8. cont.

Smpl #	SIO2	AL203	CAO	MGO	NA2O	K2O	FE*	FEO	FE203	TIO2	H2O	CO2
Tonalite sills												
133	59.10	13.90	4.61	3.42	4.14	1.79	7.92	5.4	1.92	0.99	1.6	1.50
110	66.80	12.60	3.12	0.83	3.79	1.70	8.97	6.0	2.30	0.68	1.0	0.20
99A	61.60	14.30	3.95	2.47	4.11	1.44	8.72	5.5	2.61	1.46	1.7	0.02
140	67.10	12.70	2.08	1.68	4.24	1.74	8.17	6.1	1.39	0.65	1.2	0.37
88	61.80	12.80	3.15	4.23	3.86	0.32	7.69	5.1	2.02	0.88	1.4	0.39
129	60.00	14.40	4.34	2.97	4.59	1.39	8.23	4.7	3.01	1.26	1.2	0.72
65	58.40	14.20	6.39	2.77	3.84	1.07	9.49	5.5	3.38	1.42	1.3	0.03
113	53.70	14.10	3.51	6.01	3.74	2.04	10.90	7.9	2.12	1.66	2.4	0.39
66	63.30	14.20	5.06	3.43	5.16	0.51	6.16	3.5	2.27	0.96	1.2	0.02
111	61.90	14.20	4.08	1.98	4.30	2.00	8.59	5.7	2.26	1.39	1.1	0.18
54	54.10	15.70	5.47	6.65	4.40	0.83	9.37	6.5	2.15	0.88	2.2	0.02
130	60.50	13.50	5.51	5.03	3.28	1.13	8.08	5.3	2.19	0.85	1.4	0.15
53	57.30	15.00	4.43	5.87	4.39	0.59	7.59	5.3	1.70	0.82	2.4	0.03
112D	53.50	14.20	4.95	5.87	4.46	0.61	11.60	7.4	3.38	1.74	2.5	0.01
127	67.90	12.70	2.93	0.68	4.45	1.32	7.94	3.4	4.16	0.70	1.0	0.01
148	63.80	12.90	4.94	3.88	3.66	0.59	7.21	4.5	2.21	0.87	1.6	0.01
138A	62.00	13.80	3.76	4.14	4.97	0.94	6.20	4.7	0.98	0.92	1.3	0.01
138B	63.40	14.10	6.39	4.12	3.63	2.15	7.14	3.9	2.81	0.73	1.3	0.01

* Fe^*=total iron, $Fe_2O_3 = Fe^* - 1.11134FeO$

Table 9. Trace Element Geochemistry and Alteration Type

Smpl #	CU	ZN	PB	CR	RB	SR	Y	ZR	NB	BA	Altyp*
Hyalotuffs											
17	23.0	250.0	6.0	20	190	70	90	480	60	570	2
16	8.5	130.0	12.0	10	260	190	110	360	30	980	2
32B	25.0	110.0	4.0	10	140	10	120	190	40	830	2
6	2.0	180.0	14.0	20	130	40	130	300	40	450	2
5B	0.5	240.0	6.0	20	90	40	50	310	30	940	2
15	6.0	210.0	10.0	20	150	70	120	420	50	660	2
3	4.0	89.0	16.0	20	80	50	110	220	30	340	2
68	8.0	180.0	14.0	20	190	210	150	290	50	1250	2
2A	11.0	65.0	12.0	10	140	20	100	240	50	1460	2
83B	27.0	140.0	10.0	20	110	150	30	210	10	750	4
28	5.0	110.0	6.0	40	150	30	60	230	30	1210	1
85	68.0	62.0	6.0	20	40	10	80	360	50	330	1
126	5.0	130.0	2.0	30	110	10	130	320	50	330	2
MPFW	1600.0	11000.0	150.0	10	280	10	140	490	60	610	2
171	6.5	260.0	4.0	40	120	10	90	330	30	690	4
67	31.0	65.0	4.0	40	80	40	100	280	40	530	2
19	9.0	190.0	18.0	10	270	180	100	280	40	1620	2
18	2.0	170.0	12.0	10	230	10	90	620	80	1100	2
4B	0.5	220.0	6.0	20	130	10	60	360	40	500	4
27	43.0	140.0	8.0	10	320	210	70	270	30	890	2
84	74.0	390.0	30.0	30	150	40	40	130	20	340	2
Mafic lava flows											
25	24.0	110.0	6.0	20	50	170	30	110	20	370	2
86	41.0	97.0	2.0	340	30	200	10	110	10	200	3
31B	28.0	120.0	4.0	20	50	290	20	100	30	190	1
14	21.0	130.0	6.0	20	50	250	20	120	20	220	2
33	24.0	130.0	2.0	20	40	100	10	120	20	330	1
QFP											
94	3.5	53.0	2.0	20	70	30	140	670	40	380	1
104	25.0	140.0	2.0	20	70	20	140	650	30	620	2
103	2.0	86.0	2.0	10	150	20	140	660	50	1200	2
Rhyolite lava flows											
119	1.5	52.0	2.0	10	150	20	120	310	60	770	1
155	2.5	38.0	2.0	30	40	30	190	340	50	580	1
161	4.0	35.0	2.0	30	60	40	150	310	40	860	1
122	2.5	71.0	4.0	20	110	40	130	310	40	640	2
163	2.0	83.0	2.0	10	90	10	110	330	40	700	1
101	21.0	24.0	2.0	10	100	10	120	310	50	930	2
168	12.0	21.0	6.0	20	130	10	90	320	50	900	1
139	4.0	49.0	4.0	10	110	20	130	320	40	890	1
87	4.0	65.0	2.0	10	120	40	110	310	30	730	1
90	3.0	88.0	4.0	20	60	40	140	290	40	750	1
62	22.0	87.0	8.0	340	60	220	10	120	20	390	3
128	1.0	72.0	4.0	10	130	20	80	320	50	890	1
61	20.0	31.0	28.0	20	70	30	120	240	30	870	1
136	23.0	31.0	2.0	20	100	250	130	300	30	770	2
57	10.0	48.0	2.0	10	110	20	100	330	30	900	1
149	6.0	70.0	2.0	10	130	20	100	330	50	1080	2
91	12.0	27.0	2.0	10	100	20	110	330	40	1270	1
116	7.0	180.0	12.0	10	130	190	180	360	40	500	2
55	8.0	98.0	2.0	10	200	10	110	400	40	1160	2

Table 9. cont.

Smpl #	CU	ZN	PB	CR	RB	SR	Y	ZR	NB	BA	Altyp*
Tonalite sills											
133	33.0	170.0	2.0	110	70	170	30	190	20	430	2
110	6.0	170.0	2.0	10	70	70	90	460	30	540	2
99A	27.0	120.0	4.0	10	60	160	40	210	30	400	2
140	2.5	160.0	2.0	10	80	160	80	450	30	470	2
88	11.0	100.0	2.0	140	80	190	50	210	30	520	1
129	6.5	92.0	2.0	40	70	150	20	230	20	360	2
65	19.0	120.0	2.0	30	70	140	10	170	20	280	3
113	17.0	120.0	2.0	120	130	160	20	120	30	540	3
66	3.0	49.0	6.0	100	20	210	20	190	20	240	3
111	10.0	110.0	2.0	10	60	140	30	240	30	500	3
54	32.0	110.0	2.0	220	20	170	10	130	30	230	1
130	10.0	120.0	2.0	190	50	110	10	190	30	300	3
53	18.0	86.0	2.0	150	20	200	10	130	10	160	1
112D	3.5	89.0	2.0	110	40	150	20	120	20	140	3
127	26.0	250.0	2.0	10	50	100	60	450	30	400	1
148	3.5	65.0	2.0	110	40	110	10	200	30	210	3
138A	1.0	36.0	4.0	110	40	170	30	210	20	220	3
138B	4.5	70.0	4.0	180	10	200	20	160	20	190	2

*
Alteration types:
1. least altered
2. sericite/biotite alteration
3. actinolite alteration
4. dalmatianite

Appendix III: X-Ray Diffraction and Hand Sample Staining Analyses

16 samples were analyzed by X-ray diffraction at the University of Minnesota, Duluth to identify the chlorite species present and to confirm the presence of cordierite in quartz-rich samples. In addition, one sample of a tourmaline inclusion-rich quartz vein was analyzed to determine the tourmaline species present. Unoriented and oriented slide mounts were scanned from 4-70° at 2°/minute using a Picker Diffractometer with CuK_{α} radiation. Mineral identifications were made using Switzer (1962), and Berry (1974).

8 altered samples were etched with a 0.2% solution of hydrochloric acid and then stained with a 0.2% solution of alizarin red S and a 1.0% solution of potassium ferricyanide to determine the carbonate species as outlined by Friedman (1959) and Evamy (1962).

Table 10: X-Ray Diffraction and Hand Sample Staining Results

X-Ray Diffraction

Sample #	Chlorite Species	Cordierite
Actinolite alteration		
66	Ferroan clinochlore	
124 D	Ripidolite	
Sericite, chlorite alteration		
1 A	Ferroan clinochlore, penninite	X
2 A	Ferroan clinochlore	X
14	Ferroan clinochlore, penninite	
19	Ferroan clinochlore, penninite	
31 B	Ripidolite?, penninite	X
137 A	Ripidolite?	
Dalmatianite		
4 B	Ferroan clinochlore, penninite	
5 B	Ferroan clinochlore, penninite	
171	Ferroan clinochlore, penninite	
Least altered		
2 B		X
91		X
102		X
118 BT	Chamosite	

Tourmaline Species

Quartz vein	Dravite

Chemical Staining

Sample #	Carbonate Species
Actinolite alteration	
66	Ferroan dolomite/ankerite
Sericite, chlorite alteration	
14	Ferroan dolomite/ankerite
55	Ferroan dolomite
113	Ferroan dolomite/ankerite
133	Ferroan dolomite/ankerite
Dalmatianite	
4 B	Ferroan dolomite
5 B	Ferroan dolomite